Remote Sensing Series 75

Marta Gomez Gimenez

# Monitoring Agricultural Management Practices and Nitrogen Deposition in Swiss Agroecosystems Using Remote Sensing

Remote Sensing Laboratories
Department of Geography
University of Zurich, 2017

Remote Sensing Series 75

Marta Gomez Gimenez

# Monitoring Agricultural Management Practices and Nitrogen Deposition in Swiss Agroecosystems Using Remote Sensing

Remote Sensing Laboratories
Department of Geography
University of Zurich, 2017

Front page: Photo collage showing different management practices. Pictures taken by Marta Gómez Giménez.

Gómez Giménez, Marta

*Monitoring Agricultural Management Practices and Nitrogen Deposition in Swiss Agroecosystems Using Remote Sensing.*

Remote Sensing Series, Vol.75
Remote Sensing Laboratories, Department of Geography, University of Zurich
Switzerland, 2017

ISBN: 978-3-906894-04-1



This work was approved as a PhD thesis by the Faculty of Science of the University of Zurich in the fall semester 2017. Doctorate committee: Prof. Dr. Michael E. Schaepman (chair and dissertation supervisor), Dr. Rogier de Jong, Dr. Armin Keller, PD. Dr. Guido L. B. Wiesenberg.

# MONITORING AGRICULTURAL MANAGEMENT PRACTICES AND NITROGEN DEPOSITION IN SWISS AGROECOSYSTEMS USING REMOTE SENSING

Dissertation

zur

Erlangung der naturwissenschaftlichen Doktorwürde

(Dr. sc. nat.)

vorgelegt der

Mathematisch-naturwissenschaftlichen Fakultät

der

Universität Zürich

von

Marta Gómez Giménez

aus

Spanien

Promotionskommission

Prof. Dr. Michael E. Schaepman

(Vorsitz und Leitung der Dissertation)

Dr. Rogier de Jong

Dr. Armin Keller

PD Dr. habil. Guido L. B. Wiesenberg

Zürich, 2017

## Summary

Food production is one of the main drivers of land competition. Increasing the agricultural production of a certain area usually entails the application of fertilizers that in high quantities can produce water pollution, loss of biodiversity, and greenhouse gases emission and deposition. In Switzerland, manure input is the main cause of nutrient surplus in agroecosystems. Other source of nutrient is atmospheric deposition, which also contributes to nitrogen surplus to a lesser extent. Nitrogen surplus has been monitored using farm statistics but there is a lack of assessments of spatial and temporal patterns of nitrogen surplus.

Remote sensing can contribute substantially to the monitoring and assessment of nitrogen surplus in agroecosystems, e.g., providing land cover and land use datasets to allocate farm statistics, monitoring grassland use intensity to control high manure inputs, and evaluating the impact of nitrogen deposition on carbon fixation response. Results can be integrated as part of modelling frameworks or used as ancillary information by decision-makers. The use of models brings along two challenges: first, the reliability of model outputs depends on the quality of model inputs; second, the integration of results in multidimensional frameworks may remain difficult because the same phenomenon can be characterised and analysed differently by diverse scientific disciplines. This thesis is motivated by three research questions aiming at investigating the impact of remote sensing datasets on the land allocation output, proposing a method to assess grassland use intensity following an ecological approach, and evaluating the role of nitrogen deposition and climatic factors in explaining carbon fixation responses.

The research findings revealed that the spatial resolution, classification accuracy, and segmentation process impacted on the allocation of farm statistics. Three ecological indicators of grassland use intensity i.e., mowing frequency, grazing intensity, and fertilization inputs were assessed. Further results integration helped define areas prone to nutrients surplus. Nitrogen deposition was the variable that explained mostly the carbon fixation response in grasslands, croplands, and croplands/natural vegetation mosaic. Finally, main

findings and contributions are discussed and future research lines proposed.

## Zusammenfassung

Die Nahrungsmittelproduktion gehört zu den wichtigsten Einflussfaktoren, welche den Wettbewerb um die Landnutzung antreiben. Die Steigerung der landwirtschaftlichen Produktion geht üblicherweise mit dem Einsatz von Düngemitteln einher, der in grossen Mengen zu Wasserverschmutzung, Verlust von Biodiversität sowie zu Treibhausgasemissionen und Deposition führt. In der Schweiz ist der Überschuss an Nährstoffen in Agroökosystemen hauptsächlich durch hohe Düngerzufuhr bedingt, und zu einem kleineren Anteil durch andere Quellen wie atmosphärische Deposition, welche die Kohlenstofffixierung beeinflussen und die Biodiversität in landwirtschaftlich genutzten Regionen reduzieren. Der Überschuss an Nährstoffen wird zwar mittels Agrarstatistiken überwacht, aber es fehlt an Studien welche die räumlichen und zeitlichen Muster des Stickstoffüberschusses untersuchen.

Fernerkundung kann substanziell zur Untersuchung und Überwachung von Stickstoffüberschuss in Agroökosystemen beitragen. Dies zum Beispiel durch Bereitstellung von Landbedeckungs- und Landnutzungsdaten um Agrarstatistiken zuzuweisen, durch Überwachung der Nutzungsintensität von Grasland um (zu) hohe Nährstoffeinträge zu kontrollieren und durch Untersuchung des Einflusses der Stickstoffdeposition auf die Kohlenstofffixierung. Entsprechende Resultate können in Modelle integriert oder als zusätzliche Information für Entscheidungsträger genutzt werden. Die Verwendung von Modellen bringt zwei Herausforderungen mit sich: erstens, die Zuverlässigkeit der Modellresultate hängt von den Eingangsvariablen ab; zweitens, die Integration von Resultaten in multidimensionale Strukturen kann sich als schwierig herausstellen, da das gleiche Phänomen von verschiedenen wissenschaftlichen Disziplinen unterschiedlich charakterisiert und analysiert werden kann. Diese Dissertation ist durch drei Forschungsfragen motiviert, mit dem Ziel den Einfluss von Fernerkundungsdaten auf die Landzuweisung zu untersuchen, eine Methode zur Analyse der Grasland Nutzungsintensität anhand eines ökologischen Ansatzes vorzuschlagen und die Rolle von Stickstoffdeposition und Klimafaktoren auf die Kohlenstofffixierung zu evaluieren.

Die Forschungsergebnisse zeigen, dass räumliche Auflösung, Klassifikationsgenauigkeit und der Segmentierungsprozess der Fernerkundungsdaten den stärksten Einfluss auf die Zuweisung von Agrarstatistiken haben. Drei ökologische Indikatoren der Grasland-Nutzungsintensität, nämlich Mähfrequenz, Beweidungsintensität und Düngemitteleintrag, wurden untersucht und die weiterführende Integration der Resultate half Gebiete auszuscheiden, die zu einem Nährstoffüberschuss neigen könnten. Stickstoffablagerung hatte die stärkste Vorhersagekraft für Kohlenstofffixierung in Gras- und Ackerland sowie in Mosaiken von Ackerland und natürlicher Vegetation. Schliesslich werden die wichtigsten Forschungsergebnisse und Beiträge dieser Arbeit diskutiert und zukünftige Forschungsrichtungen vorgeschlagen.

## Table of Contents

## List of Tables

## List of Figures

## List of Abbreviations

| | |
|---|---|
| a.s.l. | Above sea level |
| AGIS | Agrarpolitisches Informationssystem |
| *AI* | Accuracy index |
| APEX | Airborne Prism Experiment |
| AR | Autotrophic respiration |
| AVZH | Non-public dataset provided by a cantonal agency |
| B-P | Breuch-Pagan |
| BRDF | Bidirectional Reflectance Distribution Function |
| C | Carbon |
| $Ch_t$ | Relative changes |
| CI | Confidence interval |
| CV | Coefficient of variation |
| D-W | Durbin-Watson |
| DEM | Digital Elevation Model |
| DHM25 | Digital Height Model at scale 1:25'000 |
| DOY | Day of the year |
| ECA | Ecological Compensation Areas |
| EO | Earth observation |
| FAO | Food and Agriculture Organization of the United Nations |
| $F_c$ | Factors |
| GDD | Growing degree-days |
| GPP | Gross primary production |
| GS | Gram-Schmidt |
| HC | Heteroscedasticity-consistent |
| IFOV | Instantaneous field of view |
| IGBP | International Geosphere and Biosphere Programme |
| iMSoil | Integrated modelling framework to monitor and predict trends of agricultural management and their impact on soil functions at multiple scales |
| IR-MAD | Iteratively re-weighted multivariate alteration detection |

| | |
|---|---|
| JM | Jeffries-Matusita |
| K | Kappa statistic |
| K | Koenker |
| LAI | Leaf area index |
| LCC | Leaf chlorophyll content |
| LCLUC | Land-cover and land-use change |
| LMM | Land Management Model |
| LU | Livestock units |
| N | Nitrogen |
| NDVI | Normalized Difference Vegetation Index |
| NPP | Net primary production |
| NRP68 | National Resource Program |
| OA | Overall accuracy |
| OLI | Operational Land Imager |
| P | Phosphorous |
| PEP | Proof of ecological performance |
| RBF | Radial basis function |
| RS | Remote sensing |
| SE | Sampling error |
| SEON | Swiss Earth Observatory Network |
| SNR | Signal-to-noise ratio |
| SOC | Soil organic carbon |
| SR | Shrunken |
| STSE | Support to Science Element |
| SVM | Support Vector Machine |
| SWIR | Shortwave infrared |
| T | Tolerance |
| Thres | Threshold |
| TIRS | Thermal Infrared Sensor |
| UAA | Utilised Agricultural Area |
| UAVs | Unmanned aerial vehicles |
| VIF | Variance inflation factor |
| VIs | Vegetation indices |

| | |
|---|---|
| VNIR | Visible and near infrared |

# Chapter 1

## Introduction

## 1.1. Land cover, land use, and land management change

In the next few decades, food production and the delivery of energy and materials will be the main drivers of land competition (Garnett et al., 2013; Harvey et al., 2011). In particular, food production will be the most important biophysical basis for food security in order to meet the growing population demands (Foley et al., 2011; Tilman et al., 2001) — according to FAOSTAT (2017a), world population is projected to reach more than 9 billion people by 2050 (Figure 1.1).

Agricultural production is based on the optimal combination of means such as capital, land, fertilizers, and pesticides in order to obtain an output (Matson et al., 1997; Strijker, 2005). This output can be increased by either using larger areas of cultivated land through agricultural expansion or by obtaining higher yield per area cultivated via agricultural intensification (Turner et al., 1978). Agricultural intensification aims at increasing agricultural productivity, which is a cornerstone of competition for land. Intensification played a key role in increasing food production during the 20$^{th}$ century, with the use of fertilizers being particularly crucial (Potter et al., 2010; Verburg et al., 2013). However, the excess of fertilizers produces negative impacts on biodiversity, soil fertility, water bodies, and atmospheric compounds via the emission of greenhouse gases (Matson et al., 1997; Stoate et al., 2001). The Food and Agriculture Organization of the United Nations (FAO) highlights the world consumption of three main fertilizers: nitrogen (N), potash, and phosphate (FAOSTAT, 2017b). In the last 10 years, the differences in consumption patterns among those fertilizers have been remarkable, with N being the most used nutrient (Figure 1.2).

Even small changes in agricultural land use management practices that tend to increase food production can lead to land cover modifications (Lambin et al., 2000). Therefore, land cover and land use change (LCLUC) are major role players in global environmental change (Lambin et al., 2001; Rudel et al., 2009). Local and national markets, as well as policies, trigger LCLUC under the influence of globalization and climate change (Godfray et al., 2010; Olesen et al., 2002).

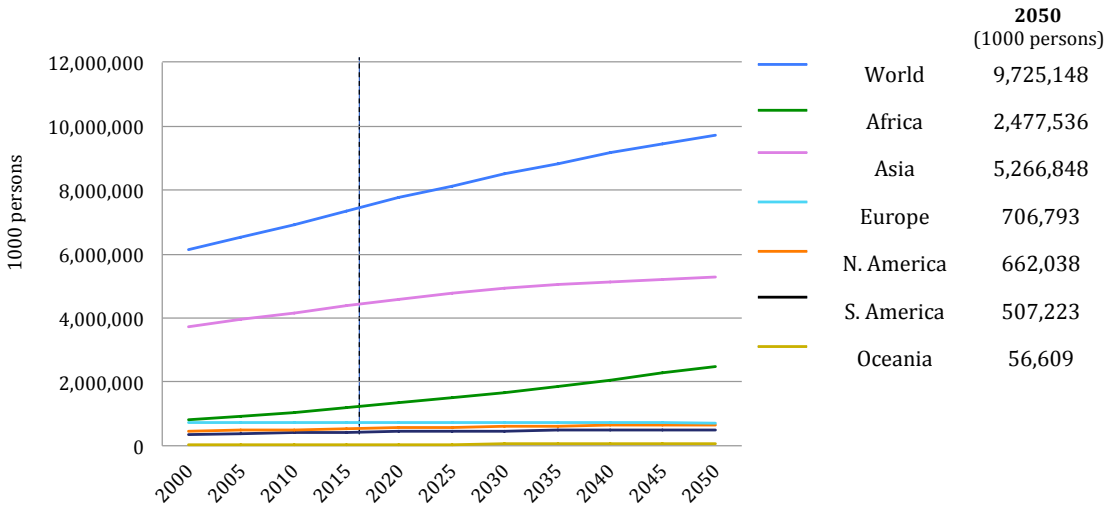


Figure 1.1 Population growth 2000-2050 according to FAOSTAT (2017a).

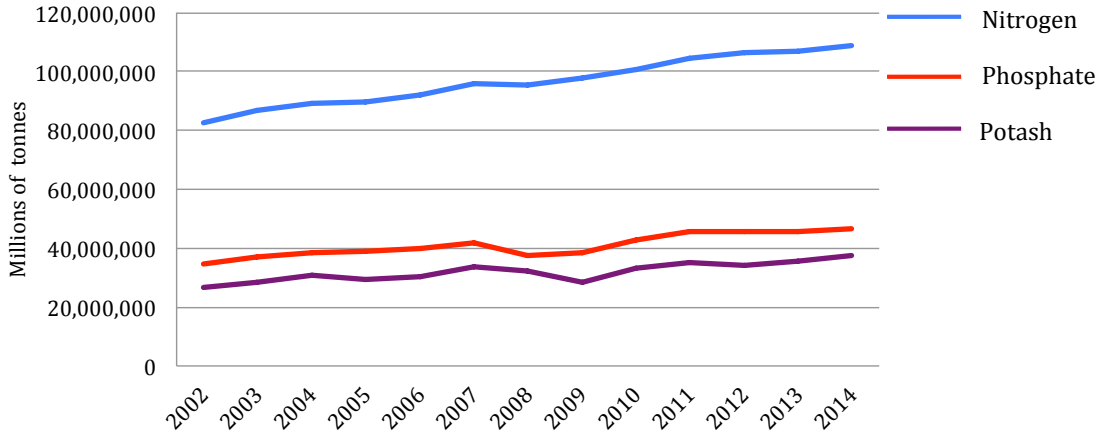


Figure 1.2 World fertilizer consumption 2002-2014 according to FAOSTAT (2017b).

In Switzerland, LCLUC have affected 15% of the total surface extent since the 1980s. The agricultural area has decreased by 5.4% because of an increase in urban areas, land abandonment, and forest encroachment. Additionally, agricultural intensification via nutrients input has caused water and air pollution and has also decreased biodiversity (FOAG, 2015b; Spiess, 2011). The Utilised Agricultural Area (UAA) (basic unit to quantify agricultural surface) represents more than 30% of the total national territory (41,285 km$^2$) with 70.9% of the total UAA (1,050,000 ha) covered by grasslands. In the last decade (1996-2013), a decline in the number of farms (from 79,500 to 55,300) has also modified the average of UAA per farm, increasing from 5.4 ha to 19 ha (FSO, 2015).

The Swiss agricultural sector plays an important role because this system has to fulfil several functions simultaneously as a result of a lack of space, e.g., ensure

food supply through sustainable production, preserve the landscape, and maintain rural areas (FOAG, 2004). Therefore, it is crucial to monitor any changes in land use and management practices that can endanger the provisioning of agricultural services for human activities.

National policies are powerful tools to reach the required agricultural productivity while reducing competition for land as well as preventing the loss of ecosystem services (Brown et al., 2014; Smith et al., 2010). In particular, the Swiss agricultural policy promotes ecological practices via direct payments (FOAG, 2004).

### 1.1.1 The Swiss agricultural policy

Since the 1990s, the Swiss government has fostered sustainability and reduction of intensity of use by means of several initiatives and programmes. For example, convert arable land to grassland, promote organic farming, increase grain production, foster permanent flower meadows, support rotated fallow land with specific crop rotations in large fields (> 3 ha), preserve areas of high ecological value, and encourage the production of renewable resources of non-food consumption (Buchli et al., 2008; OECD, 1998). In 1996, the Swiss Federal Constitution included the article 104 to turn the agricultural sector into a sustainable system binding direct payments to minimum ecological requirements (Swiss Constitution, 1999). One of the main goals was to improve species richness and to enhance biodiversity by converting 7% of farmlands into Ecological Compensation Areas (ECA) with extensive management practices (e.g., low fertilizer and pesticide input, wooded pastures, and meadows mown late in the growing season and once a year) (Swiss government, 1998). In 2001, the ordinance on eco-quality came into force in order to improve the quality of the ECAs (FOAG, 2004). Since 2014, a new policy framework has linked direct payments to specific regulations aiming at ensuring food supplies, maintaining farmland, enhancing biodiversity, preserving landscape quality, fostering animal friendly production systems, promoting resource-efficiency production techniques, and providing transitional payments for farmers who lost incomes with the new policy (Meier, 2013; OECD, 2016). In particular, farmers have to provide proof of ecological performance (PEP) about a balanced use of pesticides

and fertilizers (i.e. N and phosphorus (P) inputs must not exceed more than 10% crop requirements (Spiess, 2011)), ECAs, crop rotation, soil protection, and livestock welfare in order to receive direct payments (FOAG, 2015b).

The PEP has helped preserve biodiversity and reduce water and air pollution but some environmental issues still persist (Herzog et al., 2008; Herzog, Richner, et al., 2005). On one hand, ECAs have improved pollinator services as well as enhanced plant community composition (Albrecht et al., 2007; Aviron et al., 2009). On the other hand, N inputs still exceed crop requirements. In 2012, 88,000 tonnes of N surplus in UAAs (57 Kg/ ha) were reported (FSO, 2015; Spiess, 2011). High manure input and livestock density are the main causes of N surplus in Swiss agroecosystems, followed by inorganic and organic fertilizers, biological fixation, and atmospheric deposition (FSO, 2015). While N deposition contributes minimally to N inputs in Swiss agroecosystems, it has been identified as an important driver of changes in plant communities in Alpine regions (Bassin et al., 2013; FSO, 2015). N saturation also affects the storage and loss of N and carbon (C), which influence the C budget of ecosystems (Chapin III et al., 2006; De Deyn et al., 2009; Matson et al., 2002). Furthermore, recent analyses show that the quantities of N deposition do not meet Swiss regulations on eutrophication (Rihm et al., 2016). N deposition can increase or decrease the productivity or photosynthetic activity of plants, which impacts on ecosystems (Figure 1.3). In particular, N inputs affect supporting services (primary production, nutrient cycling, and soil formation), provisioning services (food and fibre production, biodiversity, and water supply), regulating services (C sequestration, air and water quality, and hazard regulation), and cultural services (leisure activities and aesthetic appreciation of the environment) (Foley et al., 2005; Jones et al., 2014).

In summary, monitoring N sources and the related impact on Swiss agroecosystems is crucial to meeting crop requirements, reducing N surplus caused by managed grassland systems, and controlling the influence of anthropogenic N in important ecosystem services such as C sequestration.

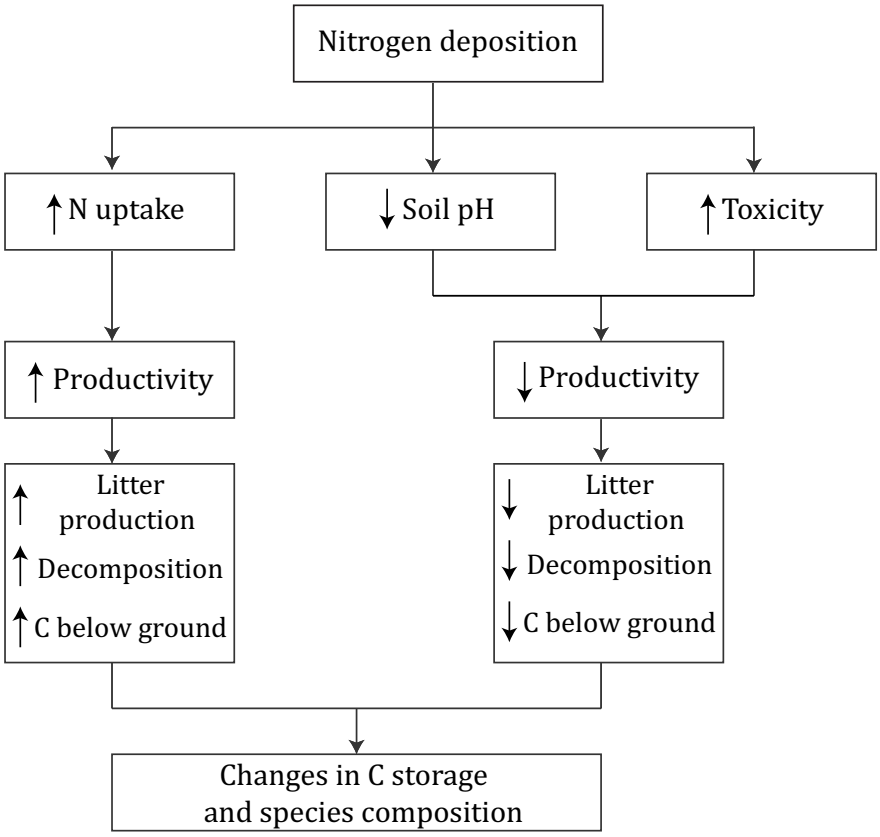


Figure 1.3. Impact of Nitrogen deposition on ecosystems. Adapted from Jones et al. (2014) and Bobbink et al. (2010).

## 1.2 Monitoring N sources in Swiss agroecosystems: the relevance of remote sensing

Farm statistics have been used to estimate N balance and to monitor the implementation of the Swiss agricultural policy (Decrem et al., 2007; Mack et al., 2017; OECD, 2015; Spiess, 2011). However, there is a lack of spatially explicit datasets to evaluate patterns of N surplus (Della Peruta R. et al., 2016). Therefore, a Land Management Model (LMM) has been developed to estimate the nutrient balance at soil surface using land cover/use maps to allocate farm statistics (Della Peruta R. et al., 2016; Gärtner et al., 2013). Earth observation (EO) sources provide land cover maps that together with farm statistics have been used to map global agricultural land use and fertilizer application (Monfreda et al., 2008; Potter et al., 2010). Furthermore, remote sensing is key to monitoring areas with high agricultural production boosted by the use of fertilizers and related atmospheric deposition (Running et al., 2004; Schulze et

al., 2010; Whitcraft et al., 2015).

Since the 1970s, the Landsat program has provided data with medium spatial (30 m) and temporal resolution (16 days revisit time) to monitor LCLUC (Loveland et al., 2012; Roy et al., 2014). Nowadays, freely available datasets with similar or improved resolutions are warranted through the Landsat continuation mission and the ongoing launch of the Sentinel constellation (Irons et al., 2012; Ramoelo et al., 2015; Wulder et al., 2011). Other commercial satellites as well as airborne sensors complement the already existing sources and provide a wide range of tailor-made remote sensing data for addressing environmental issues (Birk et al., 2003; Schaepman et al., 2015; Turner et al., 2003). In many cases, the selection and combination of different EO sources with ancillary datasets help monitor land cover, land use and land management changes, and their impact on species, C sequestration, and nutrient cycling (Rose et al., 2015; Whitcraft et al., 2015; Wulder et al., 2015). Remote sensing datasets can be used independently for mapping purposes, implemented as model inputs, and compared with model predictions (Berger et al., 2012; Malenovský et al., 2012). Models are frequently used to simulate LCLUC effects on different biochemical cycles (carbon, hydrological, and nutrients) with complex land-atmosphere interactions so that future adaptation and mitigation strategies can be developed (Liu et al., 2017; Zaehle et al., 2007).

On one hand, the quality of model inputs impacts on the reliability of model outputs (Temme et al., 2011; Zaks et al., 2011). On the other hand, land planning requires holistic approaches based on human and environmental (sub–)systems that are usually assessed with different frameworks and methods developed at several spatial scales (Turner et al., 2008; Turner II et al., 2007). As a result, barriers exist to assimilate inputs into models as well as to synthesise and connect results from different studies (Rounsevell et al., 2014).

In short, EO is a relevant data source for monitoring agricultural management practices. Particularly, remote sensing techniques are powerful tools that can contribute to the monitoring and assessment of N sources providing land cover and land use maps to allocate farm statistics, monitor areas with high manure inputs, and evaluate the role of N deposition in C fixation response. Furthermore, the remote sensing community can contribute to finding common ground

between different fields of study developing techniques based on shared frameworks. This may help integrate results in multidimensional approaches required for land planning and overcome the above-mentioned obstacles.

## 1.3 Objectives

The contribution of remote sensing to monitor N sources in agroecosystems, current research topics, and challenges ahead have been previously introduced. Accordingly, three main goals have been defined for this thesis:

1. Provide spatially explicit land cover and land use information for the Land Management Model.
2. Monitor grassland use intensity.
3. Evaluate the role of limiting factors in C fixation response.

A wide variety of remote sensing data and techniques are presented to show how EO can tackle the three aforementioned issues. The work carried out is part of an integrated modelling framework to monitor and predict trends of agricultural management and their impact on soil functions at multiple scales, iMSoil project[1], (Figure 1.4). This project aims at the optimization of nutrients and pesticides, the reduction of contaminant input to the soils, and the detection of threats to agricultural soils.

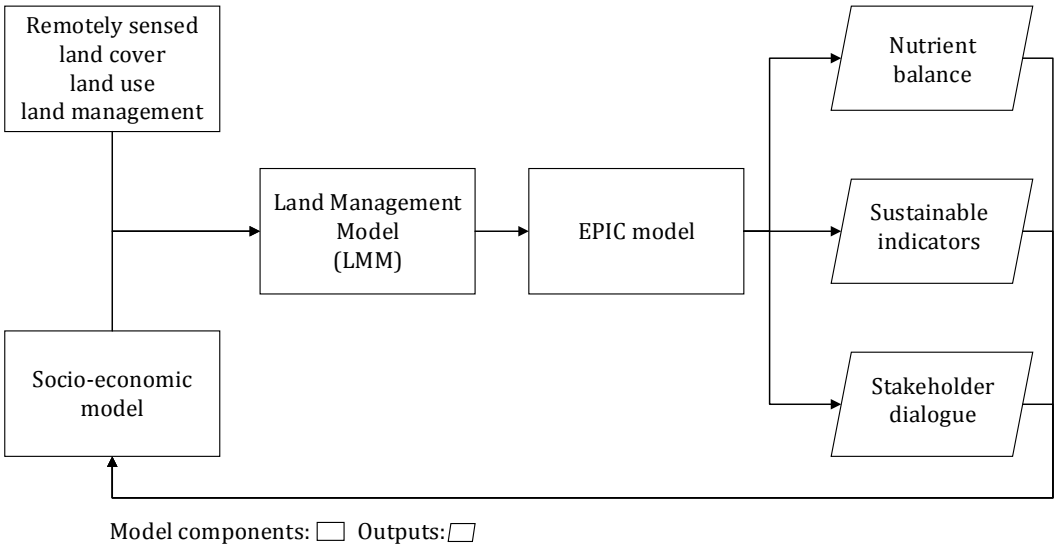


Figure 1.4 Modelling framework iMSoil. Adapted from Keller et al. (2015).

[1] http://www.nfp68.ch/en/projects/key-aspect-4-geoinformation-and-governance/early-warning-system; accessed [12/6/2017].

### 1.3.1 Research questions

Three research questions have been formulated based on the objectives presented and the research challenges identified in previous sections:

1. What is the contribution of using remote sensing data to the performance and output of the Land Management Model?
2. How can indicators of intensity of use derived from remote sensing data be used in a context of an ecological framework?
3. What is the relevance of N deposition and related climatic factors to predict remotely sensed C fixation response in land cover classes characterised by different management practices?

## 1.4 Outline

Chapter 1 introduces environmental issues that still persist despite the measures implemented through the Swiss agricultural policy. In this chapter, remote sensing datasets are highlighted as powerful tools that can contribute to monitoring and assessing N sources in Swiss agroecosystems.

Chapter 2 demonstrates the impact of remote sensing datasets on the LMM performance. Preprocessing, processing, and postprocessing chains of two satellite images are analysed in order to determine which steps have the highest impact on the land allocation module. Improvements in this part of the model can help reduce uncertainties in the LMM outputs.

Chapter 3 presents a methodology to assess grassland use intensity with five satellite images following an ecological approach. Three indicators of intensity of use are evaluated: mowing frequency, grazing intensity, and fertilization inputs within a growing season. Finally, indicators are integrated in order to find areas prone to nutrients surplus.

Chapter 4 monitors the influence of limiting factors of remotely sensed C fixation (Gross Primary Production, GPP) response in grasslands, croplands, and croplands/natural vegetation mosaic. This chapter reveals the importance of N deposition and climatic factors for predicting GPP variability in agroecosystems with different management practices.

Chapter 5 discusses the findings obtained in previous sections and provides

guidance for future research directions.

# Chapter 2

# Spatial Differentiation of Arable Land and Permanent Grassland to Improve a Land Management Model

This chapter is based on:

Gómez Giménez, M., Della Peruta, R., de Jong, R., Keller, A., and Schaepman, M.E. (2016). Spatial Differentiation of Arable Land and Permanent Grassland to Improve a Land Management Model for Nutrient Balancing. *IEEE Journal of Selected Topics in Applied Earth Observations and Remote Sensing, 9*, 5655-5665 https://doi.org/10.1109/JSTARS.2016.2551729

Authors' contributions: All authors designed the study, MGG, RDP, AK collected the data, MGG, RDP, AK, MES designed the methodology, MGG, RDP, AK, performed the analysis, all authors wrote the manuscript.

## Abstract

Agroecosystems play an important role in providing economic and ecosystem services, which directly impact society. Inappropriate land use and unsustainable agricultural management with associated nutrient cycles can jeopardize important soil functions such as food production, livestock feeding and conservation of biodiversity. The objective of this study was to integrate remotely sensed land cover information into a regional Land Management Model (LMM) to improve the assessment of spatially explicit nutrient balances for agroecosystems. Remotely sensed data and an optimized parameter set contributed to improved LMM output, allowing for a better land allocation within the model. The best-input parameter combination was based on two different land cover classifications with overall accuracies of 98%, improving the land allocation performance compared with using non-spatially explicit input. We conclude that the combined use of remote sensing data and the LMM has the potential to provide valuable guidance for farm practices. It further helps generate a spatial description of farm level nutrient balance, a crucial ability when choosing policy options related to sustainable management of agricultural soils.

**Keywords:** Agroecosystems, land allocation, land use classification, nutrient balancing, remote sensing (RS).

## 2.1 Introduction

Inappropriate management of agroecosystems can affect fundamental provisioning of ecosystem services (Díaz et al., 2007). Generally, intensification of agricultural land use degrades biodiversity, air quality, water and soil, and simplifies landscapes (Stoate et al., 2001; Tscharntke et al., 2005) by converting heterogeneous crop mosaics into homogeneous patterns. One of the most significant problems is the measurement of biogeochemical flows within agroecosystems and the assessment of changes caused by intensification (Haygarth et al., 2014). In particular, excessive input of phosphorus (P) and nitrogen (N) to agricultural soils increases the risk of soil quality degradation (Steffen et al., 2015).

Given the diverse topography, climatic conditions, geology and soil types in Switzerland, agricultural systems are relatively heterogeneous and managed by many small farms. The average farm size in Switzerland is only 18 hectares (FSO, 2015). In the past, intensification of Swiss agriculture after 1950 led to an increase in productivity. An additional suite of environmental problems arose, related to increasing N and P inputs to the agricultural system (Spiess, 2011). As a consequence, in the early 1990s the Swiss agricultural policy was re-framed and ecological programs were introduced to promote sustainability and meet market demands (FOAG, 2004; Herzog, Dreier, et al., 2005). Since the mid-1990s, agricultural management was linked to direct payments based on the environmental performance of farms. Integrated production schemes as well as organic agriculture options imposed certain environmental management requirements such as equilibrating the nutrient balance at farm level, crop rotation schemes and soil protection activities, among others (FOAG, 2004; Spiess, 2011). As a result, the surplus of nutrients decreased markedly, but not to the level specified by mitigation policies. In 2008, the national nutrient balance still indicated a nutrient surplus averaging at 108 kg N $ha^{-1}$ and 5.5 kg P $ha^{-1}$, still largely exceeding most crop requirements (Spiess, 2011).

Consequently, the Swiss agricultural policy was adapted in order to better monitor and predict the impact of agricultural management on soil quality (FOAG, 2004; Herzog, Dreier, et al., 2005). The new policy measures specifically

aimed to identify areas prone to N and P accumulation ("hot-spots"), and foster sustainable agricultural management including associated nutrient cycles in agricultural systems, without jeopardizing biodiversity and conservation goals. In order to provide a quantitative model-based assessment of those policy changes, a LMM was established, permitting the assessment of the spatially explicit nutrient balance for regional agroecosystems with sizes on the order of several hundred kilometres (Keller et al., 2017). The LMM is based on a downscaling approach (Gärtner et al., 2013) and calculates nutrient balance at the soil surface, with special emphasis on macronutrients such as N and P. The model uses geo-referenced annual farm census data for parcel allocation to farms. The LMM was extended in this study to improve this allocation procedure by incorporating the use of spatially explicit land information derived from remote sensing data.

Regional modelling of the nutrient balance for an agroecosystem requires spatially distributed land information (Heathwaite et al., 2003), apart from other data sources. Land information includes land cover, land use, and land management. Land cover "is the observed bio-physical cover on the Earth's surface; land use is characterised by the arrangements, activities and inputs that people undertake in a certain land cover type to produce, change or maintain it" (Di Gregorio et al., 1998). Both terms are frequently used interchangeably (Giri, 2012), in part because they are strongly related. Changes in land use cause changes in land cover and vice versa. In particular, mapping studies based on remote sensing are often characterised by legends entangling land cover and land use terminology (Loveland, 2012). Land use implies land management practices that are defined as the presence of human activities that affect land cover (van Oudenhoven et al., 2012; Verburg et al., 2009).

Timely and accurate land cover information is important for improving regional resource management, such as the optimization of N and P use efficiency of fertilizer input, as well as related policy formulation. Therefore, the need for land planning and management information goes hand in hand with the need for land cover information, which is an indicator of the value that society attributes to the land —and this is ultimately the basis for the decisions made (Cihlar, 2000). Remote sensing (RS) can fundamentally contribute to these needs

by making data available in support of sustainable land management practices (Lee et al., 2010; Ramoelo et al., 2012; Skidmore et al., 1997).

Recent studies have tackled the integration of farm statistics (e.g. farm surveys) and land cover information derived from RS sources (e.g. CORINE Land Cover (Kempen et al., 2011; Temme et al., 2011)) for use in regional models. The spatial accuracy requirements of regional models are dependent on the spatial resolution of input data (Britz et al., 2011; Letourneau et al., 2012). However, the impact on the model performance under spatial constraints linked to RS input data has hardly been investigated.

The objective of this study was to integrate remotely sensed land cover information into a regional land management model, which assesses spatially explicit nutrient balance for agroecosystems. The main goal of this integration was to improve the land allocation procedure within the model processing chain, on which all remaining processing stages rely on. As a consequence, the allocation procedure impacted the sustainability assessment carried out with the model. We mapped a regional agroecosystem in Switzerland (67 $km^2$), managed by approx. 250 farms, consisting mainly of dairy and mixed farms. Two land-cover classifications schemes were employed, containing bare soil and grassland. They were subsequently classified as arable land or permanent grassland; these are the major land use types for this regional case study. Finally, different variables derived from the remote sensing data as input to the LMM were analysed to study their impact on the LMM performance.

## 2.2 Study Area

The study area (Figure 2.1) is located within the Canton of Zurich (47.3667°N, 8.5500°E), Switzerland. The average altitude is 556 m above sea level (a.s.l.), and the total extent about 67 $km^2$, from which 41 $km^2$ are agricultural land (2013). It is a rich and heterogeneous floristic region (Gonseth et al., 2001) located in the Swiss plateau (cf. Figure 2.1 inset). The study area is at the transition zone between arable farming focusing on crop production, as well as dairy and mixed farming systems managing grasslands. The latter dominates the study area, with both milk and meat production in common. The area is characterised by a

relatively elevated mean precipitation rate of 1,134 mm per year, a yearly average temperature of 9.3 °C (Meteoswiss, 2015b), and a wide range of soil types. In total, permanent grassland accounts for 60% of the agricultural area, while 39% is used for arable land use. Furthermore, for about half of the arable fields, temporary grassland in crop rotation was observed in 2013. The main crop types are maize silage and corn, winter wheat, triticale, and winter barley. Special crops such as orchards, vineyards or vegetables accounted for only about 1% of the agricultural area.

The number of farms managing the agricultural land has remained quite stable over the last decade, at between 241 and 265 individual farms (FOAG, 2015a). The majority of these specialize in mixed dairy, meat or milk production. Only a few are specialized in arable farming and special crops.

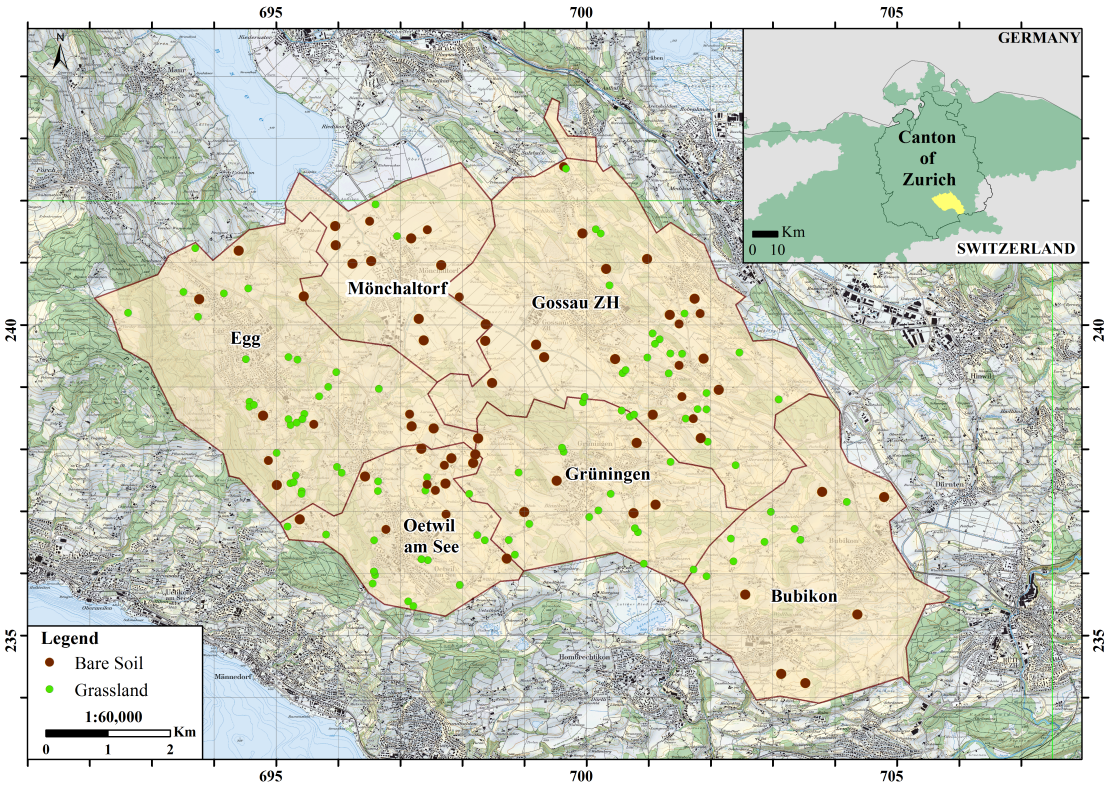


Figure 2.1 Outline of the study area located in the Canton of Zurich, Switzerland including administrative boundaries. The map inset shows the location of the study site (yellow) within the Swiss plateau (green) and the Canton of Zurich (black border). Points denote bare soil as well as grassland in situ samples used for model calibration and validation. Background: Swiss National Map 1:25'000 (Swisstopo) Coordinate System CH 1903 LV03 Hotine Oblique Mercator Azimuth Center.

## 2.3 Methods and Materials

### 2.3.1 Land Management Model

The LMM calculates yearly spatially explicit nutrient balance for Swiss agroecosystems based on available farm census and land use data. The balance approach is a simple soil surface balance (Oenema et al., 2003) accounting for all fertilizer inputs minus the nutrient export by crops excluding further possible processes such as erosion, surface flow, bio-turbation or leaching of nutrients to deeper soil layers.

The LMM algorithm follows a stepwise approach (Figure 2.2). The process starts using rule-based distribution mechanisms to allocate agricultural data spatially to the UAA belonging to an individual farm. UAA is defined in article 14 of the Swiss ordinance about agricultural terms and exploitation forms (Swiss government, 1998) and it is composed by arable land and permanent grassland among other categories. In the second step, nutrient balances at farm level are calculated using the farm census data together with average values of N and P concentration in manure and crops (Flisch et al., 2009; Keller et al., 2003). Next, a simulation of manure trading between farms is carried out following the rules provided by the national program PEP to promote a more even distribution of nutrients over the agricultural land area. Experimental farm statistics and expert interviews completed the dataset to estimate the application of manure and commercial fertilizers to each land unit. As the conditions set by the PEP program are directly linked to agricultural subsidies, they are also valid for the majority of the farms (Herzog et al., 2008). Finally, crop uptake of N and P are subtracted from the estimated inputs, obtaining spatially explicit nutrient balances. The calculation of nutrient inputs at farm level from livestock data and the export of nutrients by crops at farm level follows the method described by Keller et al. (2001).

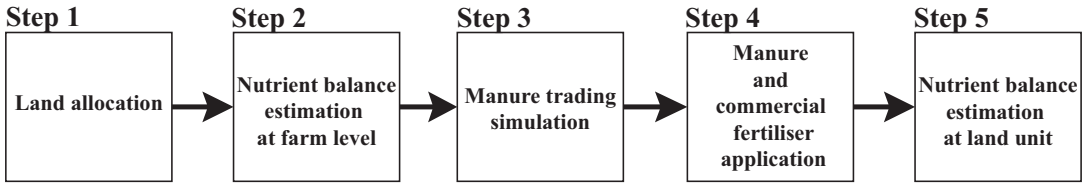


Figure 2.2 LMM workflow.

The model couples different spatial datasets such as agricultural farm census data (*Agrarpolitisches Informationssystem*, AGIS) (FOAG, 2015a) aggregated at farm level (livestock types and numbers, crop type and area), and land use information (UAA) derived from satellite images. The former data is available since 1998 on an annual basis containing coordinates of the main building for each farm. However, the data set does not contain any further spatial information about the location of the individual fields belonging to the farm. Thus, land use maps are required to allocate the agricultural area that belongs to each farm as stated in the annual farm census. We identified the main crop-type groups receiving most contrasting fertilization regimes by distinguishing arable fields and permanent grassland. Differences in fertilization strategies among crops were taken into account for the calculation of the nutrient balance at farm level. It is assumed that those differences are averaged out over the total arable land area because of a stringent crop rotation scheme; therefore, individual crops were not differentiated in a spatial fashion. On the other hand, we approximated the differences in fertilization strategies to be stable in space and time between arable land and grasslands. The spatial distinction between grassland and arable land was of great importance. Fertilization regimes for grasslands were adjusted according to the altitude derived from a digital height model (Swisstopo, 2001).

The integration of land use information in the land allocation process relied predominantly on three factors: i) spatial resolution, ii) classification accuracy and iii) parcels definition. These three aspects were crucial in processing the land use classification.

### 2.3.2 Land use classification

Land use classification process started by preprocessing the satellite images. Classification results were provided during the processing part and validated in

a next step. Finally, postprocessing was applied to delineate information at parcel level (Figure 2.3).

#### 2.3.2.1 Preprocessing

Landsat 8 data was selected as the best combination of sensor characteristics, i.e. spatial, spectral, temporal, and radiometric resolution, as well as the signal-to-noise ratio (SNR) (Irons et al., 2012; Roy et al., 2014; Wulder et al., 2008). These sensor attributes influence the classification accuracy together with other criteria such as the land cover/use classes to be distinguished, costs, and time required to carry out the analysis, the scale of study (Siu-Ngan Lam et al., 1992) or meteorological conditions that limit image acquisition. In 2013, the launch of Landsat 8 assured the program continuity with two new sensors, one optical (Operational Land Imager, OLI), and one thermal (Thermal Infrared Sensor, TIRS). OLI simultaneously records 11 spectral bands of which 8 bands within the visible, near infrared and shortwave domain have a 30-m spatial resolution, and the panchromatic band 15 m; the remaining two thermal bands were not used (Irons et al., 2012; Wulder et al., 2011).

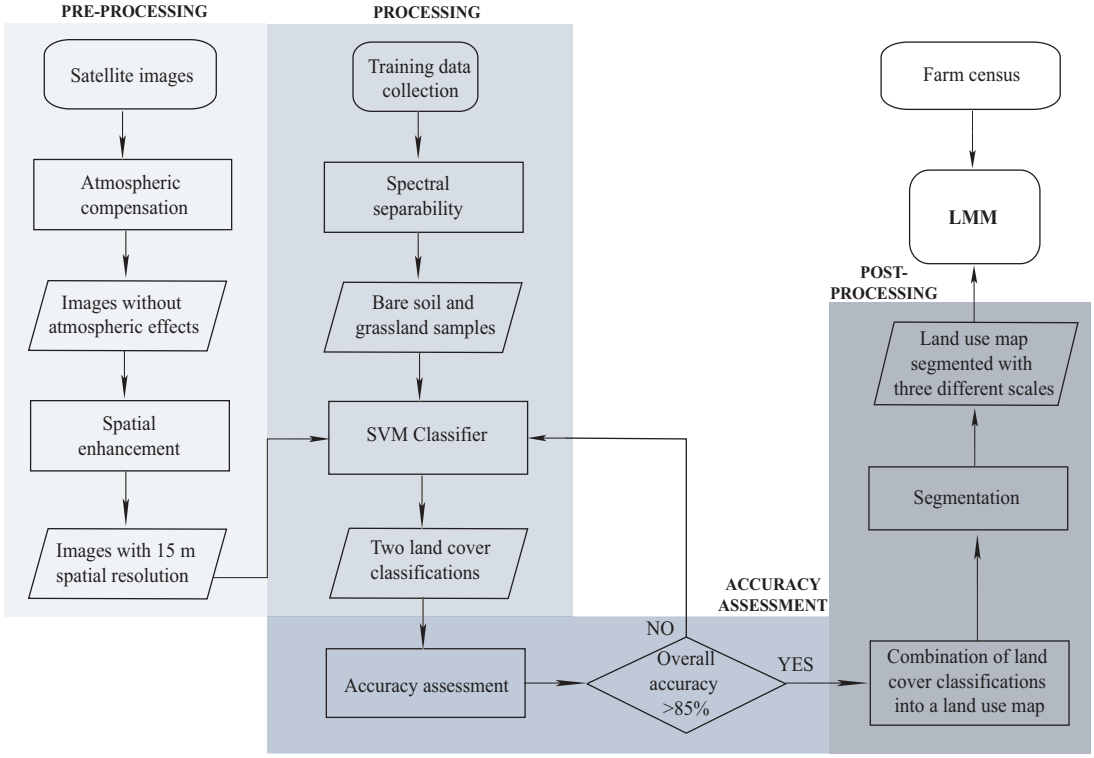


Figure 2.3 Flowchart of the model inputs processing. Colour grading shows the process sequence.

Two Level1T OLI images were recorded during June and July 2014 (path 195 and 194; row 27), and used to differentiate permanent grassland and arable land. The image acquired in June (08/06/2014) was chosen to differentiate permanent grassland from other classes because the PEP program stipulates that extensive grassland must not be cut before the 15th of June. This image contributed to select a number of statistically representative fields to characterise the spectral response of this land use class. The second image acquired in July (19/7/2014) was selected to include more bare soil area, based on a stringent crop rotation scheme applied in Switzerland. Altering crop rotation patterns therefore allowed further identification of bare soil areas, indicating arable land. Hence, the combined use of two images acquired in a time frame with high bare-soil fraction lead to an effective discrimination of arable land. This largely occurred because most of the crops were recently planted (low cover fraction) or recently harvested (tillage effect).

Previous to image processing, atmospheric correction was applied for consistency among images, and transferability to other study regions (Song et al., 2001). Atmospheric effects were compensated deriving surface reflectance values using ATCOR-2 (Richter et al., 2004). The characteristics and geographic position of the study site allowed the use of an aerosol model based on rural areas. Other effects produced by illumination differences between images, i.e. Bidirectional Reflectance Distribution Function (BRDF), or topography effects were not considered because of similar image acquisition details (date and time) with a gap of one month, and the smooth topography, e.g. slope average 3%.

The heterogeneous mosaic of cultivated land and grassland in the study area required spatial resolution enhancement. Pan-sharpening was applied to merge the multispectral lower resolution image (30 m) with the panchromatic higher resolution image (15 m). The Gram-Schmidt (GS) algorithm was used because of its high spectral and spatial performance when fusing processes of multispectral and panchromatic images of the same spatial resolution sensor (Karathanassi et al., 2007).

#### 2.3.2.2 Processing

Classification processes are based on identifying similarities and differences in the spectral domain and linking them to land cover categories (Rindfuss et al., 2004). A Support Vector Machine (SVM) classifier was used because of its high performance (Mountrakis et al., 2011).

The algorithm is based on a binary classifier that can function as multiclass classifier (Vapnik, 1998). Class separation was achieved by setting a penalty parameter, gamma function, pyramid levels, and classification probability threshold. The penalty parameter allows a certain range of misclassification. In this analysis the maximum value was used (100) because it forced the classifier to allow no misclassification during the training process (Petropoulos et al., 2012). The gamma value was the inverse of the number of bands (0.333 using three bands) as suggested in similar studies (Petropoulos et al., 2012; Petropoulos et al., 2011). Pyramid levels are used to establish a number of hierarchical processing levels, and it was set to zero, which means that the process was carried out at full spatial resolution. The classification threshold determined the probability at which pixels remained unclassified, and was set to zero, resulting in the classification of all pixels. Finally, the nonlinear radial basis function (RBF) kernel was chosen to provide the classifier with nonlinearity (EXELIS, 2015; Petropoulos et al., 2012). Three bands (OLI 2, 3, and 4) were selected because the RBF performs better, in terms of classification accuracy, when the input number of bands used in the SVM classifier is reduced (Petropoulos et al., 2011).

The classifier was trained using a dataset collected during field campaigns in April and July 2014. The sampling scheme followed a random approach combined with a systematic unaligned scheme. The stratified sampling approach is recommended when a minimum number of samples per class are selected (Congalton, 1991), and the random sampling scheme allows covering the whole area. The study region was divided in squares of 1 km x 1 km coincident with the coordinate system grid (Figure 2.1). Fields were determined applying a random selector to *a priori* information gathered from a previous vegetation mapping study accomplished in 2000 (Schüpbach et al., 2008). In case points were not

easily accessible or the land use of any particular field had changed in these years, an alternative field was randomly selected leaving at least a full pixel space between parcels to avoid spectral confusion.

Jeffries-Matusita (JM) distance and transformed divergence analyses (Iiames et al., 2013) of the possible classes involved in the land use classification, i.e. arable land (bare soil, crops and temporary grassland), and permanent grassland, were carried out to assure a good spectral separability among categories. These land use classes are defined in articles 18 and 19 of the Swiss ordinance about agricultural terms and exploitation forms (Swiss government, 1998). According to this definition, our final legend was aggregated in the following land use classes: arable land formed by crops and leys (temporary grassland or grassland in rotation), and permanent grassland composed by permanent herbaceous surfaces, meadows and pastures. The separability measurements range from 0 to 2. Values greater than 1.9 imply good separability between classes. Values ranging between 1.7 and 1.9 indicate fairly good separation. Values below 1.7 show poor separation and values under 1.0 suggest that two classes are effectively the same class (Fernandes et al., 2013; García Millán et al., 2014; Iiames et al., 2013; Li et al., 2012).

The JM values were used to define the minimum separability threshold between pair of classes because they were always lower than the transformed divergence values. 1.9 value was considered as a good spectral separability and 1.8 was set as the minimum threshold to exclude classes (Marcheggiani et al., 2008).

Thirty fields were selected to carry out the separability analyses in both images. Crops were identified using an additional image from April to monitor the change in vegetation cover between that month and June and July respectively. Field data was used to select temporary and permanent grassland fields. Bare soil samples, which were derived from Airborne Prism Experiment (APEX) (Schaepman et al., 2015) data close in time to the Landsat images, completed the dataset.

The results of these analyses (section 2.3.2) defined the final land cover classes to carry out the study. The final sample size to train the classifier with the selected classes met the heuristic criterion dependent on the dimensionality of

the input dataset (i.e. the selected Landsat bands) (Mather et al., 2011). Hundred fields were selected to collect, *a posteriori,* polygons (5 pixels) to train and assess the classifier (Congalton, 2001). Two-thirds of the ground dataset collected in total, i.e. 165 sample polygons or 330 pixels were used to calibrate, leaving one third for validation, i.e. 85 sample polygons or 170 pixels (Kotsiantis, 2007).

Urban areas, buildings, forest, and roads at scale 1:25'000 (Swisstopo, 2008) were used to mask out the images avoiding misclassifications and defining the agricultural area. A quarry and a lake were manually digitized and also masked out. The Digital Height Model at scale 1:25'000 (DHM25) (Swisstopo, 2001) was used at 30 m to study topographic effects on the images (Section 2.3.2.1).

#### 2.3.2.3 Accuracy assessment

The overall classification accuracy is commonly expressed as the percentage of the map area that has been correctly classified divided by the total number of validation samples i.e. "ground truth" data (Congalton, 2001). The classification accuracy was estimated with confusion matrices and defined in terms of overall accuracy (OA)

$$OA = \text{TDCM} / \text{TVS}. \quad (1)$$

TDCM is the total value of the diagonal in the confusion matrix and TVS is the total of validation samples. In terms of the Kappa statistic (K) (Congalton, 1991)

$$K = (\text{N} \sum_{\text{i}=1}^{\text{r}} x_{ii} - \sum_{\text{i}=1}^{\text{r}} (x_{i+} * \text{x}_{+\text{i}})) / (\text{N}^2 \sum_{i=1}^{r} (x_{i+} * x_{+i})). \quad (2)$$

where, N is the total number of validation samples, *r* is the number of rows in the confusion matrix, $x_{ii}$ the number of observations in row *i*, and column *i*, $x_{i+}$:marginal total of row *i*, and $x_{+i}$ the marginal total of column *i*. The sampling error (SE) (3) and the confidence interval (CI) at 0.05 significance level completed the validation results (4) (Chuvieco, 2008):

$$SE = \sqrt{\text{OA} * (100 - \text{OA}) / \text{TVS}}, \text{ and} \quad (3)$$

$$CI = \text{OA} \pm (1.96 * \text{SE}). \quad (4)$$

The minimum level of accuracy required in the interpretation of land cover and land use information derived from RS data for planning and management purposes was set between 85 to 90 percent by Anderson (1976). The 85% minimum overall accuracy has been a land cover standard that still used today (Loveland, 2012).

#### 2.3.2.4 Postprocessing: Segmentation

Parcels boundaries were obtained using a multi-resolution segmentation algorithm Definiens V.7.0.1.872 (Definiens, 2007). Three segmentations with different scale parameters (25, 50, and 100) were compared to analyse the sensitivity of the LMM to parcels delineation. The vector layer derived from the classification was used as boundary condition to spatially limit the segmentation process that subdivided each land use unit into parcels. The smoothness and compactness weighting parameters were set to 0.1.

### 2.3.3 Impact of land use information on the land allocation process

The main contribution of remote sensing to the reliability of the LMM is the improvement of the spatially explicit land use map and the subsequent land allocation in the LMM model. The land is now allocated following the land use pattern derived from remote sensing data. This criterion introduces an obvious constraint in land allocation processes: the parcels assigned to a given farm should match exactly the UAA managed by that farm (Kempen et al., 2011). However, the UAA as identified by remote sensing might be close but not exactly the same UAA as stated in the annual farm census data. Therefore, correction factors were introduced separately for arable land and grassland areas to adjust any mismatch. These factors were estimated for each farm separately, comparing the UAA stated in the farm census data for that farm, and the UAA assigned by the land allocation procedure. The factors ($F_c$) will reach a maximum value of 1 only in case of perfect match; otherwise nutrient input and output were rescaled.

$$F_c = UAA_{allocated} \ / \ UAA_{farm\ census.} \quad (5)$$

The term "non-allocated land" is used to define the portion of UAA that the model was not able to assign to any farms.

The effect of land use information on the land allocation process was analysed

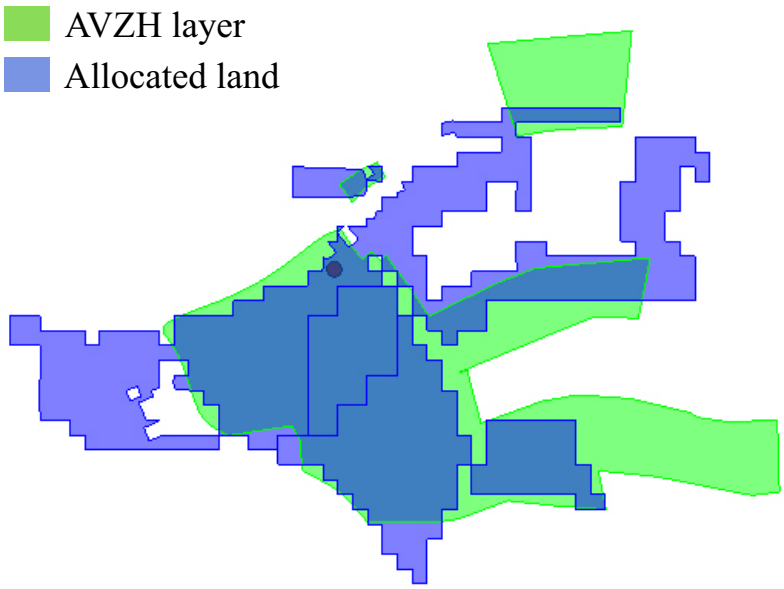


Figure 2.4 Assessment of the land allocation process: detail extracted from the overlapping between the allocated land (in violet) with the AVZH layer (in green) for one farm. The point shows the farm building location.

qualitatively and quantitatively using three different approaches. First, the spatial patterns of land allocation resulted from the LMM with and without information derived from remote sensing sources (i.e., farms census) were compared visually. Second, the effect of choosing different segmentations scales was assessed comparing the percentage of non-allocated land, and the processing time required to run the LMM with each of them. Third, the land allocation maps were compared with a confidential property map provided by the cantonal agricultural agency (AVZH), which is responsible for the annual farm census and the payment of the agricultural subsidies. This layer shows which parcels of land belong to a given property and provides land cover information, albeit incomplete. The property map was used to validate the land allocation map produced by the LMM (Figure 2.4). The two maps were overlaid and the common area (intersection) was computed. The intersection was computed farm by farm and separately for permanent grassland and arable land. The different origin and structure of these datasets made the comparison complicated. In fact, the property of a given field does not necessarily coincide with the management of that field. Thus, a semiautomated procedure and supervision by visual inspection was developed and used to exclude coarse

errors. The distance between the farm building and the land allocated was taken as criteria to rule out unrealistic assignments that could occur while linking the two datasets (allocation maps and land property map). The allocation maps and land property map referred mostly to different information and were differently codified. UAA and livestock number were used as common fields for further comparison. Only 25 farms out of 250 (14% of the total UAA area) could be considered. The accuracy of the allocation map was estimated through an accuracy index (*AI*), *AI* = intersected area / tested area * 100. Four different land allocation maps were assessed: one produced without RS information, and the remaining three produced using the remote sensing data segmented with three different scales.

## 2.4 Results and discussion

### 2.4.1 Land use classification

For satellite images from similar acquisition times, preprocessing steps (atmospheric correction and spatial enhancement) and the spectral separability analyses reduced misclassification issues.

The spectral separability analyses demonstrated that crops and temporary grassland are not distinguishable as part of arable land, with JM values lower than 1.8 (see Table 2.1 and Table 2.2). Consequently, bare soil is considered an indicator of arable land, and differentiated from grasslands in both images acquired in June and July.

Table 2.1 JM separability class pairs. Analysis applied to the Landsat 8 image in June 2014 using 7 bands (thermal and panchromatic not included)

| | Permanent grassland | Temporary grassland | Bare soil | Crops |
|---|---|---|---|---|
| Permanent grassland | | | | |
| Temporary grassland | 1.298 | | | |
| Bare soil | 1.986 | 1.999 | | |
| Crops | 0.945 | 1.066 | 1.999 | |

Table 2.2 JM separability class pairs. Analysis applied to the Landsat 8 image acquire in July 2014 using 7 bands (thermals and panchromatic not included

| | Permanent grassland | Temporary grassland | Bare soil | Crops |
|---|---|---|---|---|
| Permanent grassland | | | | |
| Temporary grassland | 0.822 | | | |
| Bare soil | 1.999 | 1.999 | | |
| Crops | 1.411 | 1.619 | 1.998 | |

The accuracy assessment of the classification suggests that the use of two land cover classifications (bare soil and grassland) from June and July helped generate a land use thematic map of arable land and permanent grassland (see Figure 2.5). The confusion matrices and Kappa statistics are listed in Table 2.3, Table 2.4, and Table 2.5 respectively.

Table 2.3 Confusion matrix for the classification using the image taken in June

| Class | Bare soil | Grassland | Total | User accuracy | Commission error |
|---|---|---|---|---|---|
| Bare soil | 85 | 0 | 85 | 100 % | 0 % |
| Grassland | 2 | 83 | 85 | 97.65 % | 2.36 % |
| Total | 87 | 83 | 170 | | |
| Producer accuracy | 97.70 % | 100 % | | | |
| Omission error | 2.3 % | 0 % | | | |

Table 2.4 Confusion matrix for the classification using the image taken in July

| Class | Bare soil | Grassland | Total | User accuracy | Commission error |
|---|---|---|---|---|---|
| Bare soil | 85 | 0 | 85 | 100 % | 0 % |
| Grassland | 4 | 81 | 85 | 95.29 % | 4.71 % |
| Total | 89 | 81 | 170 | | |
| Producer accuracy | 95.50 % | 100 % | | | |
| Omission error | 4.49 % | 0 % | | | |

Table 2.5 Classification accuracies

| | Overall Accuracy (%) | Kappa statistic | Sampling error | Interval of confidence 95 % |
|---|---|---|---|---|
| June | 98.82 | 0.97 | 0.83 | 97.2-100 |
| July | 97.65 | 0.95 | 1.16 | 95.37-99.92 |

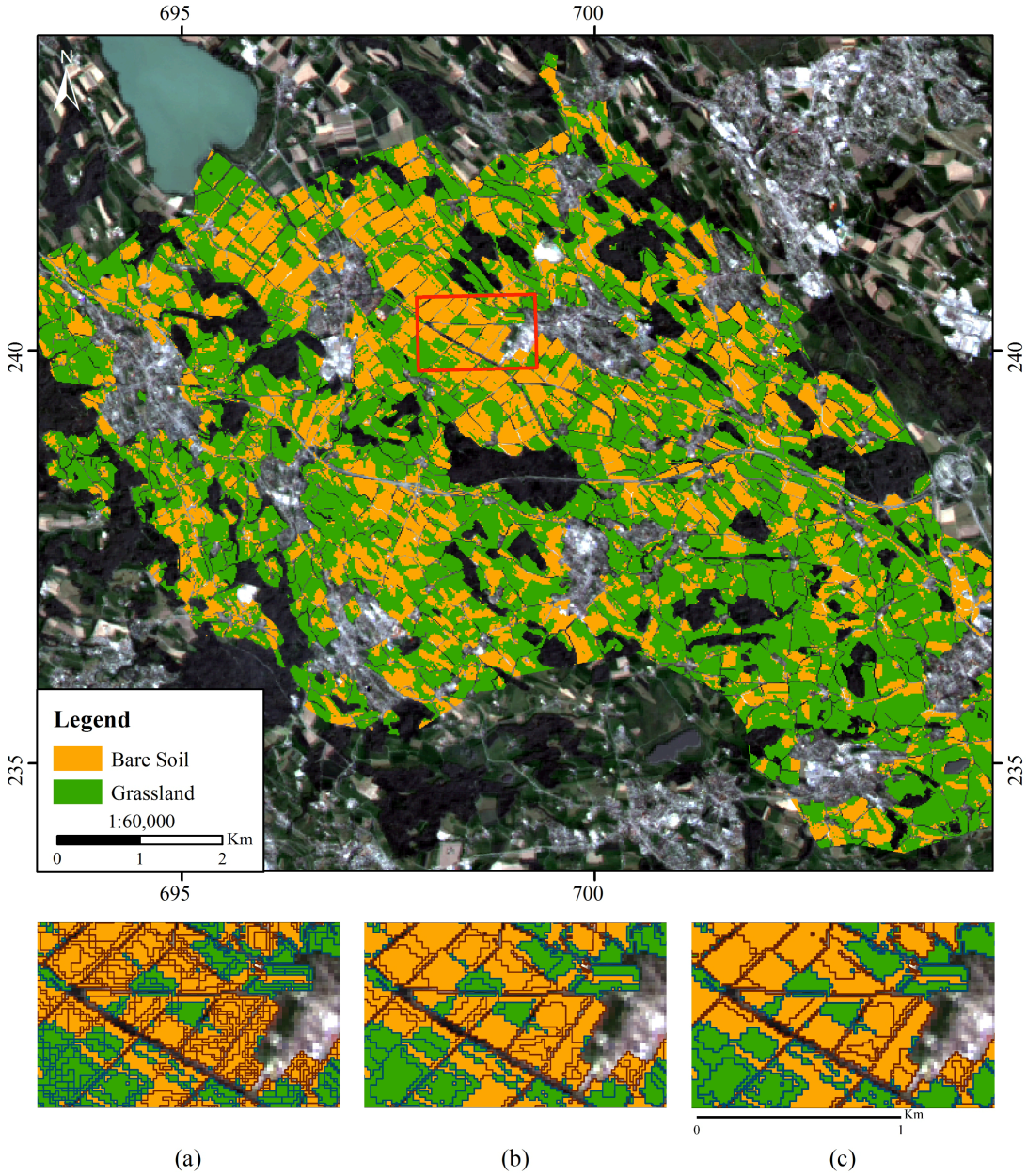


Figure 2.5 Bare soil and grassland differentiation: the upper image shows the bare soil and grassland area differentiate in June and July. On the lower side, there are three details extracted from the classification showing three different segmentations: a) scale 25, b) scale 50 and c) scale 100. Background: Landsat 8 image pan-sharpened (15 m) acquired on July 19th 2014. Path: 194. Row: 27. Coordinate System: CH 1903 LV03.

The classification from June is slightly better than the classification carried out with the image from July, with overall accuracies of 99% and 98% and Kappa coefficients of 0.97 and 0.95, respectively. The Kappa coefficients indicate that the classifications are 97% and 95% better than random chance (Table 2.5).

During the land allocation process, the high classification accuracy ultimately contributed to a low mismatch between the farm statistics and the land use dataset (Section 2.3.3). The accuracy was shown to be an important result due to the land allocation constraints. The *a priori* accuracy considered as a good input for the LMM, i.e. 85-90%, was not enough to achieve a low mismatch (5%) between the amount of UAA indicated in the farm census, with an accuracy of 95-100%, and the UAA obtained with the land use classification. The classification accuracy reached (98-99%) combining two summer images. Selecting land cover classes with high spectral separability resulted in similar UAA between both data sets. The low mismatch avoids introducing coarse errors through factor rescaling.

These classification results are regarded as accurate compared with other studies using the same classifier and similar parameters (Petropoulos et al., 2012; Petropoulos et al., 2011). Presumably, the binary classification contributes to the high performance of the classifier thanks to the high spectral separability between bare soil and grassland (Table 2.1 and Table 2.2). In fact, Knorn et al. (2009) achieved similar accuracies with a binary classification using an SVM classifier and Landsat images.

Overall, the comparison with the UAA gathered from farm census data shows that the classification provided a very good estimate of the available agricultural area (2 ha, 0.05% overestimated). However, arable land is underestimated for about 10% (159 ha), and grassland is overestimated for about 6% (161 ha) using RS (Table 2.6). There was a 4% mismatch in relative terms between the farm census data and the classification derived from RS. The farm census reported 40% of arable land and 60% of permanent grassland for the year 2011, while in the classification from 2014, 36% of the area was labelled as arable land and 64% was assigned to permanent grassland.

Table 2.6 Hectares of arable land, grassland, and agricultural area in two data sets

| Class / Source | Arable land (ha) | Permanent Grassland (ha) | Agricultural area (ha) |
|---|---|---|---|
| Farm census 2011 | 1630 | 2448 | 4078 |
| RS imagery 2014 | 1471 | 2609 | 4080 |

We attribute the overestimation of grassland area to misclassification between cultivated lands, e.g. crops vs. temporary grassland, and permanent grassland. This could not be avoided using only bare soil information from June and July. In Swiss agriculture, temporary grassland in crop rotation is quite important for the production of enough roughage in the winter. Thus, grassland seed combinations for one up to four years are often integrated in crop rotation. The accuracy of the classification might be improved if more than two time steps were considered in the classification algorithm to better distinguish temporary from permanent grassland in crop rotation. Considering the nutrient balances, this issue is quite important, as the temporary grassland is usually managed very intensively, i.e. 5-6 cuttings a year and 5-6 manure applications with biomass yields up to 13 tons dry matter per hectare (below 700 m a.s.l). Permanent grassland can also be used intensively, but in line with integration production programs, grassland systems might also be used moderately intensively or extensively. For instance, in light of the PEP requirements specified above, 7% of the farm area must be used extensively, i.e. only 1-2 cuttings per year without any fertilization.

The accuracy of the classification made it possible to further subdivide the land use units using three different segmentation scales, i.e. 25, 50 and 100 Table 2.5 a, b, and c, respectively). The mean parcel size of arable land resulting from the three segmentation scales was: 0.14, 0.33, and 0.37 ha and the mean parcel size of grassland was: 0.21, 0.72, 0.91 ha for scales 25, 50, and 100 respectively.

### 2.4.2 Impact of land use information on the land allocation process

With regard to the three key components mentioned in the section 2.3.1, implementation of RS techniques improved the land allocation performance. First, the use of spatially explicit information improved the spatial allocation output (Figure 2.6). When the land allocation was performed using only the farm census information, the land distribution followed a radial pattern as shown in

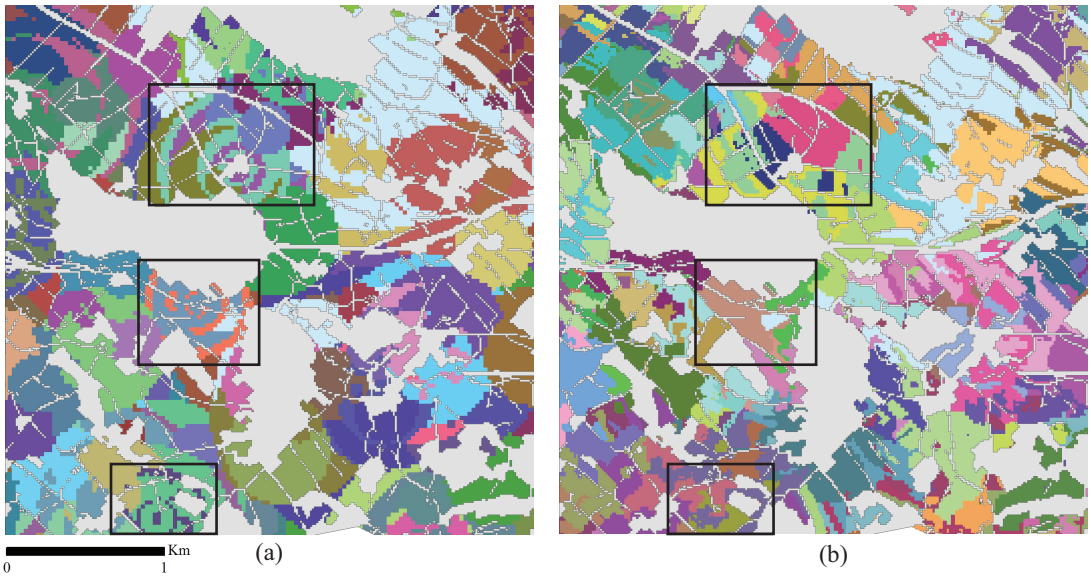


Figure 2.6 Details of the spatial pattern obtained through the land allocation process: a) Using only the farm census data, b) using also land use information. Framed in black in the left image (a), examples of artefacts that disappeared when using land use information (right image, b). Colours represent different ownership.

Figure 2.6(a). Qualitatively, the RS derived thematic map provided a boundary condition in the spatial land distribution, resulting in a pattern that better followed parcel boundaries (Figure 2.6b).

Second, the high classification accuracies ensure consistency with the farm census survey, minimizing mismatches between the data sets.

Third, the use of a suitable spatial unit to define the parcel boundaries influenced the model computation time and the amount of non-allocated land. For segmented field sizes larger than the area given in the reference data set (farm census), the non-allocated land class occurred during the allocation process. Thus, the number of fields or spatial units available to distribute the land depends on the segmentation scale chosen (Table 2.7). Based on image interpretation, the comparison of the three scales, and the land allocation assessment, we selected the segmentation 50 as the best input for the LMM. In addition, the parcel definition obtained with scale 50 represents the best trade-off between the processing time and the non-allocated area. Quantitatively, 67 $km^2$ were processed in 27 min with 4% of non-allocated land. The computing time was reduced by 146 min (85%) on a Intel Xeon CPU, W5590, 3.33 GHz (2 cores) and RAM 24 GB computer compared to the more detailed scale (25) while the amount of non-allocated land remained almost the same (Table 2.7).

Table 2.7 Influence of spatial units on the land allocation process

| Segmentation scale | Number of polygons | Computational time | Non allocated land (ha) |
|---|---|---|---|
| 25 | 23519 | 2h 53min | 164 |
| 50 | 8072 | 27min | 176 |
| 100 | 6820 | 21min | 304 |

These results indicate that the computing time would be greatly reduced when processing large areas. This is the case when the LMM is applied to all Swiss agricultural areas, covering over 14,000 km$^2$, i.e. 200 times the study area.

Assuming a linear increase in processing time with area, the time saving amounts to 29,200 minutes (i.e., > 20 days). However, the processing time of the land allocation grows exponentially, because a squared matrix is used to compute the distance between farms and fields.

The AVZH property map was used to assess the performance of the land allocation procedure. In absence of land use information derived from RS (i.e. using only the farm census data set), the accuracy index of the land allocation procedure was 39% (Section 2.3.3). Nevertheless, when RS-derived land use information was used, the accuracy increased to 51%. In other words, every second farm field can be allocated correctly, while the other fields for a given farm are allocated to the vicinity. In relative terms, the total area correctly allocated increased by 16%. Despite the improvement obtained, these results should be seen as preliminary until a validation data set can be obtained. Nonetheless, these results indicate a substantial positive influence of remotely sensed inputs on the land allocation performance. As mentioned in Section 2.3.3, a persistent problem is that the spatial units of the field ownership do not always correspond to those of the land managed, and vice versa; this complicated our validation efforts.

In this study, multispectral information was selected as the best means for improving the land allocation step. However, the LMM could be further improved with the use of imaging spectrometers. Some studies have demonstrated the potential of these sources for the extraction of biophysical and biochemical parameters from the canopy reflectance (Asner et al., 2002; Kokaly et al., 2009; Ustin et al., 2009). The wavelength range 1,500-1,700 nm helps establish relationships between nitrogen content and management practices, and

simplifies nitrogen concentration estimation, as do wavelengths close to 2,054 and 2,172 nm (Asner et al., 2015; Kokaly, 2001).

## 2.5 Conclusions

This study demonstrates the potential of using land use classification derived from RS data as spatially explicit input for agricultural management models. The LMM output is used for regional sustainable nutrient management and the formulation of related policies. We identified the importance of spatially explicit land use information for more precise allocation of farm practices, and identified three parameters that most influence the land allocation performance: spatial resolution, parcel definition, and classification accuracy. Pan-sharpened Landsat 8 OLI data made detailed parcel delineation possible, enabling the assignment of farm census data to specific fields and leaning to an improved land allocation pattern. During image segmentation, the selection of an appropriate spatial unit made it not only possible to reduce computation time, but also to substantially decrease the non-allocated land. The optimal processing cost for an area of 67 $km^2$ was established as 27 min, with a residual of 4% non-allocated land. Finally, the high classification accuracy reduced the mismatch with the farm census data set, increasing the reliability of data assigned to each field for further nutrient balance estimation. Overall, the integration of remote sensing data and derived products improved the performance of the land allocation process, by 16%. We hypothesize that the use of more advanced methods such as imaging spectroscopy would further improve the assessment of detailed fertilization practices and, in turn, help improve agricultural management estimates beyond the scope of the results presented here.

## Acknowledgements

This study is part of the "Integrated Modelling framework to monitor and predict trends of agricultural management and their impact on Soil functions at multiple scales" (iMSoil, project number 406840-143062) funded by the Swiss National Science Foundation within the National Resource Program NRP68 "Sustainable Use of Soil as a Resource (www.nfp68.ch). The Swiss Earth Observatory Network (SEON) provided airborne data. The contribution of M.E.S. is supported by the University of Zurich Research Priority Program on "Global Change and Biodiversity". We especially wish to thank the three anonymous reviewers for their valuable contributions, which highly improved the paper. We also thank Adrian Schubert for his additional comments as proofreader.

# Chapter 3

# Determination of Grassland Use Intensity Based on Multi-temporal Remote Sensing Data and Ecological Indicators

This chapter is based on:

Gómez Giménez, M., de Jong, R., Della Peruta, R., Keller, A., and Schaepman, M.E. (2017). Determination of grassland use intensity based on multi-temporal remote sensing data and ecological indicators. *Remote Sensing of Environment, 198*, 126-139. https://doi.org/10.1016/j.rse.2017.06.003

Authors' contributions: All authors designed the study, MGG, RDP, AK collected the data, MGG, RdJ, MES developed the methodology, MGG, RDP performed the analysis, MGG, RdJ, MES wrote the manuscript.

## Abstract

Grassland use intensity and its impact on biodiversity and water pollution is a topic of growing interest. In ecological studies, intensity of use has been assessed by means of three indicators: i) mowing frequency, ii) grazing intensity, and iii) fertilization input. A multidimensional approach is key for the understanding of intensification effects in terrestrial and water ecosystems. Remote sensing is a powerful tool to monitor management indicators. However, interdependencies between remote sensing methods and between indicators require new approaches to assess intensity of use. The objective of this study is to monitor ecological indicators of land use intensity based on multispectral imagery using a multidimensional approach. We performed a multi-temporal analysis using a series of RapidEye images within a growing season in the Canton of Zurich, Switzerland, in 2013. We defined mowing frequency classes distinguishing spectral changes between pairs of images. The analysis of the whole image sequence within the growing season helped differentiate grazing intensities. Furthermore, we analysed the suitability of modelled livestock density based on remote sensing derived products to determine fertilizer input. Three grassland management practices were distinguished: i) medium intensive (46%), ii) low intensive (37%), and iii) high intensive (17%). We discuss the combination of high mowing frequency and fields with high grazing intensity to define areas prone to nutrient surpluses. Finally, we demonstrate that the estimation of interrelated indicators of grassland use intensity could be carried out preserving independence between methods.

**Keywords:** Grassland use intensity, remote sensing, RapidEye, ecological indicators, mowing frequency, grazing intensity, fertilizer input, livestock density.

## 3.1 Introduction

Land management aiming at increasing the yield of the same area frequently results in land use intensification (Lambin et al., 2000). Also in Switzerland, agriculture and, especially, grassland management was progressively intensified since 1950 (Jeangros et al., 2004; Spiess, 2011). Permanent grassland covers ca. 59% of the agricultural area (Jeangros et al., 2004). Its predominant land uses are meadows, used for mowing or fodder production, and pastures, used for grazing or livestock farming (Bötsch, 2004). High nitrogen (N) input derived from manure and high livestock density has produced excess of nutrients into the soils (FSO, 2015). Since the mid-1990s, the Swiss Agricultural Policy has been dedicated to mitigate the effects of management intensification (FOAG, 2004). As a result, nutrient surpluses have been reduced by 27% (Spiess, 2011).

Land use intensification processes have implications at different spatial scales. Local and landscape changes, e.g., homogenous landscapes promoting farm efficiency and habitat fragmentation respectively, affect biodiversity world wide (Tscharntke et al., 2005). Nevertheless, there is a lack of suitable datasets to assess the effects of land use intensity globally (Kuemmerle et al., 2013). Remote sensing methods allow monitoring the spatio-temporal evolution of management indicators at different scales (Kuemmerle et al., 2013; Zaks et al., 2011). However, in Switzerland, grassland use intensity is recommended to be adjusted to local conditions to foster steady species richness (Jeangros et al., 2004). Therefore, local studies are relevant to understanding how to monitor indicators of grassland use intensity by using remote sensing data.

In ecological studies, grassland use intensity has been assessed by means of multi-temporal analysis of indicators: i) mowing frequency, ii) grazing intensity, and iii) fertilization input (Blüthgen et al., 2012; Socher et al., 2013; Socher et al., 2012). The integration of these indicators is of major relevance for the understanding of land use change effects (Erb et al., 2013), such as loss of biodiversity or water pollution (Kleijn et al., 2009; Kleijn et al., 2003; Matson et al., 1997).

The remote sensing community has widely assessed individual ecological indicators of intensity of use. For instance, mowing and grazing intensities have

been classified using leaf area index (LAI) (Dusseux et al., 2014; Numata et al., 2007). Fertilization management practices have been linked to leaf chlorophyll content (LCC), serving as an indicator of nitrogen status or content (N) (Clevers et al., 2013; Filella et al., 1994; Ramoelo et al., 2012). Equally, both traits LAI and LCC have been extensively linked to multispectral vegetation indices (VIs) using bands in the same spectral range (e.g., red edge) (Adjorlolo et al., 2014; Asam et al., 2013; Delegido et al., 2013). VIs account for vegetation greenness to which chlorophyll content largely contributes as well as LAI especially in certain wavelengths (Haboudane et al., 2004). Furthermore, same ancillary data can provide information to quantify different indicators. For example, livestock density has been not only used as quantifier of nutrient input (Herzog et al., 2006) but also of grazing intensity (Blüthgen et al., 2012). Interrelationships between indicators of intensity are also expected due to combined management practices such as mowing frequency and application of fertilizers (N inputs) (Flisch et al., 2009; Herzog et al., 2006).

Recently, Asam et al. (2015) and Franke et al. (2012) have classified grassland intensity of use using LAI and VIs based on RapidEye images. The RapidEye satellite constellation has a high temporal and spatial resolution (5 days and 5 m respectively) suitable for monitoring management practices, but low spectral resolution (5 bands). Their results showed the potential of multispectral imagery to monitor, assess, and quantify indirectly singular indicators of grassland use intensity (Asam et al., 2015; Franke et al., 2012). Quantification of individual indicators has been widely used to establish links between land use intensity and its effects on biodiversity and water quality (Herzog et al., 2006). However, there is a need to integrate these indicators to account for the multidimensional nature of land use intensity (Erb et al., 2013; Kuemmerle et al., 2013).

This study tries to bridge the gap between new ecological frameworks to assess land use intensity and remote sensing techniques. The specific goals are: i) estimate indicators of grassland use intensity based on multispectral imagery, ii) seek independence between methods to derive unique information from each indicator, and iii) integrate indicators to distinguish areas affected by high levels of intensity of use.

## 3.2 Methods

### 3.2.1 Study area

The study area is located in the Swiss Plateau within the Canton of Zurich (47.25° – 47.34° N, 8.68° – 8.84°E), Switzerland (Figure 3.1). The area is characterised by mean precipitation rates of 1134 mm per year with a wet season occurring from May to August and yearly average temperatures of 9.3 °C (Meteoswiss, 2015b).

The study site is an agroecosystem with a high presence of permanent grassland (ca. 60%) (Gómez Giménez et al., 2016). The total extent is about 67 $km^2$ placed at 556 m above sea level (a.s.l.). The study area and the local scale were selected for three reasons: i) farmers manage grassland at different intensities based on local conditions such as topography and soil type (Jeangros et al., 2004), ii) the study area was located in a well-known agroecosystem where we could better understand how indicators of grassland use intensity may interact, iii) the remote sensing data covering the study area was minimally affected by atmospheric issues.

Grazing and mowing were the main management practices observed during a field campaign accomplished in 2014. Farmers reported that in areas with high intensity of use grazing practices were combined with four to five cuts during the growing season followed by manure application. In case farmers promoted extensive practices (one or two cuts per year) to receive subsidies, fields were not mown until 15 June as mandated by Swiss regulations (Swiss government, 2013). The most common management practices in the area were around three to four mowing events combined with grazing practices. Livestock grazed in a stepwise manner. This means that farmers fenced the fields in small stripes where livestock grazed during two or three days and then moved to another fraction of the field in order to protect the soil from trampling. In more intensively used areas farmers cut the remaining patches of grassland to homogenise the field after grazing.

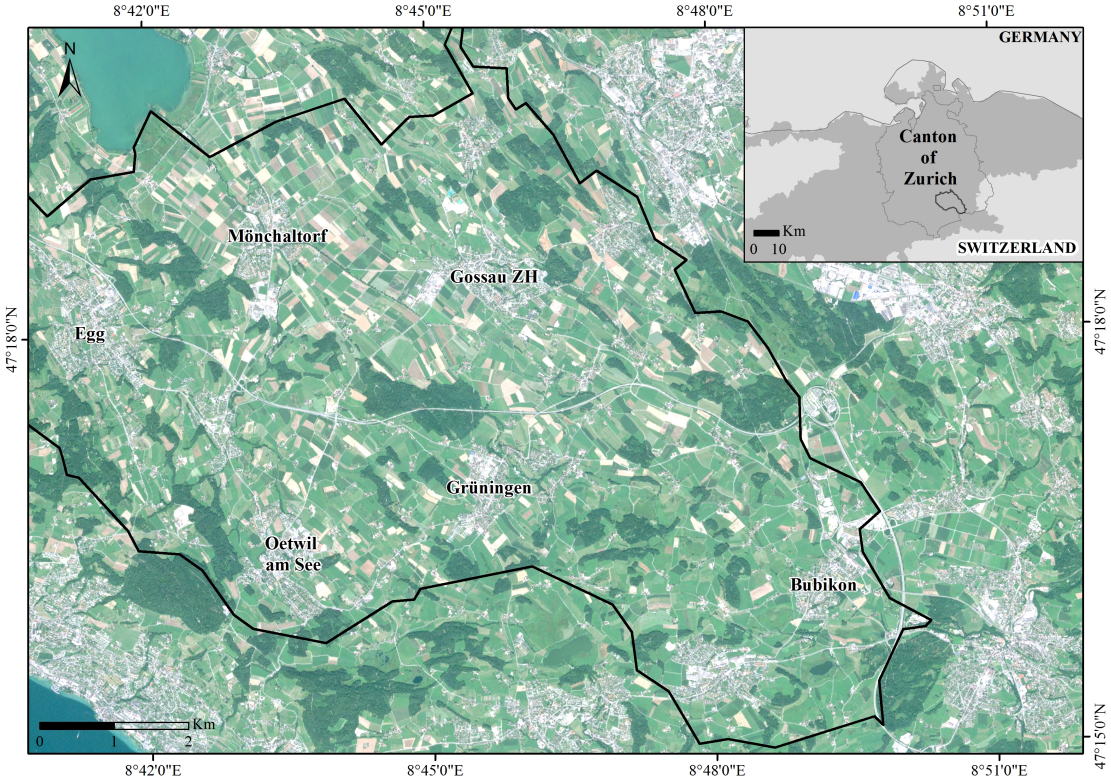


Figure 3.1 Outline of the study area and administrative boundaries located in the Canton of Zurich. The area is limited on the left by the satellite acquisition path. The map inset shows the location of the study site (black line) within the Swiss Plateau (dark grey) and the Canton of Zurich (grey border). Background data: RapidEye image acquired on August 2, 2013.

### 3.2.2 Overview

The overview of the analyses carried out is shown in Figure 3.2. Five calibrated RapidEye images (Section 3.2.3) were used to differentiate spatial units of grassland (Section 3.2.4). Spectral changes of the grassland units contributed to define a mowing frequency index. The mowing frequency index combined with the multi-temporal spectral mean of grassland units resulted in the output mowing frequency classes (Section 3.2.5). The datasets grassland units and its spectral mean were used for computing a coefficient of variation (*CV*). The result was nominally divided statistically with a K-means algorithm. On the other hand, the spectral mean was nominally divided to define levels of intensity. The statistical analysis of how both nominal variables were related to each other resulted in the output grazing intensities (Section 3.2.6). Finally, we analysed the suitability of modelled livestock density as an indicator of fertilization input. The dataset grassland units and the input farm census were used in a model to obtain the output livestock density (Section 3.2.7).

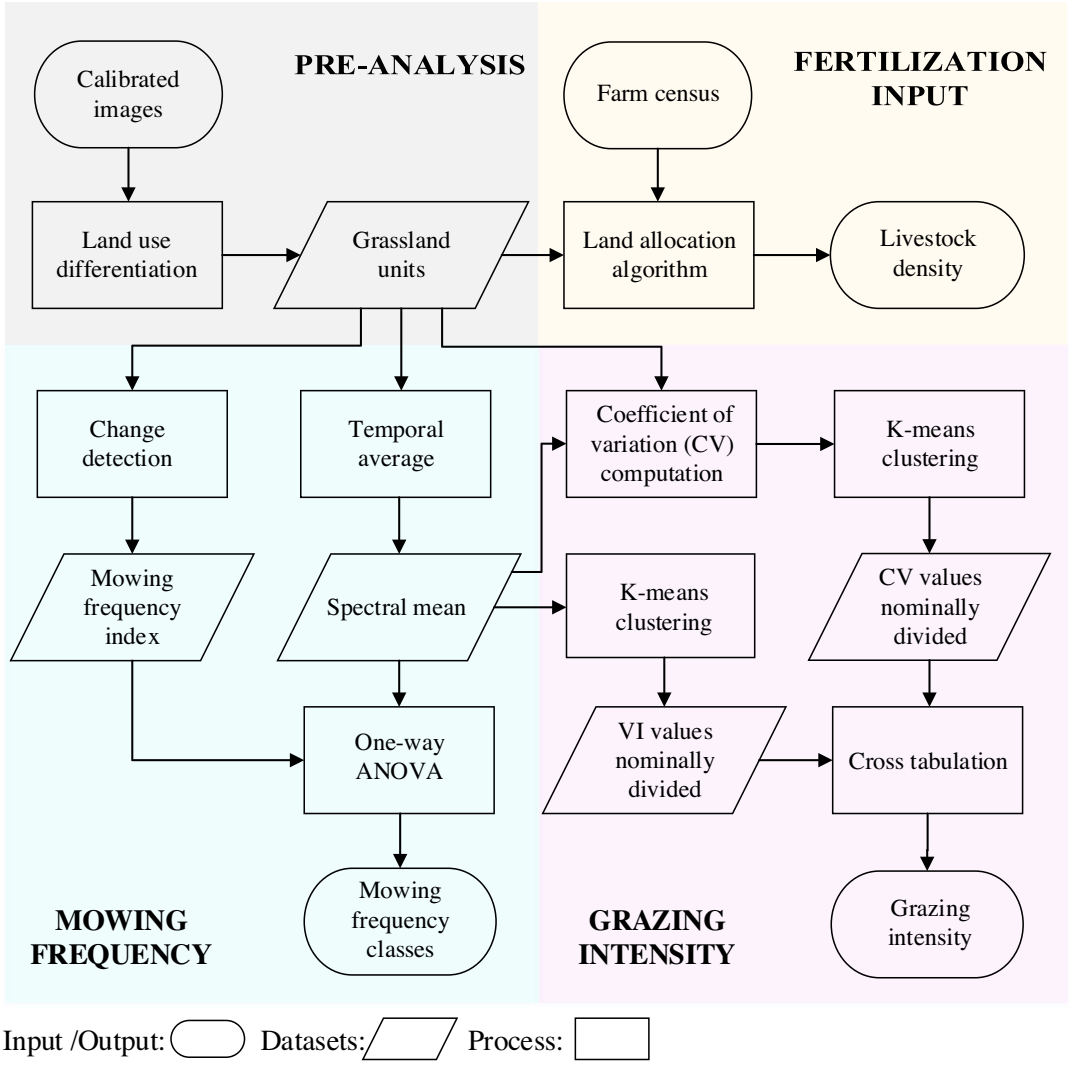


Figure 3.2 Workflow of the analysis.

### 3.2.3 Preprocessing

Five orthorectified RapidEye images (processing level 3A), (Blackbridge, 2015) were acquired on April 24, May 8, June 8, July 15, and August 2, 2013. RapidEye imagery features a red edge band (690-730 nm) within the total spectral range (440-850 nm) and has a high spatial resolution for land-use planning purposes, rendering the data well suited for the small farm sizes (ca. 18 ha.) as found in our study area. Selected images are the best available acquisitions within the study time frame and had a variable percentage of cloud coverage: 1%, 12%, 4%, 12%, and 0%. The image acquired in June (5m-pixel size) showed some signs of haze.

Change detection analyses require image pre-processing approaches to ensure physical consistency and guarantee suitable comparisons of time series. Pre-

processing steps include: i) geometric correction, ii) compensation of atmospheric effects to estimate surface reflectance, iii) topographic correction, and iv) radiometric normalisation among images (Vicente-Serrano et al., 2008). Consequently, the applicability of each component of the pre-processing chain was studied for implementation.

Geometric quality of the orthorectified RapidEye images was compared and checked visually using orthophotos acquired on April 17 and June 13, 2013 (Swisstopo, 2013); no further geometric corrections were applied. Atmospheric effects were compensated in all the images using ATCOR-2 based on a rural aerosol model for flat areas (Richter et al., 2004). Topography was characterised using the SwissALTI3D Digital Elevation Model (DEM) (Swisstopo, 2015) and found to have a minimal influence with very low average slope angles (≤ 9%). A topographic correction was therefore not implemented. A global nadir normalisation was performed in all the images using ATCOR-2 (Richter et al., 2004) to minimise varying illumination angle effects, different viewing geometries among images (across-track incidence angle), and varying across-track instantaneous field of view (IFOV) at angles >20° (RapidEye FOV = ±25°) (Konstanski et al., 2015). Radiometric normalisation was performed using iteratively re-weighted multivariate alteration detection (IR-MAD) identifying invariant features between pairs of images (Nielsen, 2007). IR-MAD is comparable with manual and time-consuming feature selection processes (Canty et al., 2004). This technique has been seldom implemented (Coppin et al., 2004). However, Schroeder et al. (2006) pointed out the reasons why MAD algorithm should be preferred rather than other traditional methods. All resulting images were normalized using a band-by-band approach. Paired *t-test* for equal mean and *F-test* for equal variance (Canty et al., 2008) quantified normalisation results (Supporting information, Tables S1-S4).

### 3.2.4 Selecting permanent grassland units for change detection.

Permanent grassland is defined in article 19 of the Swiss ordinance about agricultural terms and exploitation forms (Swiss government, 1998). The term refers to grasslands that have existed in that form at least during six years and include permanent meadows and permanent pastures. Other land-cover/ use

classes including: buildings, forest, roads, streets, lakes, a quarry, and swamps were masked out in all images using ancillary data (Swisstopo, 2008, 2014). Clouds and shadows were also masked out in all images by visual inspection. After the masking process only bare soil (defined as arable land with no vegetation cover under tillage or fallow land) and vegetation cover remained as land cover classes in the study area.

Field boundaries were used as minimum units (polygons) to analyse how spectral changes in permanent grassland evolved. All the images were segmented individually using a multi-resolution segmentation algorithm (Definiens V.70.1.872), (Definiens, 2007). Image segmentation clusters groups of pixels spectrally similar using spatial criteria including scale (number of pixels per object), and shape object characteristics, e.g., smoothness and compactness (Desclée et al., 2006). Segmentation was carried out in a chronological stepwise approach (from April to August, i.e., from lower to higher mowing frequency), and using two vector layers as spatial constraints, i.e., the layer obtained from segmenting previous images and another with roads (Swisstopo, 2008). Segmentation overlapped sequentially provided spatial consistency to analyse the same spatial units on all the images.

Polygons with vegetation cover and bare soil obtained from each image were spectrally distinguished using a $VI_{\text{red edge}}$ ranging from -1 to 1 (Equation 1). The red-edge VI has been reported as highly correlated to canopy structure (Delegido et al., 2013). Therefore, this index is expected to be highly sensitive to changes caused by management practices.

$$VI_{red\ edge} = \frac{Red\ edge - Red}{Red\ edge + Red} \quad (1)$$

Spectral thresholds for differentiating permanent vegetation cover were determined through visual inspection using reference fields. Spectral responses were not strongly affected by phenology but for management practices such as grazing and mowing. Continuous seasonal development is characteristic of semi-natural and managed grasslands as well as grasslands during the wet season (Esch et al., 2014; Numata et al., 2007). By contrast, natural grasslands normally follow natural phenological conditions (Esch et al., 2014). In the study area, we

could see phenological effects in some natural-protected grasslands (*Naturschutzgebiet*) during a field campaign. Therefore, we recorded the location of these fields and exclude them from the analysis in order to avoid misclassifications between images.

The five binary vector layers with vegetation cover and bare soil were merged and classified as arable land and permanent grassland as proposed by Gómez Giménez et al. (2016). The land-use class defined as permanent grassland was compared with available data from a farm census (FOAG, 2015a). The combination of vector layers from five images acquired at different dates during the growing season helped characterise the agricultural area.

### 3.2.5 Mowing frequency

#### 3.2.5.1 Change detection

Image differencing is one of the most commonly used change detection algorithms (Coppin et al., 2004). The implementation of this method and interpretation of results is straightforward and performs better than other bi-temporal algorithms (Lu et al., 2004; Singh, 1989). We used a bi-temporal standardized image differencing algorithm (Equation 2) to account for relative changes ($Ch_t$) (Coppin et al., 1994).

$$Ch_{t1,2} = \frac{VI_{red\ edge\ (t2)} - VI_{red\ edge\ (t1)}}{VI_{red\ edge\ (t2)} + VI_{red\ edge\ (t1)}} \quad (2)$$

Where $VI_{red\ edge}$ is the average vegetation greenness per polygon; t2 refers to the image acquired later in time, e.g. May; t1 refers to the image acquired earlier in time, e.g. April.

Bi-temporal image differencing techniques frequently rely on the assumption that data is normal distributed. In areas of no change, pixels resulting from images subtraction have values close to zero. Changes are defined with thresholds based on standard deviations from the mean (Cakir et al., 2006). Therefore, data distribution was checked between pairs of images (data not shown). Descriptive statistics: central tendency measures, box-plots, Q-Q plots, Kolmogorov-Smirnov test, and standardized kurtosis and skewness were calculated to characterise the distribution of the resulting differencing image.

### 3.2.5.2 Defining thresholds of change

A two-step thresholding approach was implemented because of asymmetries in the data distribution (Mas, 1999; Pu et al., 2008; Sinha et al., 2013). The distribution was split in two parts from the mean: decreasing and increasing values. We used a 5% trimmed mean, which trims off the 5% of the upper and lower values of the probability density function, and percentiles 95 and 5 (Figure 3.3). The use of these limits in the distribution guaranteed that outliers do not affect the definition of thresholds that could underestimate negative and positive changes. Means and standard deviations of each range were calculated to establish negative (Equation 3) and positive changes (Equation 4, Figure 3.3).

$$Thres_d = \bar{x}_d - c * \sigma_d \quad (3)$$

$$Thres_i = \bar{x}_i + c * \sigma_i \quad (4)$$

Where *Thres* $_d$: threshold of the decreasing range, $\bar{x}_d$: mean of the decreasing range, $\bar{x}_i$: mean of the increasing range, c: constant value defining the distance from the mean of the whole distribution, $\sigma_d$: standard deviation of the mean in the decreasing range, *Thres* $_i$: threshold of the increasing part, and $\sigma_i$: standard deviation of the mean in the increasing range.

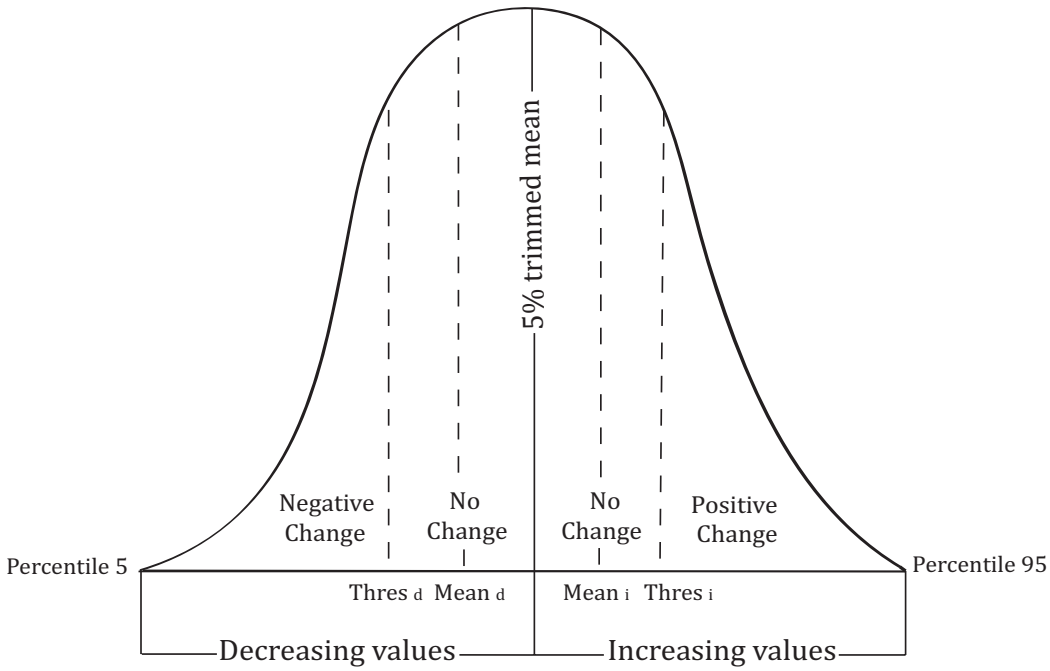


Figure 3.3 Thresholding scheme (notation: Mean $_d$ equals $\bar{x}_d$ and Mean $_i$ equals $\bar{x}_i$).

Studies splitting the distribution in two ranges to define thresholds of change usually follow a test and error approach with different constant values. Therefore, we checked the sensitivity of classes of change to different constant values: 1, 1.5, and 2 standard deviations from the $Mean_i$ and $Mean_d$. In the image pair April-May, using a constant value equals 1.5 the user accuracies in the classes negative change and no change were slightly higher than those obtained with 1 (1% and <1% respectively). A constant value of 2 diminished the user accuracies by 8% and 3% in the classes no change and positive change respectively and they increased in the class negative change (4%), all with respect to the accuracies resulting from a value of 1. In the pairs of images May-June and June-July, the highest user accuracies were obtained using a constant value of 1 for all the classes. In the pair July-August, a constant value equals 1.5 reached lower user accuracies in the classes negative change (<4%) and no change (<3%) and higher in the class positive change (>2%) than using a value of 1. In contrast with results obtained with a value of 1, the user accuracies decreased in the class negative change (2%) and increased in the classes no change (1%) and positive change (4%) using a constant value of 2 (Supporting information, Tables S5-S16). All in all, one standard deviation was chosen for the remaining analysis as the most reliable constant to achieve high overall accuracies for all pairs of images (Section 3.3.3.2 and Supporting information, Tables S17 and S18). Further, Mas (1999) and Pu et al. (2008) have obtained good results using a constant of one.

*3.2.5.2.1 Accuracy assessment*

False colour image composites and NDVI (Normalized Difference Vegetation Index) composites have been used in studies based on a two-step thresholding approach to delineating validation samples using visual inspection (Pu et al., 2008; Sinha et al., 2013). Following a similar approach, bi-temporal composites of $VI_{\text{red edge}}$ images were checked to define positive change, no change, and negative change (Figure 3.4a). However, visual inspection of randomly selected samples introduced an unquantifiable bias in each comparison because defining from which colour tonality a change should be considered was tricky. As a result, a standard approach to assessing the definition of thresholds was carried out

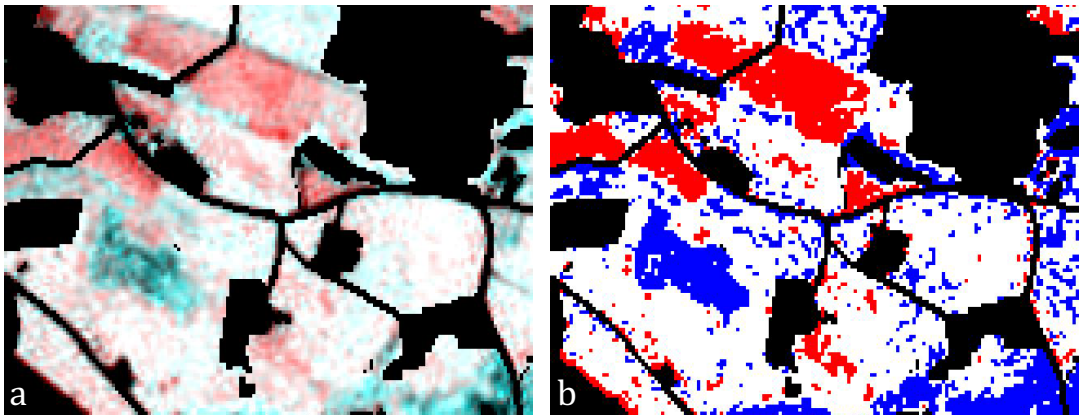


Figure 3.4 a) Detail of the bi-temporal VI $_{\text{red edge}}$ composite: image acquired on April 24, 2013 (red channel). Image from May 8, 2013 (green and blue channels); b) Detail of the ISODATA classification carried out over the bi-temporal standard differencing image using the images acquired on April 24, 2013 and May 8, 2013. Blue colours are positive changes, white colours no change and red colours are negative changes. In black are all the land cover/use classes excluded from the analysis.

using an unsupervised ISODATA algorithm. Ten iterations were used to reach convergence of cluster centres and a stable classification result (Figure 3.4b).

The sample size was estimated using a multinomial distribution equation (Equation 5). Only polygons with areas equals or higher than 225 m$^2$ (3x3 kernel, 5m pixel size) were considered (Congalton et al., 1998).

$$n = \frac{B* \Pi_i \, (1- \Pi_i)}{b_i^2} \tag{5}$$

B: was determined from a Chi-square table with one degree of freedom and $\chi^2 = \alpha/k$; $\alpha = 0.05$; $k$: number of classes in the classification, i.e. three (positive change, no change, negative change); $\Pi_i$: proportion of a population in the ith class. A worst-case scenario with 50% of the area cover of one single class was considered, $b_i = \alpha$.

The major class of change found per polygon was used to compute the assessment. The results were reported in terms of overall accuracies (OA), confusion matrices, and kappa statistics to establish the degree of agreement between the definition of thresholds of change and the ISODATA classifications (Congalton, 1991). Sampling error and confidence intervals were also reported.

### 3.2.5.3 Mowing frequency index

Following Otto et al. (2007), the beginning of the growing season was defined as the first day with a minimum temperature higher than 5°C. The end of the

growing season was the first day with a minimum temperature below 5°C. Accordingly, the growing season of grasslands in the study area for 2013 was defined from February to November. This is in line with the standard growing season defined for grasslands in Switzerland (Flisch et al., 2009).

In Switzerland, intensive grasslands can be mown five or six times per year (Flisch et al., 2009). The first cut in grasslands with high intensity of use is before flowering. In contrast, extensive grasslands are cut for first time late in the growing season (Jeangros et al., 2004). Consequently, the earlier negative changes in vegetation greenness (mowing events) occurred, the higher the expected intensity of use. On the contrary, positive changes (vegetation regrowth) or no changes (stable) in vegetation greenness early in the growing season indicated low intensity of use. Accordingly, weights were assigned to change events based on the observed date. The beginning of the growing season (February) was set to one and the end of the growing season (November) was set to zero. The average of the day of the year (DOY) between pairs of images and the corresponding weight were estimated through a linear function (Table 3.1) (further information is provided in the Supporting information, Assignment of weights).

Table 3.1 Weights assigned according to extensive management during the growing season. The mean day of the year (DOY) indicates the midpoint between the dates of observation and serves as estimate of the change date.

| Months | DOY | Mean DOY | Weight |
|---|---|---|---|
| February | 32 | | 1 |
| April | 114 | 73 | 0.85 |
| May | 128 | 121 | 0.67 |
| June | 159 | 143.5 | 0.59 |
| July | 196 | 177.5 | 0.47 |
| August | 214 | 205 | 0.37 |
| November | 305 | | 0 |

The moment within the growing season when spectral changes were observed was used to define the mowing frequency index. First, the type of change between pairs of images was defined. Second, weights were assigned to changes according to the date when they were observed. Third, weights were aggregated through the four stages of change: April-May, May-June, June-July,

and July-August. The aggregated weight provided the mowing index. For instance, a positive change observed in a polygon in May received a weight of 0.67, a no change observed in June: 0.59, a positive change observed in July: 0.47, and a negative change observed in August: -0.37 (Table 3.1). The resulting mowing index for this polygon was 1.36 (0.67 + 0.59 + 0.47 – 0.37) (Table 3.2). The index was useful to cluster groups of polygons according to their spectral pattern observed between pairs of images.

Table 3.2 Mowing frequency index. The arrows indicated if positive changes i.e., vegetation regrowth, (↑), no changes i.e., stable (→), or negative changes i.e., mowing events (↓) in vegetation greenness occurred.

| Change detection | | | | Mowing Index |
|---|---|---|---|---|
| 24 April — 8 May | 8 May — 8 June | 8 June — 15 July | 15 July — 2 August | |
| ↑ | → | → | → | 2.1 |
| → | → | ↑ | ↓ | 1.36 |
| ↑ | → | ↓ | → | 1.16 |
| → | ↓ | ↑ | → | 0.92 |
| ↓ | ↑ | → | → | 0.76 |
| → | → | ↓ | ↓ | 0.42 |
| → | ↓ | ↑ | ↓ | 0.18 |
| ↓ | ↑ | → | ↓ | 0.02 |
| → | ↓ | ↓ | → | -0.02 |
| ↓ | ↑ | ↓ | ↑ | -0.18 |
| ↓ | ↓ | ↑ | ↑ | -0.42 |
| ↓ | ↑ | ↓ | ↓ | -0.92 |
| ↓ | ↓ | ↑ | ↓ | -1.16 |

We estimated a temporal mean using the $VI_{\text{red edge}}$ values per polygon averaged through all the images ($\overline{VI}_{\text{red edge}}$). $\overline{VI}_{\text{red edge}}$ values were nominally divided in low, medium, and high through a K-means clustering algorithm with a maximum number of ten iterations, and 0.5 percentage of change allowed among clusters centres to converge. The mowing index legend was divided in three classes of mowing frequency, i.e. high, medium, and low, according to $\overline{VI}_{\text{red edge}}$ via a one-way ANOVA test. A one-way ANOVA test was performed to reduce arbitrariness dividing mowing frequency classes. Since $VI_{\text{red edge}}$ is an indicator of canopy

structure (Section 3.2.4), high $\overline{VI}_{\text{red edge}}$ values are expected to indicate low mowing frequency classes because of homogeneous vegetation greenness during the season. Low $\overline{VI}_{\text{red edge}}$ values are expected to represent areas with high fluctuations in vegetation greenness due to high mowing frequency. Therefore, medium $\overline{VI}_{\text{red edge}}$ values are assumed to occur in fields with moderate mowing frequency. Robust tests of equal means (Welch and Brown-Forsythe) were used to find significant differences among groups because the data did not follow a normal distribution. The Tukey HSD's test was carried out to report which groups were statistically significantly different (Supporting information, Table S19). Finally, summarising the relationship between mowing frequency classes and $\overline{VI}_{\text{red edge}}$ values via cross tabulation helped us understand the impact of these mowing events in terms of canopy status within the monitoring time. Chi-square tests and Cramer's V tests for nominal variables were carried out to check significance among clusters and association between variables.

*3.2.5.3.1 Accuracy assessment*

The suitability of the mowing frequency approach was compared with growing degree-days (GDD) based on the closest meteorological station (< 20 km, Fluntern, Zurich) to the study area in 2013 (Equation 6), (McMaster et al., 1997).

$$GDD = \left[\frac{(T_{max}+T_{min})}{2} + T_{base}\right] \quad (6)$$

Where $T_{max}$ is the maximum temperature per day and $T_{min}$ the minimum. $T_{base}$ is the minimum temperature from which plant growth is considered.

We chose standard values provided in Otto et al. (2007). GDD provided information about the date when a potential mowing event may occur according to the amount of times that a field could be mown within the growing season (usually 1 to 5 in that area). The expected cutting dates were compared with the mowing frequency classes defined.

### 3.2.6 Grazing intensity

Grazed fields could be differentiated using the $CV$, (Equation 7).

$$CV = \frac{\sigma}{\overline{VI}red\ edge} * 100 \quad (7)$$

$\sigma$: Standard deviation of the average $VI_{\text{red edge}}$ per polygon and image from the temporal average, $\overline{VI}_{\text{red edge}}$: temporal average through all the images.

Grazing has a similar effect on grasslands but is generally carried out in an extensive and gradual fashion compared to mowing. In contrast with the mowing frequency approach, the $CV$ provided information of the whole sequence of images instead of pairs. Since grazing practices are generally carried out in a low intensive fashion, we expected that low $CV$ values were mostly related to grazing practices. In case of more intensive use practices, farmers cut the remaining grassland patches to homogenise the field and this would be identified as a mowing event (Section 3.2.1).

$CV$ values were nominally divided in low, medium, and high through a K-means clustering algorithm with a maximum number of ten iterations, and 0.5 percentage of change allowed among clusters centres to converge. Even though grazing practices were related to low $CV$, these fields should not be considered as an indicator of high management intensity *per se* without characterising the practices along the growing season. Grazing intensities: low, medium, and high, could be distinguished statistically via cross tabulation between $CV$ and $\overline{VI}_{\text{red edge}}$ values after being nominally divided (Section 3.2.5.3). Chi-square tests and Cramer's V tests for nominal variables were carried out to check significance among clusters and association between variables respectively.

#### 3.2.6.1 Accuracy assessment

The expected relationship between low $CV$ values and grazing areas was validated using GPS points from a field campaign carried out in 2014. 30 fields characterised as home pasture (permanent grazing areas next to the farm building) were compared with fields with low $CV$ values.

The level of intensity was compared with 22 fields identified as extensive grassland during the field campaign. Additionally, 285 polygons indicating extensive meadows, and 20 extensive pastures were analysed to characterise their spectral response (non-public dataset provided by a cantonal agency, AVZH). 1048 polygons resulted from intersecting the AVZH layer and the permanent grassland layer in the study area (967 meadows and 81 pastures). Polygons with areas equal or higher than 2000 $m^2$ were selected to avoid small

polygons that were not representative of the land management type in the field: 508 extensive meadows and 75 extensive pastures.

### 3.2.7 Fertilization input

In remote sensing studies, livestock density has been mainly quantified through GPS tracking (Rinella et al., 2011; Swain et al., 2011), unmanned aerial vehicles (UAVs) (Rango et al., 2011), modelling farm census data (Robinson et al., 2014), and estimating the distance to grazing hotspots or water sources (Manthey et al., 2010; Sanderson et al., 2010). In this study we modelled livestock densities as stated in a farm census available each year (FOAG, 2015a).

Livestock density is an important factor when addressing nutrient pollution. Areas with high livestock numbers likely receive high amount of manure whereby they are prone to nutrient surpluses (Sanderson et al., 2010). Hence, livestock density was used as a proxy of elevated soil nutrient concentration.

Livestock density per grassland field was estimated through a land allocation algorithm (Gärtner et al., 2013) using the farm census of 2013 (FOAG, 2015a) and the layer of permanent grassland. We used 800 $m^2$ as minimum grazing area according to Swiss regulations (Swiss government, 2013). The number of animals per farm stated in the farm census was allocated to the farm fields (Gärtner et al., 2013) considering the area of grassland belonging to each farm and not the whole farmland. The range of livestock units (LU) was established based on Swiss guidelines for nutrients balance (AGRIDEA et al., 2015); LU/ha≤ 1: fields with low livestock density and extensive management, 1 >LU/ha< 2: medium livestock density with moderate management, and LU/ha≥ 2: high livestock density with intensive practices. Correlations between livestock density values and $\overline{VI}_{\text{red edge}}$ values were checked in order to establish a link between nutrient inputs and the spectral response.

## 3.3 Results

### 3.3.1 Preprocessing

The best radiometric normalisation results were achieved using the image acquired in August (Supporting information, Table S1-S4). Nevertheless, normalising issues and some atmospheric effects that were not completely

removed with the atmospheric compensation could be the causes of mean values slightly deviated from zero after images subtraction (Table 3.3).

### 3.3.2 Selecting permanent grassland units for change detection

The total area of permanent grassland was 2,472 ha, which was similar to the area reported in the farm census of 2013: 2,435 ha (-37 ha). The total amount of spatial units obtained from the segmentation process was 6197 polygons.

### 3.3.3 Mowing frequency

#### 3.3.3.1 Change detection

All the pairs of images showed a nearly normal distribution but all of them were skewed. We identified outliers as changes in management and differences in shadows cast by forest areas. Similar results for the mean, 5% trimmed mean, median, and mode including and excluding outliers indicated minimal effect of outliers on the data distribution (Table 3.3). Thus, outliers were neither removed nor truncated to avoid removing significant information about management practices and increasing artificially the number of values in the tails of the distribution. This would have affected the definition of thresholds of change. False alarms caused by shadows were avoided with a buffer of 30 m around forest areas.

Table 3.3 Descriptive statistics of pairs of standardize differencing images.

| Statistics | May — April | | June — May | | July — June | | August — July | |
|---|---|---|---|---|---|---|---|---|
| | Outliers | No outliers | Outliers | No outliers | Outliers | No outliers | Outliers | No Outliers |
| Mean | 0.063 | 0.061 | -0.067 | -0.067 | 0.024 | 0.024 | 0.009 | 0.011 |
| 5% trimmed mean | 0.062 | 0.061 | -0.066 | -0.066 | 0.023 | 0.024 | 0.010 | 0.011 |
| Median | 0.061 | 0.061 | -0.054 | -0.055 | 0.021 | 0.021 | 0.007 | 0.008 |
| Mode | 0.048 | 0.048 | 0.14 | 0.14 | 0.002 | 0.0022 | -0.026 | -0.026 |
| Standard skewness | 12.35 | 0.62 | -11.2 | -11.7 | 0.2 | 1.95 | -4.15 | 1.95 |
| Standard kurtosis | 53.97 | 4.05 | -9.08 | -12.5 | 6 | -5.48 | -0.38 | -0.85 |

### 3.3.3.2 Defining thresholds of change

Thresholds of change are shown in Table 3.4 using a constant value equals one.

Table 3.4 Thresholds of change. (Decr: decreasing; Incr.: increasing, SD: standard deviation).

| | Whole distribution | | Decr. Part | | Incr. Part | | | |
|---|---|---|---|---|---|---|---|---|
| Stages of change | 5% trimmed mean | SD | Mean | SD | Mean | SD | Threshold Decr. Part | Threshold Incr. Part |
| April—May | 0.062 | 0.065 | 0.026 | 0.027 | 0.1 | 0.028 | -0.001 | 0.127 |
| May—June | -0.066 | 0.099 | 0.141 | 0.048 | -0.003 | 0.038 | -0.189 | 0.035 |
| June—July | 0.023 | 0.091 | -0.033 | 0.040 | 0.082 | 0.041 | -0.073 | 0.123 |
| July—August | 0.010 | 0.094 | -0.049 | 0.041 | 0.074 | 0.044 | -0.090 | 0.117 |

The images resulting from the standard differencing process reached 80% concordance with the ISODATA classifications, also in line with similar studies (Mas, 1999). Results were 70% better than chance agreement based on Kappa statistics (Table 3.5). Confusion matrices (Supporting information, Tables S5-16) revealed that the class no change was the most problematic to be distinguished in terms of user accuracy.

Table 3.5 Classification accuracies of classes of change (thresholds defined with a constant of 1).

| Time steps | Overall Accuracy (%) | Kappa Statistic | Sampling Error | Interval of confidence 95% |
|---|---|---|---|---|
| April—May | 79.19 | 0.69 | 1.67 | 75.91-82.46 |
| May—June | 79.70 | 0.70 | 1.65 | 76.45-82.94 |
| June—July | 82.23 | 0.73 | 1.57 | 79.15-85.31 |
| July—August | 77.50 | 0.66 | 1.72 | 74.13-80.86 |

### 3.3.3.3 Mowing frequency index

Three statistically significantly different classes resulted from the one-way ANOVA test (Table 3.6). The upper end of the mowing index values (2.1 and 1.36) was defined as low mowing frequency, the middle range as moderate mowing frequency, and the lower range (-0.42 to -1.16) as high mowing frequency classes.

Table 3.6 Mowing frequency classes characterised with the mean and standard deviation of $\overline{VI}_{\text{red edge}}$. Classes statistically significantly different at a 0.05 level.

| Mowing frequency | Number of polygons | Mean | Standard deviation |
|---|---|---|---|
| Low | 4426 | 0.6735 | 0.0583 |
| Moderate | 1745 | 0.6678 | 0.0445 |
| High | 26 | 0.6346 | 0.0471 |
| Total | 6197 | 0.6718 | 0.0549 |

$\overline{VI}_{\text{red edge}}$ values ranged from 0.404 to 0.840 and were defined with a K-means algorithm in three ranges: low, $\overline{VI} \leq 0.621$ (1027 polygons, 17%), medium, $0.621 \geq \overline{VI} \leq 0.693$ (2885 polygons, 46%), and high, $\overline{VI} \geq 0.694$ (2285 polygons, 37%). The results from the cross tabulation between the mowing frequency and the $\overline{VI}_{\text{red edge}}$ clusters characterised high and moderate mowing frequencies by medium $\overline{VI}_{\text{red edge}}$ values (Table 3.7). Low mowing frequencies were mainly represented by medium and high $\overline{VI}_{\text{red edge}}$ values. Pearson Chi-square test indicated significant association between the indicators (p-value < 0.05), although the strength of this association was weak, Cramer's V = 0.112.

Table 3.7 Cross tabulation between mowing frequency and clusters of $\overline{VI}_{\text{red edge}}$ values defining low, medium, and high ranges.

| Mowing frequency | $\overline{VI}_{\text{red edge}}$ clusters | | | Total |
|---|---|---|---|---|
| | Low | Medium | High | |
| Low | 690 | 1552 | 1584 | 3826 |
| Moderate | 329 | 1316 | 700 | 2345 |
| High | 8 | 17 | 1 | 26 |
| Total | 1027 | 2885 | 2285 | 6197 |

The results from estimating GDD showed that in areas with high intensity of use the first cut is early in the growing season, and in fields with low intensity of use this occurs later. The images acquired on 8 May and 8 June were useful to identify early changes. The image acquired the 2 August provided also useful information to find areas with low intensity of use. The expected cuts at the beginning and ending of the growing season matched with high and low mowing frequency classes defined (Table 3.8 and Figure 3.5).

Table 3.8 Expected mowing dates according to GDD and the potential number of cuts carried out in that region. The difference in days from the expected mowing event and the date of the next image acquired is indicated in brackets.

| Date cuts / Num. cuts | 1st cut | 2nd cut | 3rd cut | 4th cut | 5th cut | Others |
|---|---|---|---|---|---|---|
| 1 | 7 Sep 2013 | | | | | |
| 2 | 19 Jun 2013 | 1 Aug 2013 | | | | |
| | (Δ26 days) | (Δ1 day) | | | | |
| 3 | 27 May2013 | 28 Jun2013 | 1 Aug 2013 | | | |
| | (Δ12 days) | (Δ17 days) | (Δ1 day) | | | |
| 4 | 27 May2013 | 28 Jun 2013 | 17 Jul 2013 | 25 Aug 2013 | | |
| | (Δ12 days) | (Δ17 days) | (Δ16 days) | | | |
| 5 | 27 May2013 | 28 Jun 2013 | 1 Aug 2013 | 25 Aug 2013 | 5 Oct 2013 | |
| | (Δ12 days) | (Δ17 days) | (Δ1 day) | | | |
| >5 | 4 May 2013 | 7 Jun 2013 | 5 Jul 2013 | 27 Jul 2013 | 25 Aug 2013 | 19 Oct 2013 |
| | (Δ4 days) | (Δ1 day) | (Δ10 days) | (Δ6 days) | | |

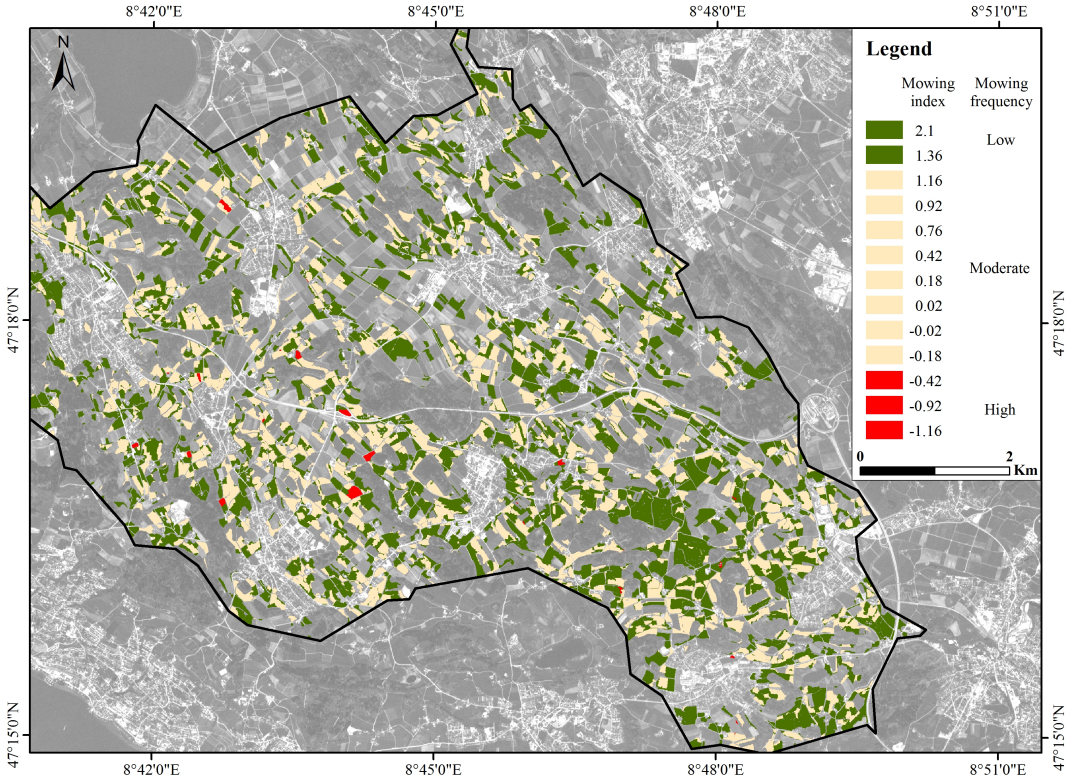


Figure 3.5 Mowing index and mowing frequency intensity levels. Background data: RapidEye image acquired on 24 April 2013; image displayed in grey scale and transparency 50%.

### 3.3.4 Grazing intensity.

The $CV$ values defined with a K-means algorithm ranged from 3.6 to 34 and were divided as low, $CV \leq 10.596$ (2491 polygons, 40%), medium, $10.599 \geq CV \leq 16.647$ (2421 polygons, 39%), and high, $CV \geq 16.653$ (1285 polygons, 21%).

23 out of 30 fields identified as home pasture had low $CV$ values. Five out of 30 fields reached medium $CV$ values and only two out of 30 fields had high $CV$ values. Therefore, the expected relationship between grazing practices and low $CV$ values could be confirmed. As a result, low $CV$ values were identified as grazing areas (Figure 3.6).

The independent dataset acquired from a field campaign indicated that 64% of the fields identified as extensive areas reached high $\overline{VI}_{\text{red edge}}$ values. According to the AVZH dataset, extensive meadows mostly reached high $\overline{VI}_{\text{red edge}}$ values (47%) followed by medium (44%), and low values (9%). The analysis of extensive pastures revealed that 53% reached medium $\overline{VI}_{\text{red edge}}$ values, 33% high, and 13% low values.

The results from the grazing areas defined with low $CV$ (home pastures, 2491 polygons) reached mainly high $\overline{VI}_{\text{red edge}}$ values (1204 polygons, 48%), followed by medium $\overline{VI}_{\text{red edge}}$ values (874 polygons, 35%) and low $\overline{VI}_{\text{red edge}}$ values (413 polygons, 17%). Pearson Chi-Square test indicated a significant association between $\overline{VI}_{\text{red edge}}$ and $CV$ (p-value < 0.05), but the Cramer's V symmetric measure showed that this association was weak, i.e., 0.173.

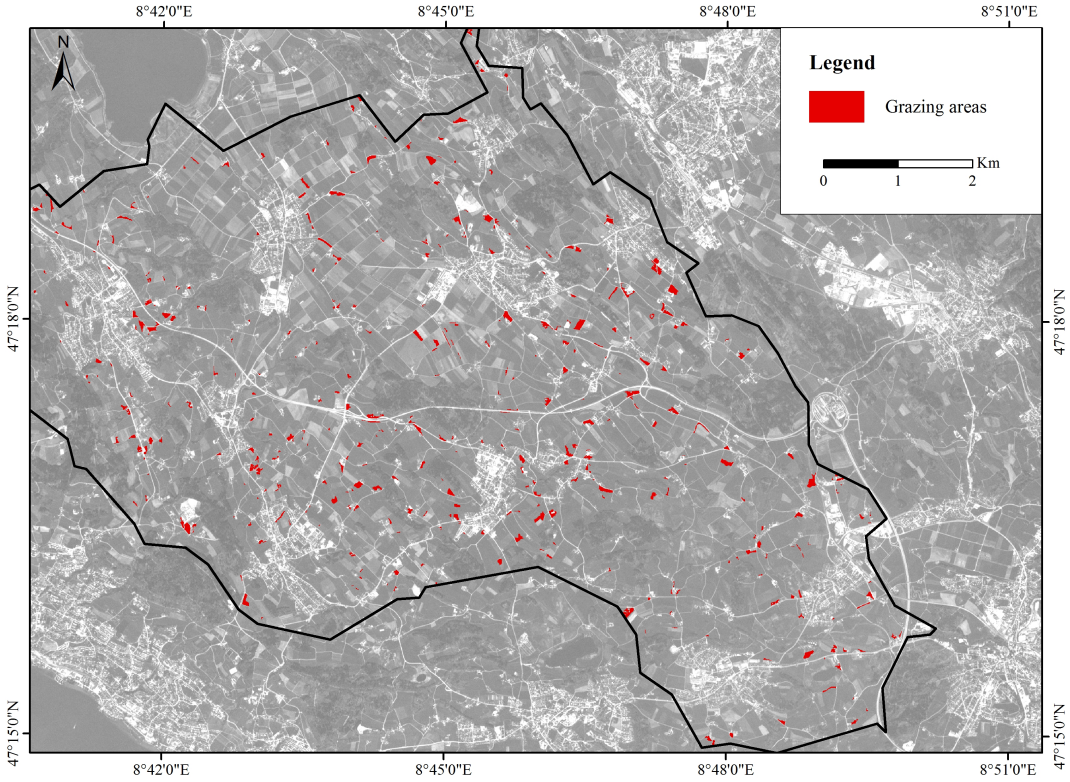


Figure 3.6 Grazing areas. Background data: RapidEye image acquired on 24 April 2013; image displayed in grey scale and transparency 50%.

### 3.3.5 Fertilization input

Livestock density as stated in the farm census was allocated to the farmland based on the grassland units (Section 3.2.7). No correlation was found between allocated livestock density (Figure 3.7) and $\overline{VI}_{\text{red edge}}$ values (Figure 3.8). High $\overline{VI}_{\text{red edge}}$ values indicate low intensity of use, medium $\overline{VI}_{\text{red edge}}$ values show medium intensities, and low $\overline{VI}_{\text{red edge}}$ values indicate high intensities. Pearson's correlation = -0.038 (statistically significant with p-value < 0.05). Therefore, no impact of livestock density on the spectral response of the vegetation was found. Consequently, the suitability of livestock density as an indicator of nutrient input could not be demonstrated.

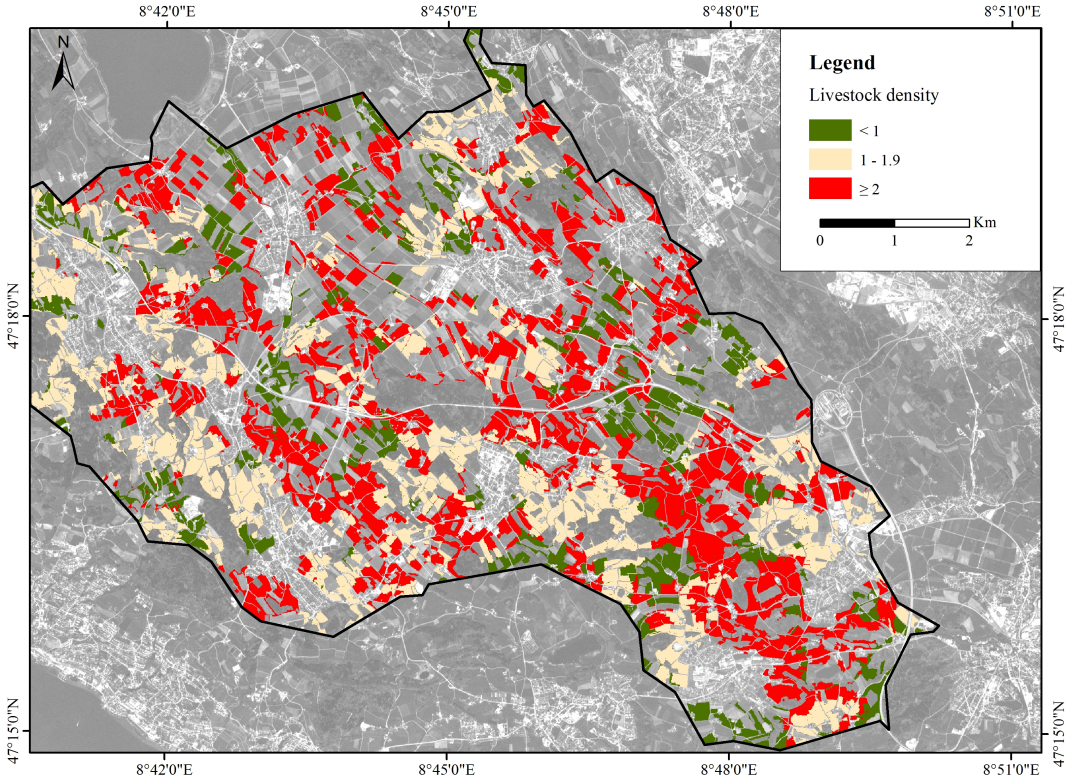


Figure 3.7 Livestock density. Background data: RapidEye image acquired on 24 April 2013; image displayed in grey scale transparency 50%. Units: livestock count / ha.

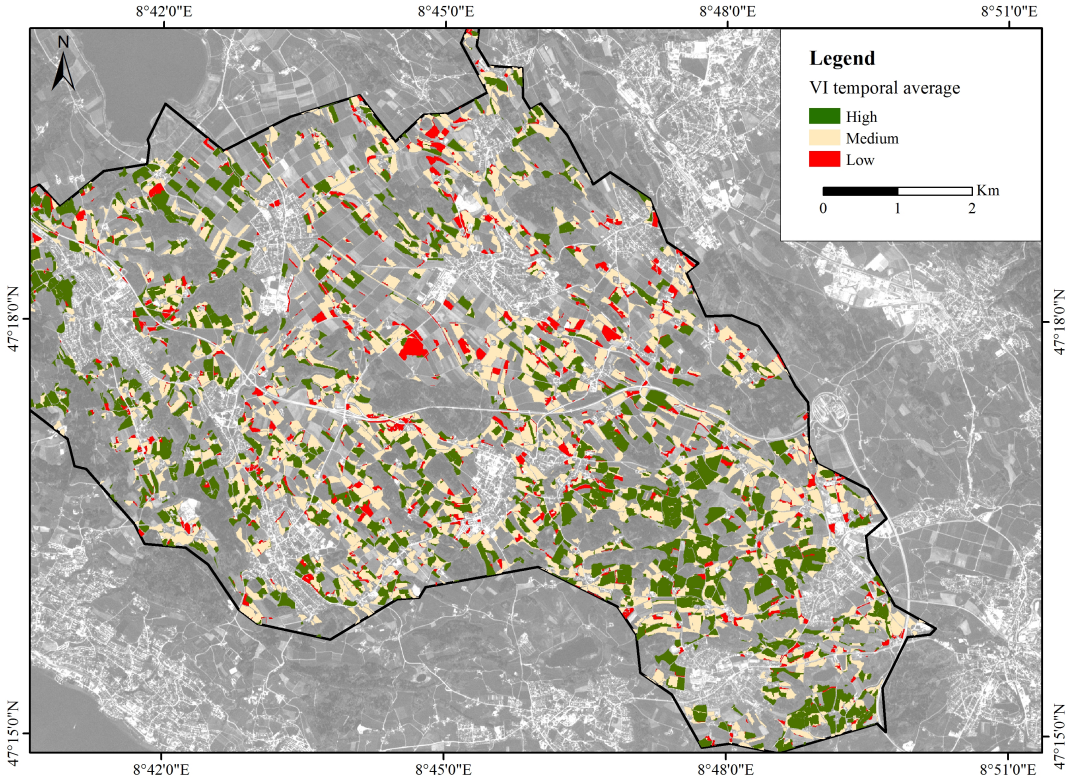


Figure 3.8 $\overline{VI}_{\text{red edge}}$ values. Background data: RapidEye image acquired on 24 April 2013; image displayed in grey scale and transparency 50%.

## 3.4 Discussion

### 3.4.1 Change detection and thresholds of change

The good overall agreement between the definition of thresholds of change and unsupervised classifications shows that this type of classification is a fast method to obtain change detection results. Nevertheless, we emphasise that methods accounting for asymmetries in the data distribution can play a relevant role in the results when strong asymmetries are present. Positive asymmetries were observed when a high percentage of fields between a pair of images presented growing vegetation or vegetation regrowth that increased vegetation greenness. We observed negative asymmetries when most of the fields between a pair of images were mown.

### 3.4.2 Mowing frequency, grazing intensity, and fertilization inputs

The comparison between the mowing frequency index and the GDD show the plausibility of the method applied. Chi-Square tests indicated significant relationships between $\overline{VI}_{\text{red edge}}$ values and mowing frequency classes as well as between $\overline{VI}_{\text{red edge}}$ and $CV$ values. However, Cramer's V measures indicated that the strength of these associations was weak in both cases. These results imply that the relationships between these variables were not exactly as expected. For example, fields with high mowing frequency mostly reached medium $\overline{VI}_{\text{red edge}}$ values (Table 3.7) and fields with high grazing intensity mainly obtained high $\overline{VI}_{\text{red edge}}$ values (Section 3.3.4).

According to the $\overline{VI}_{\text{red edge}}$ values observed in independent datasets recording management practices (Section 3.3.4), high $\overline{VI}_{\text{red edge}}$ values were related to extensive practices, especially extensive meadows. However, these values decreased to medium $\overline{VI}_{\text{red edge}}$ range for extensive pastures. Heterogeneous canopies caused by grazing may produce lower spectral means than homogeneous canopies found in meadows. Nevertheless, it is interesting to observe that grazing areas defined with low $CV$ values and identified as home pastures mainly reached high $\overline{VI}_{\text{red edge}}$ results. We presume that those fields next to the farm building generally receive high amounts of manure.

In this study, the amount of grassland units identified as extensive meadows

was higher than extensive pastures, 92% and 8% respectively (Section 3.2.6.1). Hence, we consider that high $\overline{VI}_{\text{red edge}}$ values are representative of low intensity of use. Moreover, high $\overline{VI}_{\text{red edge}}$ were in line with spectral values for healthy managed grasslands (Morawitz et al., 2006). Medium $\overline{VI}_{\text{red edge}}$ values were characteristic of values reported for grasslands in normal conditions of water and nutrients (Gu et al., 2007), or managed and well preserved grasslands (Poças et al., 2012). As a result, these values indicate management practices with medium intensity of use. Low $\overline{VI}_{\text{red edge}}$ values were similar to those observed in frequently grazed and mown grasslands (Dusseux et al., 2014). Consequently, we assign these values to high intensity of use. According to the levels of intensity of use, the management practices in the area were: i) medium intensive (46%), ii) low intensive (37%), and iii) high intensive (17%), (Section 3.3.3.3).

On one hand, seasonal patterns of VIs in extensive and intensive areas show spectral values within the same range as well as reaching similar maxima in particular during the summer season (Franke et al., 2012; Metzger et al., 2016). VIs sensitive to biomass and chlorophyll content such as $\text{VI}_{\text{red edge}}$ may saturate in fields with different fertilization strategies at similar development stages (Hollberg et al., 2017). This could result in spectral responses in areas with high intensity of use such as home pastures reaching high $\overline{VI}_{\text{red edge}}$ values.

On the other hand, the suitability of $\overline{VI}_{\text{red edge}}$ values to determine levels of intensity of use and by contrast the weak associations found with mowing frequencies as well as with *CV* values, indicate that vegetation greenness could be providing additional information about management practices such as fertilization inputs. Furthermore, we argue that accounting for the importance of the moment when a mowing event occurs within the growing season provides information about grassland growing rate and canopy recovery. Following this reasoning, we expect that high $\overline{VI}_{\text{red edge}}$ values found in fields with high mowing frequency and high grazing intensity to be indicators of high nutrients input. These fields are prone to nutrient surplus whereby vegetation growth may be boosted and strong spectral response driven by high N content may be observed. As a result, we defined areas prone to nutrient surplus as those fields with high and medium-high mowing frequency classes (two and three cuts, from -1.16 to 0.42, see Table 3.2) with medium and high $\overline{VI}_{\text{red edge}}$ values.

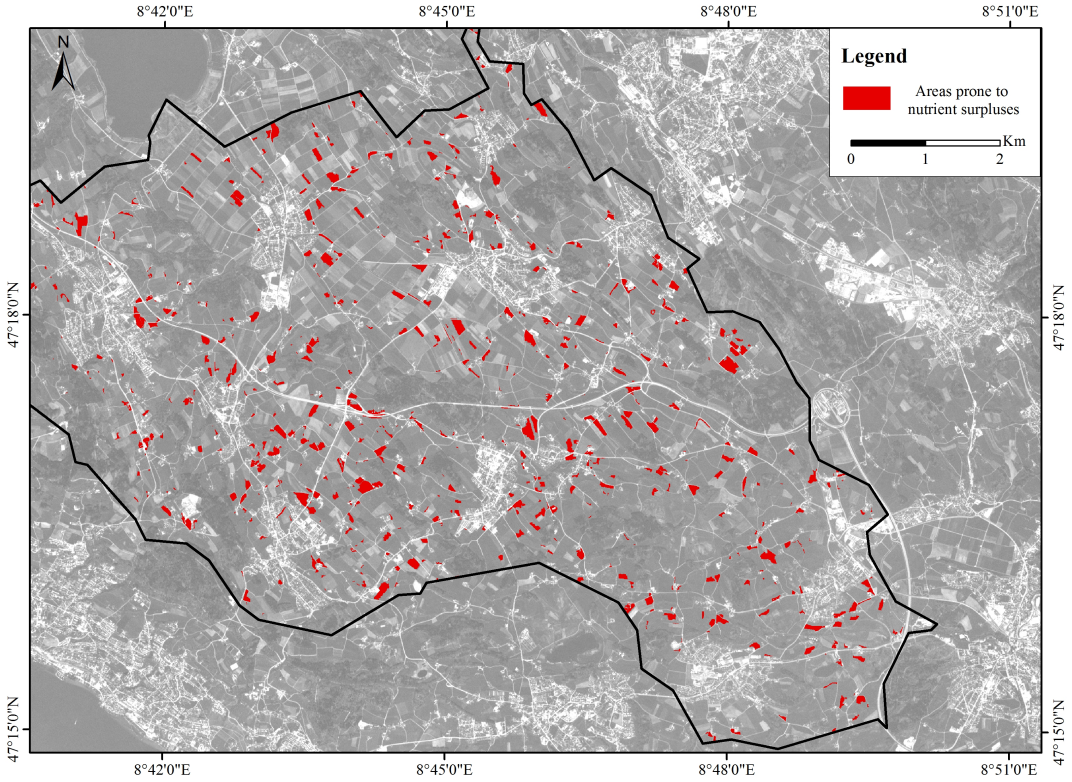


Figure 3.9 Areas prone to nutrient surplus. Background data: RapidEye image acquired on 24 April 2013; image displayed in grey scale and transparency 50%.

Additionally, we included areas with low $CV$ (mostly observed as grazed areas), and low $\overline{VI}_{\text{red edge}}$ values (indicator of high frequency of use). These fields represent 12% of the total area (Figure 3.9).

### 3.4.3 Limitations and outlook

Change detection analyses of vegetation cover are affected by phenology and climate, apart from scene dependent issues, which have been already addressed. Blooming effects could be identified as a mowing event in case of long gaps between image dates. In this study, frequent image acquisition covering the blooming period at the beginning of the growing season minimised this type of misclassification between pairs of images. However, in areas with high blooming effects we recommend analysing in detail their impact on the results. Other areas that may cause misclassifications are unmanaged natural protected areas and swamps. There is no high spatial resolution cartography of swamps but they were not representative of our study area due to their small size. On the other hand, we recommend the use of standard approaches to assess changes because visual interpretation of randomly selected samples may produce biased results.

The methodology proposed accounts for the potential number of cuts carried out in a field based on observing a mowing event within the growing season. Classification analyses highly rely on the number and date of the images acquired (Asam et al., 2015; Franke et al., 2012), which may be a limiting and bias factor in cloud prone areas. Nevertheless, the beginning and ending of the growing season were crucial to defined mowing frequency classes.

The use of a standard constant to define thresholds of change that achieves good accuracy results and avoids large iterations is key to standardize the methodology and upscale it to larger areas. Additionally, we provided statistically significantly different variables that could be implemented in rule-based classification approaches to standardize the definition of branches in decision tree algorithms. On the other hand, a higher density of images with higher spatial resolution would contribute to a more accurate definition of grazing practices. We emphasise the potential of new sensors such as Sentinel-2A/2B (launched in June 2015 and March 2017 respectively) to extrapolate this analysis to larger areas. The Sentinels constellation has a revisiting time of five days and 13 spectral bands. Spatial resolution varies from 10 m (visible and near-infrared bands) to 20 m (red-edge/shortwave-infrared bands) and 60 m (three atmospheric correction bands). Once operational, these sensors will be a relevant source of remote sensing data to transfer the proposed methods.

Further work is required to assess livestock density as a reliable indicator of nutrient input. Information about the real amount of livestock per field, the period of time that animals graze, and the total amount of manure applied per field, would help quantify how these factors contribute to nutrient surplus at field scale. Furthermore, information about manure trading, soil type, and nutrient fluxes into the soil should be taken into account to avoid over- or underestimating nutrient surpluses at farm level. Environmental models are able to integrate interrelated inputs and we highlight them as important tools to monitor nutrient balance in agroecosystems. Spatial information of grassland use intensity will help modellers to quantify regional nutrient budget in agroecosystems.

## 3.5 Conclusions

We demonstrated the potential of multispectral imagery to analyse and monitor grassland intensity of use within new ecological frameworks. Monitoring abrupt changes between pairs of images contributed to define mowing frequency classes. Accounting for the importance of the moment when a mowing event occurs within the growing season provided the methodology with certain independence on the number of images acquired. However, the acquisition time was crucial. In particular, we highlighted the relevance of the beginning and ending of the growing season. On the other hand, we showed that analyses of the whole sequence of images help distinguish grazing practices.

Livestock density proved ambiguities because of no correlation with the spectral response. Hence, we could not prove the suitability of allocated livestock density as proxy of fertilizer input. We emphasised the need of further research to define reliable independent indicators of fertilizer input, more validation datasets, as well as, information about soil type, and nutrient fluxes into the soil. In that sense, we pointed out models as powerful tools to integrate multiple datasets.

All in all, the straightforward methodology applied could be adapted to study intensity of use at larger scales and different years via remote sensing data. In particular, we point out the Sentinel constellation as relevant source of remote sensing data to transfer the proposed methods. Therefore, indicators of intensity of use could be characterised in areas with limited ancillary information. Additionally, we presented statistically significantly different variables that could be used as part of rule-based classification algorithms in a more standard fashion. We think that common approaches will lead to a better interdisciplinary understanding of land use intensification processes.

## Acknowledgements

This study was a part of the "Integrated modelling framework to monitor and predict trends of agricultural management and their impact on soil functions at multiple scales" (iMSoil) under Project 406840-143062 funded by the Swiss National Science Foundation within the National Resource Program NRP68 "Sustainable Use of Soil as a Resource" (www.nfp68.ch). The RapidEye data was provided with support of ESA EO Cat 1 project No. 9524 in the context of the ESA Support to Science Element (STSE) '3D-VegetationLab' project, ESRIN Contract No. AO/1-6529/10/I-NB. The University of Zurich Research Priority Program on "Global Change and Biodiversity" supported the work of M. E. Schaepman. The authors thank Michael Müller providing livestock density data. We thank the three anonymous reviewers for excellent comments that highly improved the manuscript.

## Supporting information

Table S1 T-test, p-values and F-test for equal means and variances of the images 24 April 2013 and 2 August 2013 normalized using the IR-MAD transformation.

| | | B1 | B2 | B3 | B4 | B5 |
|---|---|---|---|---|---|---|
| Mean | t-stat. | -0.484477 | -0.907635 | -0.832065 | -0.219624 | -1.75543 |
| | p-value | 0.628193 | 0.364429 | 0.405701 | 0.826245 | 0.0796796 |
| Variance | F-stat. | 1.12477 | 1.03477 | 1.06604 | 1.01549 | 1.01504 |
| | p-value | 0.143508 | 0.670584 | 0.426174 | 0.848304 | 0.852630 |

Table S2 T-test, p-values and F-test for equal means and variances of the images 8 May 2013 and 2 August 2013 normalized using the IR-MAD transformation.

| | | B1 | B2 | B3 | B4 | B5 |
|---|---|---|---|---|---|---|
| Mean | t-stat. | -0.808773 | -0.841909 | -1.73525 | -0.292721 | -0.854726 |
| | p-value | 0.418666 | 0.399861 | 0.0827397 | 0.769213 | 0.392752 |
| Variance | F-stat. | 1.13678 | 1.01334 | 1.00223 | 1.01380 | 1.00856 |
| | p-value | 1.01565e-9 | 0.527600 | 0.915512 | 0.513723 | 0.684525 |

Table S3 T-test, p-values and F-test for equal means and variances of the images 8 June 2013 and 2 August 2013 normalized using the IR-MAD transformation.

| | | B1 | B2 | B3 | B4 | B5 |
|---|---|---|---|---|---|---|
| Mean | t-stat. | -0.323230 | -0.0313101 | -0.356325 | -0.0619989 | 0.781816 |
| | p-value | 0.746578 | 0.975167 | 0.721704 | 0.950838 | 0.434479 |
| Variance | F-stat. | 1.02528 | 1.01823 | 1.01737 | 1.01577 | 1.00602 |
| | p-value | 0.658927 | 0.749350 | 0.760807 | 0.782089 | 0.915467 |

Table S4 T-test, p-values and F-test for equal means and variances of the images 15 July 2013 and 2 August 2013 normalized using the IR-MAD transformation.

| | | B1 | B2 | B3 | B4 | B5 |
|---|---|---|---|---|---|---|
| Mean | t-stat. | -0.919389 | -0.384706 | -0.690833 | -0.237744 | -0.951202 |
| | p-value | 0.357975 | 0.700462 | 0.489732 | 0.811770 | 0.341549 |
| Variance | F-stat. | 1.01811 | 1.04857 | 1.01883 | 1.00099 | 1.00021 |
| | p-value | 0.596925 | 0.162347 | 0.582641 | 0.976642 | 0.995157 |

Table S5 Confusion matrix of the classes of change estimated using a constant value of 1 standard deviation to define thresholds of change. Standard differencing image obtained from subtracting May from April image.

| | Negative change | No change | Positive change | Total | User accuracy | Commission accuracy |
|---|---|---|---|---|---|---|
| Negative change | 173 | 18 | 6 | 197 | 87.82% | 12.18% |
| No change | 21 | 147 | 29 | 197 | 74.62% | 25.38% |
| Positive change | 18 | 31 | 148 | 197 | 75.13% | 24.87% |
| Total | 212 | 196 | 183 | 591 | | |
| Producer accuracy | 81.60% | 75% | 80.87% | | | |
| Omission error | 18.40% | 25% | 19.13% | | | |

Table S6 Confusion matrix of the classes of change estimated using a constant value of 1.5 standard deviations from the mean to define thresholds of change. Standard differencing image obtained from subtracting May from April image.

| | Negative change | No change | Positive change | Total | User accuracy | Commission accuracy |
|---|---|---|---|---|---|---|
| Negative change | 175 | 19 | 3 | 197 | 88.83% | 11.17% |
| No change | 26 | 148 | 23 | 197 | 75.13% | 24.87% |
| Positive change | 12 | 37 | 148 | 197 | 75.13% | 24.87% |
| Total | 213 | 204 | 174 | 591 | | |
| Producer accuracy | 82.16% | 72.55% | 85.06% | | | |
| Omission error | 17.84% | 27.45% | 14.94% | | | |

Table S7 Confusion matrix of the classes of change estimated using a constant value of 2 standard deviations from the mean to define thresholds of change. Standard differencing image obtained from subtracting May from April image. There were no enough points (197) to define positive changes using 2 standard deviations.

| | Negative change | No change | Positive change | Total | User accuracy | Commission accuracy |
|---|---|---|---|---|---|---|
| Negative change | 180 | 14 | 3 | 197 | 91.37% | 8.63% |
| No change | 28 | 132 | 37 | 197 | 67.01% | 32.99% |
| Positive change | 15 | 39 | 141 | 195 | 72.31% | 27.69% |
| Total | 223 | 185 | 181 | 589 | | |
| Producer accuracy | 80.72% | 71.35% | 77.90% | | | |
| Omission error | 19.28% | 28.65% | 22.10% | | | |

Table S8 Confusion matrix of the classes of change estimated using a constant value of 1 standard deviation from the mean to define thresholds of change. Change detection carried out using the standard differencing image obtained from subtracting June from May image.

| | Negative change | No change | Positive change | Total | User accuracy | Commission accuracy |
|---|---|---|---|---|---|---|
| Negative change | 177 | 8 | 12 | 197 | 89.85% | 10.15% |
| No change | 31 | 108 | 58 | 197 | 54.82% | 45.18% |
| Positive change | 1 | 10 | 186 | 197 | 94.42% | 5.58% |
| Total | 209 | 126 | 256 | 591 | | |
| Producer accuracy | 84.69% | 85.71% | 72.66% | | | |
| Omission error | 15.31% | 14.29% | 27.34% | | | |

Table S9 Confusion matrix of the classes of change estimated using a constant value of 1.5 standard deviations from the mean to define thresholds of change. Change detection carried out using the standard differencing image obtained from subtracting June from May image.

| | Negative change | No change | Positive change | Total | User accuracy | Commission accuracy |
|---|---|---|---|---|---|---|
| Negative change | 176 | 11 | 10 | 197 | 89.34% | 10.66% |
| No change | 38 | 107 | 52 | 197 | 54.31% | 45.69% |
| Positive change | 4 | 19 | 174 | 197 | 88.32% | 11.68% |
| Total | 218 | 137 | 236 | 591 | | |
| Producer accuracy | 80.73% | 78.10% | 73.73% | | | |
| Omission error | 19.27% | 21.90% | 26.27% | | | |

Table S10 Confusion matrix of the classes of change estimated using a constant value of 2 standard deviations from the mean to define thresholds of change. Change detection carried out using the standard differencing image obtained from subtracting June from May image.

| | Negative change | No change | Positive change | Total | User accuracy | Commission accuracy |
|---|---|---|---|---|---|---|
| Negative change | 172 | 12 | 13 | 197 | 87.31% | 12.69% |
| No change | 49 | 95 | 53 | 197 | 48.22% | 51.78% |
| Positive change | 4 | 20 | 173 | 197 | 87.82% | 12.18% |
| Total | 225 | 127 | 239 | 591 | | |
| Producer accuracy | 76.44% | 74.80% | 72.38% | | | |
| Omission error | 23.56% | 25.20% | 27.62% | | | |

Table S11 Confusion matrix of the classes of change estimated using a constant value of 1 standard deviation from the mean to define thresholds of change. Change detection carried out using the standard differencing image obtained from subtracting July from June image.

| | Negative change | No change | Positive change | Total | User accuracy | Commission accuracy |
|---|---|---|---|---|---|---|
| Negative change | 171 | 19 | 7 | 197 | 86.80% | 13.20% |
| No change | 27 | 146 | 24 | 197 | 74.11% | 25.89% |
| Positive change | 7 | 21 | 169 | 197 | 85.79% | 14.21% |
| Total | 205 | 186 | 200 | 591 | | |
| Producer accuracy | 83.42% | 78.50% | 84.5% | | | |
| Omission error | 16.58% | 21.50% | 15.5% | | | |

Table S12 Confusion matrix of the classes of change estimated using a constant value of 1.5 standard deviations from the mean to define thresholds of change. Change detection carried out using the standard differencing image obtained from subtracting July from June image.

| | Negative change | No change | Positive change | Total | User accuracy | Commission accuracy |
|---|---|---|---|---|---|---|
| Negative change | 160 | 29 | 8 | 197 | 81.22% | 18.78% |
| No change | 32 | 134 | 31 | 197 | 68.02% | 31.98% |
| Positive change | 4 | 25 | 168 | 197 | 85.28% | 14.72% |
| Total | 196 | 188 | 207 | 591 | | |
| Producer accuracy | 81.63% | 71.28% | 81.16% | | | |
| Omission error | 18.37% | 28.72% | 18.84% | | | |

Table S13 Confusion matrix of the classes of change estimated using a constant value of 2 standard deviations from the mean to define thresholds of change. Change detection carried out using the standard differencing image obtained from subtracting July from June image.

| | Negative change | No change | Positive change | Total | User accuracy | Commission accuracy |
|---|---|---|---|---|---|---|
| Negative change | 157 | 31 | 9 | 197 | 79.70% | 20.30% |
| No change | 34 | 121 | 42 | 197 | 61.42% | 38.58% |
| Positive change | 8 | 30 | 159 | 197 | 80.71% | 19.29% |
| Total | 199 | 182 | 210 | 591 | | |
| Producer accuracy | 78.89% | 66.48% | 75.71% | | | |
| Omission error | 21.11% | 33.52% | 24.29% | | | |

Table S14 Confusion matrix of the classes of change estimated using a constant value of 1 standard deviation from the mean to define thresholds of change. Change detection carried out using the standard differencing image obtained from subtracting August from July image.

| | Negative change | No change | Positive change | Total | User accuracy | Commission accuracy |
|---|---|---|---|---|---|---|
| Negative change | 175 | 17 | 5 | 197 | 88.83% | 11.17% |
| No change | 55 | 106 | 36 | 197 | 53.81% | 46.19% |
| Positive change | 9 | 11 | 177 | 197 | 89.85% | 10.15% |
| Total | 239 | 134 | 218 | 591 | | |
| Producer accuracy | 73.22% | 79.10% | 81.19% | | | |
| Omission error | 26.78% | 20.90% | 18.81% | | | |

Table S15 Confusion matrix of the classes of change estimated using a constant value of 1.5 standard deviations from the mean to define thresholds of change. Standard differencing image obtained from subtracting August from July image.

| | Negative change | No change | Positive change | Total | User accuracy | Commission accuracy |
|---|---|---|---|---|---|---|
| Negative change | 167 | 23 | 7 | 197 | 84.77% | 15.23% |
| No change | 52 | 100 | 45 | 197 | 50.76% | 49.24% |
| Positive change | 6 | 9 | 182 | 197 | 92.39% | 7.61% |
| Total | 225 | 132 | 234 | 591 | | |
| Producer accuracy | 74.22% | 75.76% | 77.78% | | | |
| Omission error | 25.78% | 24.24% | 22.22% | | | |

Table S16 Confusion matrix of the classes of change estimated using a constant value of 2 standard deviations from the mean to define thresholds of change. Standard differencing image obtained from subtracting August from July image.

| | Negative change | No change | Positive change | Total | User accuracy | Commission accuracy |
|---|---|---|---|---|---|---|
| Negative change | 171 | 21 | 5 | 197 | 86.80% | 13.20% |
| No change | 50 | 108 | 39 | 197 | 54.82% | 45.18% |
| Positive change | 5 | 8 | 184 | 197 | 93.40% | 6.60% |
| Total | 226 | 137 | 228 | 591 | | |
| Producer accuracy | 75.66% | 78.83% | 80.70% | | | |
| Omission error | 24.34% | 21.17% | 19.30% | | | |

Table S17 Classification accuracies of classes of change (thresholds defined with a constant of 1.5).

| Time steps | Overall Accuracy (%) | Kappa Statistic | Sampling Error | Interval of confidence 95% |
|---|---|---|---|---|
| April—May | 79.69 | 0.69 | 1.65 | 76.45-82.94 |
| May—June | 77.33 | 0.66 | 1.72 | 73.95-80.70 |
| June—July | 78.17 | 0.67 | 1.70 | 74.84-81.50 |
| July—August | 78.34 | 0.67 | 1.69 | 75.02-81.66 |

Table S18 Classification accuracies of classes of change (thresholds defined with a constant of 2).

| Time steps | Overall Accuracy (%) | Kappa Statistic | Sampling Error | Interval of confidence 95% |
|---|---|---|---|---|
| April—May | 76.65 | 0.65 | 1.74 | 73.23-80.07 |
| May—June | 74.45 | 0.62 | 1.72 | 70.93-77.97 |
| June—July | 73.94 | 0.61 | 1.80 | 70.40-77.48 |
| July—August | 75.97 | 0.64 | 1.76 | 72.53-79.42 |

Table S19 Tukey HSD's test comparing mowing frequency clusters.

| Mowing frequency cluster comparison | | Mean difference | Standard error | Sig. |
|---|---|---|---|---|
| Low | Moderate | 0.0057* | 0.0016 | 0.001 |
| | High | 0.0389* | 0.0108 | 0.001 |
| Moderate | Low | -0.0057* | 0.0015 | 0.001 |
| | High | 0.0332* | 0.0108 | 0.006 |
| High | Low | -0.0389* | 0.0107 | 0.001 |
| | Moderate | -0.0332* | 0.0108 | 0.006 |

*. Mean difference is significant at the 0.05 level.

## Assignment of weights

Weights were assigned to change events according to a linear function. An alternative to this approach could be to assign weights according to the seasonal development of the species. However, in our study area there were not only cool-season species such as: *Festuca rubra, Lolium multiflorum, Lolium perenne,* and *Alopecurus pratensis* but also perennials that can be distributed in the warm season, for instance: *Ranunculus bulbosus Taraxacum officinalis,* and *Achillea millefolium*. Since the growing development of cool- and warm-season species is

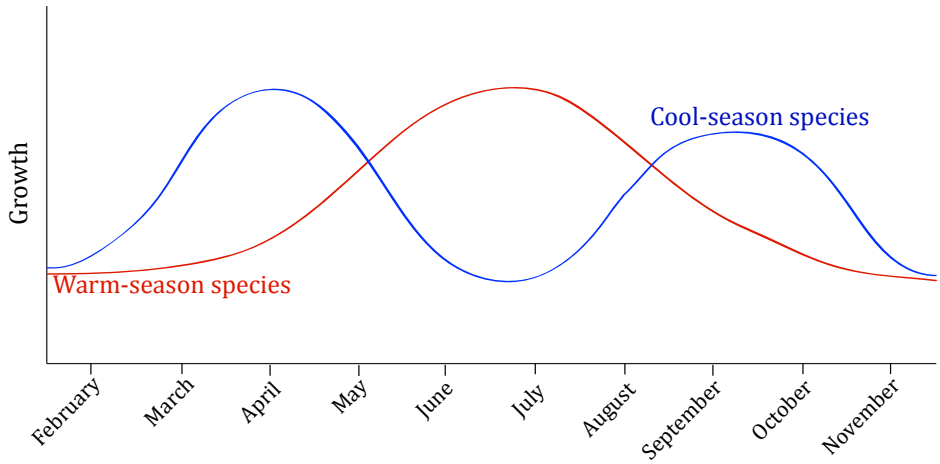


Figure S1 Growth development of grassland species within the growing season (adapted from Agriculture and natural resources 2016).[2]

complementary we decided to use the criterion of the date when a mowing event was observed to define mowing frequency classes. Consequently, a linear function was implemented.

[2] Agriculture and Natural resources, U.C (2016). Seasonal growth pattern of grasses. In. Oct. 19, 2016 http://ipm.ucanr.edu/TOOLS/TURF/ESTABLISH/seasongrth.html

# Chapter 5

# Synthesis

## 5.1 Main findings

Reaching the agricultural productivity that society needs while avoiding the loss of ecosystem services requires the monitoring of agricultural management practices and the assessment of environmental issues derived from them. This thesis demonstrates the potential of Earth observation (EO) sources to monitor agricultural management practices and to assess the impact of Nitrogen (N) deposition on carbon (C) fixation. Here, the research questions pointed out in Section 1.3.1 and the main findings of this thesis are reviewed.

### 5.1.1 What is the contribution of using remote sensing data to the performance and output of the Land Management Model?

Chapter 2 sheds light on how to reduce uncertainties in the spatially explicit distribution of farm statistics using remote sensing datasets. The propagation of errors from the allocation process to the model outputs has been pointed out in several studies, e.g., Gärtner et al. (2013); Kempen et al. (2011); Temme et al. (2011) but, as explained in Chapter 2, there is a lack of sensitivity analyses for this procedure. The analyses revolved around matching the Utilised Agricultural Area (UAA) stated in the farm census and the area derived from EO sources as well as finding an optimum spatial unit to carry out the allocation process.

The Land Management Model (LMM) requires information about arable land that is formed by land use classes e.g., croplands and temporary grassland, receiving different fertilization strategies. However, the low spectral separability between these classes led to define an approach that identified croplands through bare soil. The crop rotation scheme in the area is supposed to reduce differences in N inputs among fields; therefore the distinction of land cover classes following this approach was considered sound. On one hand, the selection of land cover classes (bare soil and permanent vegetation cover) with high spectral separability is key to achieve high classification accuracies (e.g., 98-99% accuracies were reached in Chapter 2). On the other hand, this procedure can lead to over- and under-estimations because not all the fields cultivated with temporary grassland can be identified with two images acquired during the summer season. In Chapter 3, this process was extended to five images.

However, taking into account the legal definition of permanent grasslands, a time frame of seven years should be monitored to account for all the temporary grassland of an agroecosystem (Swiss government, 1998), with the corresponding cost. The use of ancillary information contributed to defining the agricultural area with high accuracy (+2 ha with respect to the farm census). This strategy was also applied in Chapter 3 in order to differentiate permanent grassland and to minimise inconsistencies between the farm census and the remotely sensed land use dataset.

The evaluation of three spatial units to carry out the allocation process allowed identifying the best trade-off between computational time and allocated farm statistics. 67 $km^2$ were computed in 27 min with 4% of non-allocated land. This means a computational gain of more than 20 days to process all Swiss agricultural land. These results were used as a basis for the segmentation process carried out in Chapter 3.

Finally, the comparison of the land allocated in 14% of the study area with a land property layer showed a preliminary improvement of 12% using the remote sensing dataset. However, further efforts are required to validate the land belonging to each farm.

In summary, Chapter 2 helped define benchmarks for spatial resolution, classification accuracy, and segmentation units that improved the land allocation module of the LMM and served as a reference for some analysis in Chapter 3.

### 5.1.2 How can indicators of intensity of use derived from remote sensing data be used in a context of an ecological framework?

Chapter 3 poses challenges derived from monitoring ecological indicators of grassland use intensity (mowing frequency, grazing intensity, and fertilization inputs) by means of satellite images with high temporal and spatial resolution but low spectral information. In addition, interrelationships between indicators are expected because grazing periods are often combined with cuts, which are followed by manure application (Chapter 2 and Chapter 3). The method proposed in Chapter 3 attempted to ensure the added value of each indicator for the computation of grassland use intensity and to bridge the gap between ecological approaches and the remote sensing techniques employed for

assessing intensity of use.

Mowing management practices were determined by tracking abrupt changes between pairs of images. Classes of change were differentiated accounting for asymmetries in the data distribution, which can be particularly important when strong asymmetries occur. The classes of change reached 80% concordance with respect to the results obtained from an unsupervised ISODATA classification. Furthermore, monitoring the beginning of the growing season was relevant in order to define intensive management practices. Three levels of intensity of use were distinguished using spectral information: medium intensive (46%), low intensive (37%), and high intensive (17%). In addition, grazing areas were determined by small spectral changes using the coefficient of variation. However, allocated livestock could not be used as indicator of fertilizer inputs. This simplification of the relationship animal presence — manure application may need to be better represented with additional information such as manure trading and importation of fodder so that the environmental pressure caused by livestock can be comprehensively determined. Finally, cross tabulation between mowing frequency and grazing areas with levels of intensity of use allowed finding unexpected relationships. This helped identify areas prone to N surplus, i.e., 12% of the study area.

### 5.1.3 What is the relevance of nitrogen deposition and related climatic factors to predict remotely sensed carbon fixation response in land cover classes characterised by different management practices?

Chapter 4 monitors the variation of remotely sensed Gross Primary Production (GPP) as indicator of C fixation, according to precipitation, relative sunshine, temperature, and N deposition in three land cover classes: grasslands, croplands, and croplands/natural vegetation mosaic. The selection of land cover classes located in areas with different soil characteristics, i.e., cropland aptitude, stone content, water and nutrient storage capacity provided information about the relevance of the selected limiting factors to control GPP in areas with different management practices.

The outcomes of the multiple linear regressions stratified per land cover class indicate that N deposition produces the strongest impact on GPP. High

correlations between N deposition and temperature have overshadowed the latter variable as part of the models. As a result, precipitation stood out with respect to the remaining climatic factors i.e., temperature and relative sunshine.

In grasslands, the selected explanatory variables explained up to 80% of the GPP response, 47% in croplands, and 19% in croplands/natural vegetation mosaic. In particular, N deposition can explain between 14% and 68% GPP variance. However, atmospheric deposition together with high manure application and livestock density (Chapter 3) can contribute to producing negative effects in water bodies and biodiversity, as explained in Chapter 1 and Chapter 4; these consequences of N surplus should be further studied.

The observed impact of N deposition on C fixation for all the agroecosystems considered can have an influence on the design of future studies on the C budget at national scale. Verstraeten et al. (2006) highlighted that C budget studies have been predominantly focused on studying the influence of temperature on C fixation. Nevertheless, other climatic factors such as sunshine and precipitation, which are also relevant to controlling C uptake via photosynthesis, have been progressively used to monitor GPP variation (Beer et al., 2010; Yang et al., 2015; Zhang et al., 2014) as well as to study the influence of nutrients and their interaction with precipitation (Guo et al., 2016; He et al., 2016). Therefore, the findings shown in Chapter 4 provide an insight into the relevance of these controlling factors of C fixation at large scale. Not only does N deposition provide information about nutrient effects on GPP response but also about the N status of the land cover classes, which can be relevant to understanding relationships between C and N cycles.

## 5.2 Main contributions

In line with the objectives pointed out in Chapter 1, the main contributions of this thesis can be summarised as follows: improvement of a modelling tool to assess N balance in agroecosystems, development of a methodology to monitor ecological indicators of grassland use intensity with remote sensing techniques, and comprehension of the relevance of limiting factors of C fixation in biogeographic regions characterised by different management practices.

In particular, this thesis raises awareness about the required quality and characteristics of remotely sensed land cover and land use datasets to allocate farm statistics. The findings imply a step forward to reduce sources of error in the model outputs i.e., N surplus assessments at local and regional scales. Consequently, this work can improve the reliability of policy assessment tools, which is crucial to meeting policy goals and developing further objectives. The recommendations highlighted in Chapter 2 can be implemented in other land system models because land cover datasets are widely used to allocate point grid land use information (Cantelaube et al., 2012; Kempen et al., 2011; Letourneau et al., 2012). Therefore, this work could contribute to improving policy formulation in other regions as well.

Furthermore, this thesis attempts to bridge the gap between scientific disciplines seeking common ground to monitor grassland use intensity. In particular, ecological indicators were evaluated as well as integrated as proposed in new ecological frameworks (Erb et al., 2013; Kuemmerle et al., 2013). Besides, the use of robust thresholds and standard values provide a sound basis for reproducing the methodology. Accounting for the moment within the growing season when management practices are being observed can contribute to a better planning of image acquisition campaigns as well as to a reduction of the number of images required to monitor certain indicators with high accuracy, as reported in other studies (Asam et al., 2015; Franke et al., 2012). The latter directly impacts on the processing time and the budget needed for image acquisition in case of selecting commercial satellite or airborne sensors. In conclusion, this work contributes to achieving complementarity between ecological and remote sensing studies in order to develop standard methods that can be used in multiple analyses and produce results that can be implemented in models.

Finally, this thesis provides an insight into the relevance of several limiting factors of C fixation in different biogeographic regions. The findings obtained can play a key role in the assessment of the C budget at national scale. In particular, the impact of N deposition observed on GPP variance can help promote the future inclusion of this variable in C models (Schulze et al., 2010; Stevens et al., 2015). Besides, these findings can be used as a basis for developing studies in

other regions. The comparison of results from different analyses can help understand underlying relationships among factors, which can shift their relevance as explanatory variables of GPP.

The coalescence of the findings presented in this thesis constitutes a link between the causes and the consequences of intensive management practices in agricultural land as well as a reflection on the use of techniques that foster multidimensional approaches. These multi-faceted strategies are vital to understanding complex systems, which can only be done when different scientific communities combine their expertise.

## 5.3 Outlook

This section discusses potential improvements of the analyses carried out as well as future focuses of research based on the main findings of this thesis.

### 5.3.1 Data assimilation in the Land Management Model (LMM) and carbon budget models

Future research could aim at defining the best approach to assimilating remotely sensed mowing frequency, grazing intensity, and areas prone to N surplus into the LMM. Different methods have been proposed to assimilate remote sensing datasets in agroecosystems models such as direct or forcing (datasets used as observed variables), sequential or updating (datasets used to update state variables of the model when observations are available), and variational or calibration (method used to minimise differences between observed remote sensing products and model outputs) (Dorigo et al., 2007; Fang et al., 2013). Additionally, the integration of these datasets with an improved estimation of fertilizer inputs derived from livestock density, manure trading, and nutrient fluxes would provide a more comprehensive set of indicators to assess N balance in grassland systems. However, further efforts to validate the allocation process of the LMM are required. Better assessment of model outputs will contribute to improving the reliability of the model.

He et al. (2010) has recommended that N deposition should be included as part of nutrient balance estimates in intensive use areas. However, the contribution of N deposition to N inputs in Swiss agroecosystems remains small (FSO, 2015).

Therefore, additional evaluation about whether including or not this information in the LMM to assess N balance could be carried out. Nevertheless, the relevance of N deposition to explain GPP variance indicates the importance that this factor may have in C budget models at national scale, especially for understanding vegetation dynamics and ecosystem functioning. Further research could be based on the integration of N cycles in C models. Some scientists have demonstrated that this integration can change NPP variation along temperature and water availability gradients, avoid overestimation of $CO_2$ sequestration at high-latitudes, contribute to reducing anthropogenic $CO_2$ emissions at regional scales, properly account for the relevance of drivers in C dynamics and improve projections of ecosystem behaviour (Smith et al., 2014; Zaehle et al., 2010; Zhang et al., 2005).

### 5.3.2 Spectral information to assess fertilizer inputs

Remote sensing datasets with higher spectral resolution could provide additional information about the relationship between N content and management practices. In this thesis, only spectral information from the visible and near infrared (VNIR) range was used (400—1300 nm). The chlorophyll absorption feature in the VNIR has been widely used to derive leaf N content (Clevers et al., 2013; Mutanga et al., 2003; Ramoelo et al., 2012), but this effect can only account for a small part of the spectral response, which is influenced by other leaf properties (Kokaly et al., 2009). Kokaly (2001) found that absorptions features in the shortwave infrared (SWIR) region centered at 2100 nm are sensitive to different N concentrations. Therefore, potential lines of research could be focused on determining the suitability of datasets with wavelengths in the SWIR range to quantify fertilizer inputs and assess intensity of use. Furthermore, resulting maps could be used to calibrate the LMM or for cross-comparison with model outputs. However, the spatial resolution selected in Chapter 2 and 3 (15 and 5 m respectively) would have to be changed because these wavelengths are available at 30 m in Landsat-8 and at 20 m in Sentinel-2 sensors respectively. The temporal resolution would remain similar.

### 5.3.3 Impact of intensive management practices on biodiversity

Species composition and its abundance vary according to the intensity of

management practices (Kampmann et al., 2008; Kleijn et al., 2009; Köhler et al., 2005). For instance, intensive grazing may favour rosette-forming species with ruderal strategies, annual growth with seasonal seed regeneration, early flowering, and perennial grasses with small seeds (Köhler et al., 2005; Pakeman, 2004; Peco et al., 2005). In such cases of high disturbance and trampling, the competition between invasive and native species diminishes, facilitating the establishment of opportunistic species (Byers et al., 2006; Pavlů et al., 2008). Additionally, the high application of fertilizers together with additional nutrient sources such as atmospheric deposition affects biodiversity at the expense of some species (Bassin et al., 2013; Matson et al., 2002).

In disturbed grasslands, *Taraxacum officinale* (dandelions) is a common weed that colonises open areas by windborne seeds mainly produced in spring (Martinkova et al., 2014). Dandelions have a nutritious quality and palatability comparable with any sown species at the same stage of development. However, high richness decreases the yield of the fields and can produce problems in livestock health (Clark et al., 2006; Pavlů et al., 2008). Moreover, the reduction of plant communities composition can diminish N and C storage in soils and consequently soil fertility (De Deyn et al., 2009).

Remote sensing techniques have been successfully applied for weed monitoring through appropriate selection of the spectral, spatial, and temporal resolution (Hunt Jr et al., 2003). In particular, differentiation of weeds can be achieved when their spectral characteristics differ from those in the invaded ecosystem (Andrew et al., 2008). Flowering status has been used as indicator of species abundance using multispectral imagery (Hunt Jr et al., 2006; Müllerová et al., 2013) and imaging spectrometer data (Chen et al., 2009; Landmann et al., 2015; Miao et al., 2006; Mirik et al., 2013) both at very high (1-5m) and high (20m) spatial resolution. Therefore, it would be interesting to determine the effects of levels of grassland use intensity defined in this work on weeds abundance.

Summarizing everything considered, remote sensing will be able to contribute increasingly in the future to assessing environmental impact as well as policy, allowing to monitor and forecast agroecosystems and their productivity.

## Bibliography

Adjorlolo, C., Mutanga, O., & Cho, M. A. (2014). Estimation of canopy nitrogen concentration across c3 and c4 grasslands using worldview-2 multispectral data. *IEEE Journal of Selected Topics in Applied Earth Observations and Remote Sensing, 7*(11), 4385-4392. doi:10.1109/JSTARS.2014.2320601

AGRIDEA, & FOAG. (2015). *Wegleitung Suisse-Bilanz.* Swiss Federal Office for Agriculture. Dec, 6, 2016. https://www.agridea.ch/de/publikationen/publikationen/aufzeichnungen-nachweis/suisse-bilanz/wegleitung-suisse-bilanz-2015/

Albrecht, M., Duelli, P., Müller, C., Kleijn, D., & Schmid, B. (2007). The Swiss agri-environment scheme enhances pollinator diversity and plant reproductive success in nearby intensively managed farmland. *Journal of Applied Ecology, 44*(4), 813-822. doi:10.1111/j.1365-2664.2007.01306.x

Anav, A., Friedlingstein, P., Beer, C., Ciais, P., Harper, A., Jones, C., Murray-Tortarolo, G., Papale, D., Parazoo, N. C., Peylin, P., Piao, S., Sitch, S., Viovy, N., Wiltshire, A., & Zhao, M. (2015). Spatiotemporal patterns of terrestrial gross primary production: A review. *Reviews of Geophysics, 53*(3), 785-818. doi:10.1002/2015RG000483

Anderson, J. R. (1976). *A land use and land cover classification system for use with remote sensor data* Vol. 964. (pp. 41).

Andrew, M. E., & Ustin, S. L. (2008). The role of environmental context in mapping invasive plants with hyperspectral image data. *Remote Sensing of Environment, 112*(12), 4301-4317. doi:10.1016/j.rse.2008.07.016

Asam, S., Fabritius, H., Klein, D., Conrad, C., & Dech, S. (2013). Derivation of leaf area index for grassland within alpine upland using multi-temporal RapidEye data. *International Journal of Remote Sensing, 34*(23), 8628-8652. doi:10.1080/01431161.2013.845316

Asam, S., Klein, D., & Dech, S. (2015). *Estimation of grassland use intensities based on high spatial resolution LAI time series.* Paper presented at the International Archives of the Photogrammetry, Remote Sensing and Spatial Information Sciences - ISPRS Archives.

Asner, G. P., & Heidebrecht, K. B. (2002). Spectral unmixing of vegetation, soil and dry carbon cover in arid regions: Comparing multispectral and hyperspectral observations. *International Journal of Remote Sensing, 23*(19), 3939-3958. doi:10.1080/01431160110115960

Asner, G. P., Martin, R. E., Anderson, C. B., & Knapp, D. E. (2015). Quantifying forest canopy traits: Imaging spectroscopy versus field survey. *Remote Sensing of Environment, 158*, 15-27. doi:10.1016/j.rse.2014.11.011

Aviron, S., Nitsch, H., Jeanneret, P., Buholzer, S., Luka, H., Pfiffner, L., Pozzi, S., Schüpbach, B., Walter, T., & Herzog, F. (2009). Ecological cross compliance promotes farmland biodiversity in Switzerland. *Frontiers in Ecology and the Environment, 7*(5), 247-252. doi:10.1890/070197

Bassin, S., Volk, M., & Fuhrer, J. (2013). Species Composition of Subalpine Grassland is Sensitive to Nitrogen Deposition, but Not to Ozone, After Seven Years of Treatment. *Ecosystems, 16*(6), 1105-1117. doi:10.1007/s10021-013-9670-3

Bassin, S., Volk, M., Suter, M., Buchmann, N., & Fuhrer, J. (2007). Nitrogen deposition but not ozone affects productivity and community composition of subalpine grassland after 3 yr of treatment. *New Phytologist, 175*(3), 523-534. doi:10.1111/j.1469-8137.2007.02140.x

Bassin, S., Volk, M., Sutter, M., Buchmann, N., & Fuhrer, J. (2007). Nitrogen Deposition but Not Ozone Affects Productivity and Community Composition of Subalpine Grassland after 3 yr of Treatment. *The New Phytologist, 175*(3), 523-534.

Beer, C., Reichstein, M., Tomelleri, E., Ciais, P., Jung, M., Carvalhais, N., Rödenbeck, C., Arain, M. A., Baldocchi, D., Bonan, G. B., Bondeau, A., Cescatti, A., Lasslop, G., Lindroth, A., Lomas, M., Luyssaert, S., Margolis, H., Oleson, K. W., Roupsard, O., Veenendaal, E., Viovy, N., Williams, C., Woodward, F. I., & Papale, D. (2010). Terrestrial gross carbon dioxide uptake: Global distribution and covariation with climate. *Science, 329*(5993), 834-838. doi:10.1126/science.1184984

Berger, M., Moreno, J., Johannessen, J. A., Levelt, P. F., & Hanssen, R. F. (2012). ESA's sentinel missions in support of Earth system science. *Remote Sensing of Environment, 120*, 84-90. doi:10.1016/j.rse.2011.07.023

Bergström, A. K., & Jansson, M. (2006). Atmospheric nitrogen deposition has caused nitrogen enrichment and eutrophication of lakes in the northern hemisphere. *Global Change Biology, 12*(4), 635-643. doi:10.1111/j.1365-2486.2006.01129.x

Birk, R. J., Stanley, T., Snyder, G. I., Hennig, T. A., Fladeland, M. M., & Policelli, F. (2003). Government programs for research and operational uses of commercial remote sensing data. *Remote Sensing of Environment, 88*(1–2), 3-16. doi:10.1016/j.rse.2003.07.007

Blackbridge. (2015). Satellite Imagery Product Specifications V.6.1 April Jun. 25, 2016, http://www.e-geos.it/images/Satellite_data/RAPIDEYE/RE_Product_Specifications_ENG.pdf

Blüthgen, N., Dormann, C. F., Prati, D., Klaus, V. H., Kleinebecker, T., Hölzel, N., Alt, F., Boch, S., Gockel, S., Hemp, A., Müller, J., Nieschulze, J., Renner, S. C., Schöning, I., Schumacher, U., Socher, S. A., Wells, K., Birkhofer, K., Buscot, F., Oelmann, Y., Rothenwöhrer, C., Scherber, C., Tscharntke, T., Weiner, C. N., Fischer, M., Kalko, E. K. V., Linsenmair, K. E., Schulze, E. D., & Weisser, W. W. (2012). A quantitative index of land-use intensity in grasslands: Integrating mowing, grazing and fertilization. *Basic and Applied Ecology, 13*(3), 207-220. doi:10.1016/j.baae.2012.04.001

Bobbink, R., Hicks, K., Galloway, J., Spranger, T., Alkemade, R., Ashmore, M., Bustamante, M., Cinderby, S., Davidson, E., Dentener, F., Emmett, B., Erisman, J. W., Fenn, M., Gilliam, F., Nordin, A., Pardo, L., & De Vries, W. (2010). Global assessment of nitrogen deposition effects on terrestrial plant diversity: A synthesis. *Ecological Applications, 20*(1), 30-59. doi:10.1890/08-1140.1

Bötsch, M. (2004). *Swiss agricultural policy and its focus on grassland. In: Land Use Systems in Grassland Dominated Regions: Proceedings of the 20th General Meeting of the European Grassland Federation, Luzern, Switzerland, 21-24 June 2004. Grassland Science in Europe*.

Britz, W., Verburg, P. H., & Leip, A. (2011). Modelling of land cover and

agricultural change in Europe: Combining the CLUE and CAPRI-Spat approaches. *Agriculture, Ecosystems and Environment, 142*(1-2), 40-50. doi:10.1016/j.agee.2010.03.008

Brown, C., Murray-Rust, D., Van Vliet, J., Alam, S. J., Verburg, P. H., & Rounsevell, M. D. (2014). Experiments in globalisation, food security and land use decision making. *PLoS ONE, 9*(12). doi:10.1371/journal.pone.0114213

Buchli, S., Blum, J., Brönnimann, A., Escher, L., Eugster, L., Forni, D., Furrer, S., Gantenbein, R., Giezendanner, U., Gilg, R., Keil, N., Keller, L., Keller, M., Läng, J., Niederberger, H., Steiger, R., Wanzenried, V., & Zbinden, W. (2008). *KIP-Richtlinien für den ökologischen Leistungsnachweis (ÖLN), BTS and RAUS. Inspektions-organisationen, Kantonale Beratung und Verwaltung.* Lindau.

Byers, R. A., Curran, W. S., Pennypacker, B. W., & Badruddin, A. K. (2006). Invertebrate Pests, Weeds, and Diseases of Forage-Livestock Systems. In E. B. Rayburn (Ed.), *Forage production for pasture-based livestock production* (Vol. 172, pp. 141). Ithaca, New York: NRAES.

Cakir, H. I., Khorram, S., & Nelson, S. A. C. (2006). Correspondence analysis for detecting land cover change. *Remote Sensing of Environment, 102*(3-4), 306-317. doi:10.1016/j.rse.2006.02.023

Camargo, J. A., & Alonso, Á. (2006). Ecological and toxicological effects of inorganic nitrogen pollution in aquatic ecosystems: A global assessment. *Environment International, 32*(6), 831-849. doi:10.1016/j.envint.2006.05.002

Cantelaube, P., Jayet, P. A., Carré, F., Bamps, C., & Zakharov, P. (2012). Geographical downscaling of outputs provided by an economic farm model calibrated at the regional level. *Land Use Policy, 29*(1), 35-44. doi:10.1016/j.landusepol.2011.05.002

Canty, M. J., & Nielsen, A. A. (2008). Automatic radiometric normalization of multitemporal satellite imagery with the iteratively re-weighted MAD transformation. *Remote Sensing of Environment, 112*(3), 1025-1036. doi:10.1016/j.rse.2007.07.013

Canty, M. J., Nielsen, A. A., & Schmidt, M. (2004). Automatic radiometric normalization of multitemporal satellite imagery. *Remote Sensing of Environment, 91*(3-4), 441-451. doi:10.1016/j.rse.2003.10.024

Chapin III, F. S., Woodwell, G. M., Randerson, J. T., Rastetter, E. B., Lovett, G. M., Baldocchi, D. D., Clark, D. A., Harmon, M. E., Schimel, D. S., Valentini, R., Wirth, C., Aber, J. D., Cole, J. J., Goulden, M. L., Harden, J. W., Heimann, M., Howarth, R. W., Matson, P. A., McGuire, A. D., Melillo, J. M., Mooney, H. A., Neff, J. C., Houghton, R. A., Pace, M. L., Ryan, M. G., Running, S. W., Sala, O. E., Schlesinger, W. H., & Schulze, E. D. (2006). Reconciling Carbon-Cycle Concepts, Terminology, and Methods. *Ecosystems, 9*(7), 1041-1050. doi:10.1007/s10021-005-0105-7

Chen, J., Shen, M., Zhu, X., & Tang, Y. (2009). Indicator of flower status derived from in situ hyperspectral measurement in an alpine meadow on the Tibetan Plateau. *Ecological Indicators, 9*(4), 818-823. doi:10.1016/j.ecolind.2008.09.009

Chuvieco, E. (2008). *Teledetección ambiental: La observación de la tierra desde el espacio.* Barcelona: Ariel.

Cihlar, J. (2000). Land cover mapping of large areas from satellites: Status and

research priorities. *International Journal of Remote Sensing, 21*(6-7), 1093-1114. doi:10.1080/014311600210092

Clark, E. A., Karsten, H., Murphy, W. M., & Tracy, B. F. (2006). Ecology of Plant Communities in Forage-Livestock Systems. In E. B. Rayburn (Ed.), *Forage production for pasture-based livestock production* (Vol. 172, pp. 141). Ithaca, New York: NRAES.

Clevers, J. G. P. W., & Gitelson, A. A. (2013). Remote estimation of crop and grass chlorophyll and nitrogen content using red-edge bands on sentinel-2 and-3. *International Journal of Applied Earth Observation and Geoinformation, 23*(1), 344-351. doi:10.1016/j.jag.2012.10.008

Congalton, R. G. (1991). A review of assessing the accuracy of classifications of remotely sensed data. *Remote Sensing of Environment, 37*(1), 35-46. doi:10.1016/0034-4257(91)90048-B

Congalton, R. G. (2001). Accuracy assessment and validation of remotely sensed and other spatial information. *International Journal of Wildland Fire, 10*(3-4), 321-328. doi:10.1071/WF01031

Congalton, R. G., & Green, K. (1998). Sample Design *Assessing the Accuracy of Remotely Sensed Data*: CRC Press.

Coppin, P., Jonckheere, I., Nackaerts, K., Muys, B., & Lambin, E. (2004). Digital change detection methods in ecosystem monitoring: A review. *International Journal of Remote Sensing, 25*(9), 1565-1596. doi:10.1080/0143116031000101675

Coppin, P. R., & Bauer, M. E. (1994). Processing of Multitemporal Landsat TM Imagery to Optimize Extraction of Forest Cover Change Features. *IEEE Transactions on Geoscience and Remote Sensing, 32*(4), 918-927. doi:10.1109/36.298020

Darlington, R. B., & Hayes, A. F. (2016). *Regression analysis and linear models: Concepts, applications, and implementation*: Guilford Publications.

De Deyn, G. B., Quirk, H., Yi, Z., Oakley, S., Ostle, N. J., & Bardgett, R. D. (2009). Vegetation composition promotes carbon and nitrogen storage in model grassland communities of contrasting soil fertility. *Journal of Ecology, 97*(5), 864-875. doi:10.1111/j.1365-2745.2009.01536.x

Decrem, M., Spiess, E., Richner, W., & Herzog, F. (2007). Impact of Swiss agricultural policies on nitrate leaching from arable land. *Agronomy for Sustainable Development, 27*(3), 243-253. doi:10.1051/agro:2007012

Definiens. (2007). *Developer 7, User Guide, Definiens AG,* . Retrieved from Munich, Germany

Delegido, J., Verrelst, J., Meza, C. M., Rivera, J. P., Alonso, L., & Moreno, J. (2013). A red-edge spectral index for remote sensing estimation of green LAI over agroecosystems. *European Journal of Agronomy, 46*, 42-52. doi:10.1016/j.eja.2012.12.001

Della Peruta R., & Keller A. (2016). A regional modelling tool to assess the risk of accumulation of nutrients, trace metals and pesticides in agricultural soils (iMSoil). BGS-Bulletin 37: 9-15 In S. s. d. pédologie (Ed.), *Année internationale des sols - et maintenant?* Genève, Jun. 2 2017 http://www.soil.ch/cms/publikationen/bulletins/bulletin-37/

Desclée, B., Bogaert, P., & Defourny, P. (2006). Forest change detection by statistical object-based method. *Remote Sensing of Environment, 102*(1-2), 1-11. doi:10.1016/j.rse.2006.01.013

Di Gregorio, A., & Jansen, L. J. M. (1998). *Land Cover Classification System (LCCS): Classification concepts and user manual.Environment and Natural Resources Service, GCP/RAF/287/ITA Africover - East Africa Project and Soil Resources, Management and Conservation Service. FAO, Rome.* (pp. 157).

Díaz, S., Lavorel, S., de Bello, F., Quétier, F., Grigulis, K., & Robson, T. M. (2007). Incorporating plant functional diversity effects in ecosystem service assessments. *Proceedings of the National Academy of Sciences, 104*(52), 20684-20689. doi:10.1073/pnas.0704716104

Dorigo, W. A., Zurita-Milla, R., de Wit, A. J. W., Brazile, J., Singh, R., & Schaepman, M. E. (2007). A review on reflective remote sensing and data assimilation techniques for enhanced agroecosystem modeling. *International Journal of Applied Earth Observation and Geoinformation, 9*(2), 165-193. doi:10.1016/j.jag.2006.05.003

Dusseux, P., Vertès, F., Corpetti, T., Corgne, S., & Hubert-Moy, L. (2014). Agricultural practices in grasslands detected by spatial remote sensing. *Environmental Monitoring and Assessment, 186*(12), 8249-8265. doi:10.1007/s10661-014-4001-5

Erb, K. H., Haberl, H., Jepsen, M. R., Kuemmerle, T., Lindner, M., Müller, D., Verburg, P. H., & Reenberg, A. (2013). A conceptual framework for analysing and measuring land-use intensity. *Current Opinion in Environmental Sustainability, 5*(5), 464-470. doi:10.1016/j.cosust.2013.07.010

Esch, T., Metz, A., Marconcini, M., & Keil, M. (2014). Combined use of multi-seasonal high and medium resolution satellite imagery for parcel-related mapping of cropland and grassland. *International Journal of Applied Earth Observation and Geoinformation, 28*(0), 230-237. doi:10.1016/j.jag.2013.12.007

EXELIS. (2015). Support Vector Machine Background.

Fan, Z., Neff, J. C., & Wieder, W. R. (2016). Model-based analysis of environmental controls over ecosystem primary production in an alpine tundra dry meadow. *Biogeochemistry, 128*(1), 35-49. doi:10.1007/s10533-016-0193-9

Fang, H., Liang, S., & Hoogenboom, G. (2013). Assimilation of remote sensing data and crop simulation models for agricultural study: Recent advances and future directions *Land Surface Observation, Modeling and Data Assimilation* (pp. 405-440).

FAOSTAT. (2017a). *Annual population. FAO statistics database. Food and Agriculture Organization of the United Nations*.

FAOSTAT. (2017b). *Fertilizers. FAO statistics database. Food and Agriculture Organization of the United Nations*.

Fernandes, M. R., Aguiar, F. C., Ferreira, M. T., & Pereira, J. M. C. (2013). Spectral separability of riparian forests from small and medium-sized rivers across a latitudinal gradient using multispectral imagery. *International Journal of Remote Sensing, 34*(7), 2375-2401. doi:10.1080/01431161.2012.744491

Filella, I., & Peñuelas, J. (1994). The red edge position and shape as indicators of plant chlorophyll content, biomass and hydric status. *International Journal of Remote Sensing, 15*(7), 1459-1470.

doi:10.1080/01431169408954177

Flisch, R., Sinaj, S., Charles, R., & Richtner, W. (2009). GRUDAF-Grundlagen für die Düngung im Acker- und Futterbau. *Agrarforschung, 16*(2), 97.

FOAG. (1980). *Digital soil suitability map of Switzerland. Federal Office for Agriculture (FOAG).*

FOAG. (2004). *Swiss Agricultural Policy* Oct. 10, 2016. https://www.cbd.int/financial/pes/swiss-pesagriculturalpolicy.pdf Swiss Federal Office for Agriculture.

FOAG. (2015a). Agrarpolitisches Informationssystem AGIS. Swiss Federal Office for Agriculture.

FOAG. (2015b). *Biodiversity for food and agriculture in Switzerland*. Berne, May 30, 2017 https://www.blw.admin.ch/blw/en/home/services/publikationen/berichte.html

FOEN. (2004). Biogeographic regions of Switzerland (CH). Federal Office for the Environment Federal Office for Environment / Species, Ecosystems, Landscapes Division (FOEN). . Mar. 8, 2017 https://map.geo.admin.ch/?lang=en&topic=bafu&X=190000.00&Y=660000.00&zoom=1&bgLayer=ch.swisstopo.pixelkarte-farbe&catalogNodes=766,767,784,798,804,806,768,781,1361

FOEN. (2016). Nitrogen deposition. Meteotest and Federal Office of the Environment. Federal Office for the Environment (FOEN) Mar. 2, 2017 https://www.bafu.admin.ch/bafu/en/home/topics/air/state/data/historical-data/maps-of-annual-values/map-of-nitrogen-deposition.html

Foley, J. A., DeFries, R., Asner, G. P., Barford, C., Bonan, G., Carpenter, S. R., Chapin, F. S., Coe, M. T., Daily, G. C., Gibbs, H. K., Helkowski, J. H., Holloway, T., Howard, E. A., Kucharik, C. J., Monfreda, C., Patz, J. A., Prentice, I. C., Ramankutty, N., & Snyder, P. K. (2005). Global Consequences of Land Use. *Science, 309*(5734), 570-574. doi:10.1126/science.1111772

Foley, J. A., Ramankutty, N., Brauman, K. A., Cassidy, E. S., Gerber, J. S., Johnston, M., Mueller, N. D., O'Connell, C., Ray, D. K., West, P. C., Balzer, C., Bennett, E. M., Carpenter, S. R., Hill, J., Monfreda, C., Polasky, S., Rockström, J., Sheehan, J., Siebert, S., Tilman, D., & Zaks, D. P. M. (2011). Solutions for a cultivated planet. *Nature, 478*(7369), 337-342. doi:10.1038/nature10452

Franke, J., Keuck, V., & Siegert, F. (2012). Assessment of grassland use intensity by remote sensing to support conservation schemes. *Journal for Nature Conservation, 20*(3), 125-134. doi:http://dx.doi.org/10.1016/j.jnc.2012.02.001

Freibauer, A., Rounsevell, M. D. A., Smith, P., & Verhagen, J. (2004). Carbon sequestration in the agricultural soils of Europe. *Geoderma, 122*(1), 1-23. doi:10.1016/j.geoderma.2004.01.021

Friedl, M. A., Sulla-Menashe, D., Tan, B., Schneider, A., Ramankutty, N., Sibley, A., & Huang, X. (2010). MODIS Collection 5 global land cover: Algorithm refinements and characterization of new datasets. *Remote Sensing of Environment, 114*(1), 168-182. doi:10.1016/j.rse.2009.08.016

FSO. (2005). Swiss Land-Use Statistics, ha-grid (Arealstatistik Schweiz). Federal Statistical Office. Neuchâtel, May. 5, 2017 https://www.bfs.admin.ch/bfs/de/home/statistiken/raum-umwelt/erhebungen/area.html

FSO. (2015). *Agriculture and Forestry. Swiss Agriculture. Pocket Statistics. Federal Statistics Office. Federal Department of Home Affairs.* Neuchâtel, May 29, 2017 https://www.bfs.admin.ch/bfs/en/home/statistics/agriculture-forestry.assetdetail.349914.html

García Millán, V. E., Sánchez-Azofeifa, A., Málvarez García, G. C., & Rivard, B. (2014). Quantifying tropical dry forest succession in the Americas using CHRIS/PROBA. *Remote Sensing of Environment, 144*(0), 120-136. doi:10.1016/j.rse.2014.01.010

Garnett, T., Appleby, M. C., Balmford, A., Bateman, I. J., Benton, T. G., Bloomer, P., Burlingame, B., Dawkins, M., Dolan, L., Fraser, D., Herrero, M., Hoffmann, I., Smith, P., Thornton, P. K., Toulmin, C., Vermeulen, S. J., & Godfray, H. C. J. (2013). Sustainable intensification in agriculture: Premises and policies. *Science, 341*(6141), 33-34. doi:10.1126/science.1234485

Gärtner, D., Keller, A., & Schulin, R. (2013). A simple regional downscaling approach for spatially distributing land use types for agricultural land. *Agricultural Systems, 120*, 10-19. doi:10.1016/j.agsy.2013.04.006

Giri, C. P. (2012). Brief Overview of Remote Sensing of Land Cover. In C. P. Giri (Ed.), *Remote sensing of land use and land cover: principles and applications,* (Vol. 35, pp. 3-12, 413). Boca Ratón: Taylor & Francis.

Godfray, H. C. J., Beddington, J. R., Crute, I. R., Haddad, L., Lawrence, D., Muir, J. F., Pretty, J., Robinson, S., Thomas, S. M., & Toulmin, C. (2010). Food security: The challenge of feeding 9 billion people. *Science, 327*(5967), 812-818. doi:10.1126/science.1185383

Gómez Giménez, M., de Jong, R., Della Peruta, R., Keller, A., & Schaepman, M. E. (2017). Determination of grassland use intensity based on multi-temporal remote sensing data and ecological indicators. *Remote Sensing of Environment, 198*, 126-139. doi:10.1016/j.rse.2017.06.003

Gómez Giménez, M., Della Peruta, R., de Jong, R., Keller, A., & Schaepman, M. E. (2016). Spatial Differentiation of Arable Land and Permanent Grassland to Improve a Land Management Model for Nutrient Balancing. *IEEE Journal of Selected Topics in Applied Earth Observations and Remote Sensing, 9*(12), 5655-5665. doi:10.1109/JSTARS.2016.2551729

Gonseth, Y., Wohlgemuth, T., Sansonnens, B., & Buttler, A. (2001). *Les régions biogéographiques de la Suisse – Explications et division standard. Cahier de l'environnement n° 137. Office fédéral de l'environnement, des forêts et du paysage.* Berne.

Gu, Y., Brown, J. F., Verdin, J. P., & Wardlow, B. (2007). A five-year analysis of MODIS NDVI and NDWI for grassland drought assessment over the central Great Plains of the United States. *Geophysical Research Letters, 34*(6). doi:10.1029/2006GL029127

Guo, Q., Hu, Z. M., Li, S. G., Yu, G. R., Sun, X. M., Li, L. H., Liang, N. S., & Bai, W. M. (2016). Exogenous N addition enhances the responses of gross primary productivity to individual precipitation events in a temperate grassland. *Scientific Reports, 6*. doi:10.1038/srep26901

Haboudane, D., Miller, J. R., Tremblay, N., Pattey, E., & Vigneault, P. (2004). *Estimation of leaf area index using ground spectral measurements over agriculture crops: Prediction capability assessment of optical indices.* Paper presented at the International Archives of the Photogrammetry, Remote Sensing and Spatial Information Sciences - ISPRS Archives.

Harvey, M., & Pilgrim, S. (2011). The new competition for land: Food, energy, and climate change. *Food Policy, 36, Supplement 1*, S40-S51. doi:10.1016/j.foodpol.2010.11.009

Hayes, A. F., & Cai, L. (2007). Using heteroskedasticity-consistent standard error estimators in OLS regression: An introduction and software implementation. *Behavior Research Methods, 39*(4), 709-722. doi:10.3758/BF03192961

Haygarth, P. M., Jarvie, H. P., Powers, S. M., Sharpley, A. N., Elser, J. J., Shen, J., Peterson, H. M., Chan, N. I., Howden, N. J. K., Burt, T., Worrall, F., Zhang, F., & Liu, X. (2014). Sustainable Phosphorus Management and the Need for a Long-Term Perspective: The Legacy Hypothesis. *Environmental Science and Technology, 48*, 8417-8419. doi:10.1021/es502852s

He, C. E., Wang, X., Liu, X., Fangmeier, A., Christie, P., & Zhang, F. (2010). Nitrogen deposition and its contribution to nutrient inputs to intensively managed agricultural ecosystems. *Ecological Applications, 20*(1), 80-90. doi:10.1890/08-0582.1

He, K., Qi, Y., Huang, Y., Chen, H., Sheng, Z., Xu, X., & Duan, L. (2016). Response of aboveground biomass and diversity to nitrogen addition-a five-year experiment in semi-arid grassland of Inner Mongolia, China. *Scientific Reports, 6*. doi:10.1038/srep31919

Heathwaite, A. L., Fraser, A. I., Johnes, P. J., Hutchins, M., Lord, E., & Butterfield, D. (2003). The phosphorus indicators tool: A simple model of diffuse P loss from agricultural land to water. *Soil Use and Management, 19*(1), 1-11. doi:10.1079/SUM2002174

Heinsch, F. A., Zhao, M., Running, S. W., Kimball, J. S., Nemani, R. R., Davis, K. J., Bolstad, P. V., Cook, B. D., Desai, A. R., Ricciuto, D. M., Law, B. E., Oechel, W. C., Kwon, H., Luo, H., Wofsy, S. C., Dunn, A. L., Munger, J. W., Baldocchi, D. D., Xu, L., Hollinger, D. Y., Richardson, A. D., Stoy, P. C., Siqueira, M. B. S., Monson, R. K., Burns, S. P., & Flanagan, L. B. (2006). Evaluation of remote sensing based terrestrial productivity from MODIS using regional tower eddy flux network observations. *IEEE Transactions on Geoscience and Remote Sensing, 44*(7), 1908-1923. doi:10.1109/TGRS.2005.853936

Herzog, F., Dreier, S., Hofer, G., Marfurt, C., Schüpbach, B., Spiess, M., & Walter, T. (2005). Effect of ecological compensation areas on floristic and breeding bird diversity in Swiss agricultural landscapes. *Agriculture, Ecosystems and Environment, 108*(3), 189-204.

Herzog, F., Prasuhn, V., Spiess, E., & Richner, W. (2008). Environmental cross-compliance mitigates nitrogen and phosphorus pollution from Swiss agriculture. *Environmental Science and Policy, 11*(7), 655-668. doi:10.1016/j.envsci.2008.06.003

Herzog, F., Richner, W., & Walter, T. (2005). Moderately positive effects of ecolofical measures. *12 (10)*, 454-459.

Herzog, F., Steiner, B., Bailey, D., Baudry, J., Billeter, R., Bukácek, R., De Blust, G., De Cock, R., Dirksen, J., Dormann, C. F., De Filippi, R., Frossard, E., Liira, J., Schmidt, T., Stöckli, R., Thenail, C., Van Wingerden, W., & Bugter, R. (2006). Assessing the intensity of temperate European agriculture at the landscape scale. *European Journal of Agronomy, 24*(2), 165-181. doi:10.1016/j.eja.2005.07.006

Hitz, C., Egli, M., & Fitze, P. (2001). Below-ground and above-ground production

of vegetational organic matter along a climosequence in alpine grasslands. *Journal of Plant Nutrition and Soil Science, 164*(4), 389-397. doi:10.1002/1522-2624(200108)164:4<389::AID-JPLN389>3.0.CO;2-A

Hollberg, J., & Schellberg, J. (2017). Distinguishing Intensity Levels of Grassland Fertilization Using Vegetation Indices. *Remote Sensing, 9*(1), 81. doi:10.3390/rs9010081

Hunt Jr, E. R., Everitt, J. H., Ritchie, J. C., Moran, M. S., Booth, D. T., Anderson, G. L., Clark, P. E., & Seyfried, M. S. (2003). Applications and research using remote sensing for rangeland management. *Photogrammetric engineering and remote sensing, 69*(6), 675-693. doi:10.14358/PERS.69.6.675

Hunt Jr, E. R., & Williams, A. E. P. (2006). Detection of flowering leafy spurge with satellite multispectral imagery. *Rangeland Ecology and Management, 59*(5), 494-499. doi:10.2111/05-216R.1

IBM Corp. (2012). IBM SPSS Statistics for Windows, Version 21.0. Armonk, NY: IBM Corp.

Iiames, J. S., Congalton, R. G., & Lunetta, R. S. (2013). Analyst variation associated with land cover image classification of Landsat ETM + data for the assessment of coarse spatial resolution regional/global land cover products. *GIScience and Remote Sensing, 50*(6), 604-622. doi:10.1080/15481603.2013.865399

Irons, J. R., Dwyer, J. L., & Barsi, J. A. (2012). The next Landsat satellite: The Landsat Data Continuity Mission. *Remote Sensing of Environment, 122*, 11-21. doi:10.1016/j.rse.2011.08.026

Jeangros, B., & Thomet, P. (2004). *Multi-functionality of grassland systems in Switzerland. In: Land Use Systems in Grassland Dominated Regions: Proceedings of the 20th General Meeting of the European Grassland Federation, Luzern, Switzerland, 21-24 June 2004. Grassland Science in Europe*.

Johnson, J. M. F., Allmaras, R. R., & Reicosky, D. C. (2006). Estimating source carbon from crop residues, roots and rhizodeposits using the national grain-yield database. *Agronomy Journal, 98*(3), 622-636. doi:10.2134/agronj2005.0179

Jones, L., Provins, A., Holland, M., Mills, G., Hayes, F., Emmett, B., Hall, J., Sheppard, L., Smith, R., Sutton, M., Hicks, K., Ashmore, M., Haines-Young, R., & Harper-Simmonds, L. (2014). A review and application of the evidence for nitrogen impacts on ecosystem services. *Ecosystem Services, 7*, 76-88. doi:10.1016/j.ecoser.2013.09.001

Kampmann, D., Herzog, F., Jeanneret, P., Konold, W., Peter, M., Walter, T., Wildi, O., & Lüscher, A. (2008). Mountain grassland biodiversity: Impact of site conditions versus management type. *Journal for Nature Conservation, 16*(1), 12-25. doi:10.1016/j.jnc.2007.04.002

Karathanassi, V., Kolokousis, P., & Ioannidou, S. (2007). A comparison study on fusion methods using evaluation indicators. *International Journal of Remote Sensing, 28*(10), 2309-2341. doi:10.1080/01431160600606890

Keller, A., Della Peruta, R., Gómez Giménez, M., Schaepman, M., & Schulin, R. (2017). Development of a land management model to monitor and predict nutrient and trace element balances for agricultural soils (in preparation).

Keller, A., Della Peruta, R., Mann, S., Zimmermann, A., Schulin, R., Gómez Giménez, M., de Jong, R., & Schaepman, M. E. (2015). A regional monitoring tool for

agricultural land management and to assess the impact on soil functions (iMSoil): part 1 *III Conference of NRP68: Soil as a Resource*. Montreaux.

Keller, A., & Schulin, R. (2003). Modelling regional-scale mass balances of phosphorus, cadmium and zinc fluxes on arable and dairy farms. *European Journal of Agronomy, 20*(1-2), 181-198. doi:10.1016/S1161-0301(03)00075-3

Keller, A., Von Steiger, B., Van der Zee, S. E. A. T. M., & Schulin, R. (2001). A stochastic empirical model for regional heavy-metal balances in agroecosystems. *Journal of Environmental Quality, 30*(6), 1976-1989, PMID: 11790004.

Kempen, M., Elbersen, B. S., Staritsky, I., Andersen, E., & Heckelei, T. (2011). Spatial allocation of farming systems and farming indicators in Europe. *Agriculture, Ecosystems and Environment, 142*(1-2), 51-62. doi:10.1016/j.agee.2010.08.001

Kleijn, D., Kohler, F., Báldi, A., Batáry, P., Concepción, E. D., Clough, Y., Díaz, M., Gabriel, D., Holzschuh, A., Knop, E., Kovács, A., Marshall, E. J., Tscharntke, T., & Verhulst, J. (2009). On the relationship between farmland biodiversity and land-use intensity in Europe. *Proceedings. Biological sciences / The Royal Society, 276*(1658), 903-909. doi:10.1098/rspb.2008.1509

Kleijn, D., & Sutherland, W. J. (2003). How effective are European agri-environment schemes in conserving and promoting biodiversity? *Journal of Applied Ecology, 40*(6), 947-969. doi:10.1111/j.1365-2664.2003.00868.x

Knorn, J., Rabe, A., Radeloff, V. C., Kuemmerle, T., Kozak, J., & Hostert, P. (2009). Land cover mapping of large areas using chain classification of neighboring Landsat satellite images. *Remote Sensing of Environment, 113*(5), 957-964. doi:10.1016/j.rse.2009.01.010

Köhler, B., Gigon, A., Edwards, P. J., Krüsi, B., Langenauer, R., Lüscher, A., & Ryser, P. (2005). Changes in the species composition and conservation value of limestone grasslands in Northern Switzerland after 22 years of contrasting managements. *Perspectives in Plant Ecology, Evolution and Systematics, 7*(1), 51-67. doi:10.1016/j.ppees.2004.11.003

Kokaly, R. F. (2001). Investigating a physical basis for spectroscopic estimates of leaf nitrogen concentration. *Remote Sensing of Environment, 75*(2), 153-161. doi:10.1016/S0034-4257(00)00163-2

Kokaly, R. F., Asner, G. P., Ollinger, S. V., Martin, M. E., & Wessman, C. A. (2009). Characterizing canopy biochemistry from imaging spectroscopy and its application to ecosystem studies. *Remote Sensing of Environment, 113*(SUPPL. 1), S78-S91. doi:10.1016/j.rse.2008.10.018

Konstanski, H., Choi, M., & Brunn, A. (2015). White paper: Explanation of angles documented in the RapidEye image metadata (pp. 10). Berlin, Oct. 27, 2017: BlacBridge.

Kotsiantis, S. B. (2007). Supervised machine learning: A review of classification techniques. *Informatica (Ljubljana), 31*(3), 249-268.

Krupa, S. V. (2003). Effects of atmospheric ammonia (NH3) on terrestrial vegetation: a review. *Environmental Pollution, 124*(2), 179-221. doi:10.1016/S0269-7491(02)00434-7

Kuemmerle, T., Erb, K., Meyfroidt, P., Müller, D., Verburg, P. H., Estel, S., Haberl, H.,

Hostert, P., Jepsen, M. R., Kastner, T., Levers, C., Lindner, M., Plutzar, C., Verkerk, P. J., van der Zanden, E. H., & Reenberg, A. (2013). Challenges and opportunities in mapping land use intensity globally. *Current Opinion in Environmental Sustainability, 5*(5), 484-493. doi:10.1016/j.cosust.2013.06.002

Lal, R. (2004a). Soil Carbon Sequestration Impacts on Global Climate Change and Food Security. *Science, 304*(5677), 1623-1627. doi:10.1126/science.1097396

Lal, R. (2004b). Soil carbon sequestration to mitigate climate change. *Geoderma, 123*(1-2), 1-22. doi:10.1016/j.geoderma.2004.01.032

Lambin, E. F., Rounsevell, M. D. A., & Geist, H. J. (2000). Are agricultural land-use models able to predict changes in land-use intensity? *Agriculture, Ecosystems and Environment, 82*(1-3), 321-331. doi:10.1016/S0167-8809(00)00235-8

Lambin, E. F., Turner, B. L., Geist, H. J., Agbola, S. B., Angelsen, A., Bruce, J. W., Coomes, O. T., Dirzo, R., Fischer, G., Folke, C., George, P. S., Homewood, K., Imbernon, J., Leemans, R., Li, X., Moran, E. F., Mortimore, M., Ramakrishnan, P. S., Richards, J. F., Skånes, H., Steffen, W., Stone, G. D., Svedin, U., Veldkamp, T. A., Vogel, C., & Xu, J. (2001). The causes of land-use and land-cover change: moving beyond the myths. *Global Environmental Change, 11*(4), 261-269. doi:10.1016/S0959-3780(01)00007-3

Landmann, T., Piiroinen, R., Makori, D. M., Abdel-Rahman, E. M., Makau, S., Pellikka, P., & Raina, S. K. (2015). Application of hyperspectral remote sensing for flower mapping in African savannas. *Remote Sensing of Environment, 166*, 50-60. doi:10.1016/j.rse.2015.06.006

Ledgard, S. F. (2001). Nitrogen cycling in low input legume-based agriculture, with emphasis on legume/grass pastures. *Plant and Soil, 228*(1), 43-59. doi:10.1023/A:1004810620983

Lee, W. S., Alchanatis, V., Yang, C., Hirafuji, M., Moshou, D., & Li, C. (2010). Sensing technologies for precision specialty crop production. *Computers and Electronics in Agriculture, 74*(1), 2-33. doi:10.1016/j.compag.2010.08.005

Leifeld, J., Bassin, S., & Fuhrer, J. (2005). Carbon stocks in Swiss agricultural soils predicted by land-use, soil characteristics, and altitude. *Agriculture, Ecosystems and Environment, 105*(1-2), 255-266. doi:10.1016/j.agee.2004.03.006

Leifeld, J., Zimmermann, M., Fuhrer, J., & Conen, F. (2009). Storage and turnover of carbon in grassland soils along an elevation gradient in the Swiss Alps. *Global Change Biology, 15*(3), 668-679. doi:10.1111/j.1365-2486.2008.01782.x

Letourneau, A., Verburg, P. H., & Stehfest, E. (2012). A land-use systems approach to represent land-use dynamics at continental and global scales. *Environmental Modelling and Software, 33*, 61-79. doi:10.1016/j.envsoft.2012.01.007

Li, G., Lu, D., Moran, E., Dutra, L., & Batistella, M. (2012). A comparative analysis of ALOS PALSAR L-band and RADARSAT-2 C-band data for land-cover classification in a tropical moist region. *ISPRS Journal of Photogrammetry and Remote Sensing, 70*(0), 26-38. doi:10.1016/j.isprsjprs.2012.03.010

Liu, S., Bond-Lamberty, B., Boysen, L. R., Ford, J. D., Fox, A., Gallo, K., Hatfield, J.,

Henebry, G. M., Huntington, T. G., Liu, Z., Lovelan, T. R., Norby, R. J., Soh, T., Steiner, A. L., Yuan, W., Zhang, Z., & Zhao, S. (2017). Grand challenges in understanding the interplay of climate and land changes. *Earth Interactions, 21*(2). doi:10.1175/EI-D-16-0012.1

Lorenz, K. (2013). Ecosystem Carbon Sequestration. In R. Lal, K. Lorenz, R. F. Hüttl, B. U. Schneider, & J. von Braun (Eds.), *Ecosystem Services and Carbon Sequestration in the Biosphere* (pp. 39-62). Dordrecht: Springer Netherlands.

Lorenz, K., & Lal, R. (2012). Cropland soil carbon dynamics *Recarbonization of the Biosphere: Ecosystems and the Global Carbon Cycle* (pp. 303-346).

Loveland, T. R. (2012). History of Land-Cover Mapping. In C. P. Giri (Ed.), *Remote Sensing of Land Use and Land Cover:principles and applications* (Vol. 35, pp. 13-22, 413). Boca Ratón: Taylor & Francis.

Loveland, T. R., & Dwyer, J. L. (2012). Landsat: Building a strong future. *Remote Sensing of Environment, 122*, 22-29. doi:10.1016/j.rse.2011.09.022

Lu, D., Mausel, P., Brondízio, E., & Moran, E. (2004). Change detection techniques. *International Journal of Remote Sensing, 25*(12), 2365-2407. doi:10.1080/0143116031000139863

Mack, G., & Huber, R. (2017). On-farm compliance costs and N surplus reduction of mixed dairy farms under grassland-based feeding systems. *Agricultural Systems, 154*, 34-44. doi:10.1016/j.agsy.2017.03.003

Malenovský, Z., Rott, H., Cihlar, J., Schaepman, M. E., García-Santos, G., Fernandes, R., & Berger, M. (2012). Sentinels for science: Potential of Sentinel-1, -2, and -3 missions for scientific observations of ocean, cryosphere, and land. *Remote Sensing of Environment, 120*, 91-101. doi:10.1016/j.rse.2011.09.026

Manthey, M., & Peper, J. (2010). Estimation of grazing intensity along grazing gradients - the bias of nonlinearity. *Journal of Arid Environments, 74*(10), 1351-1354. doi:10.1016/j.jaridenv.2010.05.007

Marcheggiani, E., Galli, A., Bernardini, A., Malinverni, E. S., & Zingaretti, P. (2008). *Selection criteria of training set for optimal land cover discrimination with a view to automatic segmentation.* Paper presented at the Remote Sensing for a Changing Europe: Proceedings of the 28th Symposium of the European Association of Remote Sensing Laboratories, Istanbul, Turkey, 2-5 June.

Martinkova, Z., & Honek, A. (2014). The establishment of Taraxacum officinale plants in grassland. *Weed Research, 54*(5), 501-510. doi:10.1111/wre.12096

Mas, J. F. (1999). Monitoring land-cover changes: A comparison of change detection techniques. *International Journal of Remote Sensing, 20*(1), 139-152. doi:10.1080/014311699213659

Maskell, L. C., Smart, S. M., Bullock, J. M., Thompson, K., & Stevens, C. J. (2010). Nitrogen deposition causes widespread loss of species richness in British habitats. *Global Change Biology, 16*(2), 671-679. doi:10.1111/j.1365-2486.2009.02022.x

Mather, P., & Koch, M. (2011). *Computer Processing of Remotely-Sensed Images: An Introduction* (4th Edition ed.). Chichester: Wiley-Blackwell.

Matson, P., Lohse, K. A., & Hall, S. J. (2002). The globalization of nitrogen deposition: Consequences for terrestrial ecosystems. *Ambio, 31*(2), 113-

119, PMID: 12077999.

Matson, P. A., Parton, W. J., Power, A. G., & Swift, M. J. (1997). Agricultural Intensification and Ecosystem Properties. *Science, 277*(5325), 504-509. doi:10.1126/science.277.5325.504

McMaster, G. S., & Wilhelm, W. W. (1997). Growing degree-days: One equation, two interpretations. *Agricultural and Forest Meteorology, 87*(4), 291-300. doi:10.1016/S0168-1923(97)00027-0

Meier, T. (2013). Ausführungsbestimmungen der Agrarpolitik 2014 – 2017 (Vol. 4, pp. 492-497). Agrarforschung Schweiz Jul. 2, 2017 http://www.agrarforschungschweiz.ch/archiv_11en.php?id_artikel=1930

Meteoswiss. (2013). MeteoSwiss Grid-Data products. In Meteoswiss (Ed.). Mar. 7, 2017, http://www.meteoswiss.admin.ch/home/climate/present-day/monthly-and-annual-maps.html

Meteoswiss. (2014). Climate of Switzerland. Mar. 8, 2017, http://www.meteoswiss.admin.ch/home/climate/past/climate-of-switzerland.html

Meteoswiss. (2015a). Climate change in Switzerland Mar. 8, 2017, http://www.meteoswiss.admin.ch/content/dam/meteoswiss/de/Klima/Zukunft/doc/mch_klimawandel_63-13_high.pdf?query=sunshine

Meteoswiss. (2015b). Climate diagrams and normal values per station (Zurich, Fluntern). Dec. 6, 2016 http://www.meteoswiss.admin.ch/home/climate/past/climate-normals/climate-diagrams-and-normal-values-per-station.html?region=Map

Metzger, C. M. H., Heinichen, J., Eickenscheidt, T., & Drösler, M. (2016). Impact of land-use intensity on the relationships between vegetation indices, photosynthesis and biomass of intensively and extensively managed grassland fens. *Grass and Forage Science*. doi:10.1111/gfs.12223

Miao, X., Gong, P., Swope, S., Pu, R., Carruthers, R., Anderson, G. L., Heaton, J. S., & Tracy, C. R. (2006). Estimation of yellow starthistle abundance through CASI-2 hyperspectral imagery using linear spectral mixture models. *Remote Sensing of Environment, 101*(3), 329-341. doi:10.1016/j.rse.2006.01.006

Midi, H., Sarkar, S. K., & Rana, S. (2010). Collinearity diagnostics of binary logistic regression model. *Journal of Interdisciplinary Mathematics, 13*(3), 253-267.

Mirik, M., Ansley, R. J., Steddom, K., Jones, D. C., Rush, C. M., Michels Jr, G. J., & Elliott, N. C. (2013). Remote distinction of a noxious weed (Musk Thistle: Carduus Nutans) using airborne hyperspectral imagery and the support vector machine classifier. *Remote Sensing, 5*(2), 612-630. doi:10.3390/rs5020612

Monfreda, C., Ramankutty, N., & Foley, J. A. (2008). Farming the planet: 2. Geographic distribution of crop areas, yields, physiological types, and net primary production in the year 2000. *Global Biogeochemical Cycles, 22*(1). doi:10.1029/2007GB002947

Morawitz, D. F., Blewett, T. M., Cohen, A., & Alberti, M. (2006). Using NDVI to assess vegetative land cover change in Central Puget Sound. *Environmental Monitoring and Assessment, 114*(1-3), 85-106. doi:10.1007/s10661-006-1679-z

Mountrakis, G., Im, J., & Ogole, C. (2011). Support vector machines in remote sensing: A review. *ISPRS Journal of Photogrammetry and Remote Sensing, 66*(3), 247-259. doi:10.1016/j.isprsjprs.2010.11.001

Müllerová, J., Pergl, J., & Pyšek, P. (2013). Remote sensing as a tool for monitoring plant invasions: Testing the effects of data resolution and image classification approach on the detection of a model plant species Heracleum mantegazzianum (giant hogweed). *International Journal of Applied Earth Observation and Geoinformation, 25*(1), 55-65. doi:10.1016/j.jag.2013.03.004

Mutanga, O., Skidmore, A. K., & Van Wieren, S. (2003). Discriminating tropical grass (Cenchrus ciliaris) canopies grown under different nitrogen treatments using spectroradiometry. *ISPRS Journal of Photogrammetry and Remote Sensing, 57*(4), 263-272. doi:10.1016/S0924-2716(02)00158-2

Nielsen, A. A. (2007). The regularized iteratively reweighted MAD method for change detection in multi- and hyperspectral data. *IEEE Transactions on Image Processing, 16*(2), 463-478. doi:10.1109/TIP.2006.888195

Numata, I., Roberts, D. A., Chadwick, O. A., Schimel, J., Sampaio, F. R., Leonidas, F. C., & Soares, J. V. (2007). Characterization of pasture biophysical properties and the impact of grazing intensity using remotely sensed data. *Remote Sensing of Environment, 109*(3), 314-327. doi:10.1016/j.rse.2007.01.013

OECD. (1998). *The Environmental Effects of Reforming Agricultural Policies*. Paris: OECD.

OECD. (2015). Impact of Swiss policy reforms on the economic and environmental performance of agriculture *OECD Review of Agricultural Policies: Switzerland 2015*. Paris: OECD Publishing.

OECD. (2016). *Switzerland in Agricultural Policy and Evaluatoin*. Paris: OECD Publishing.

Oenema, O., Kros, H., & De Vries, W. (2003). Approaches and uncertainties in nutrient budgets: Implications for nutrient management and environmental policies. *European Journal of Agronomy, 20*(1-2), 3-16. doi:10.1016/S1161-0301(03)00067-4

Olesen, J. E., & Bindi, M. (2002). Consequences of climate change for European agricultural productivity, land use and policy. *European Journal of Agronomy, 16*(4), 239-262. doi:10.1016/S1161-0301(02)00004-7

Otto, S., Masin, R., Chistè, G., & Zanin, G. (2007). Modelling the correlation between plant phenology and weed emergence for improving weed control. *Weed Research, 47*(6), 488-498. doi:10.1111/j.1365-3180.2007.00594.x

Pakeman, R. J. (2004). Consistency of plant species and trait responses to grazing along a productivity gradient: A multi-site analysis. *Journal of Ecology, 92*(5), 893-905. doi:10.1111/j.0022-0477.2004.00928.x

Pavlů, V., Gaisler, J., Hejcman, M., & Pavlů, L. (2008). Effect of different grazing intensity on weed control under conditions of organic farming. *Journal of Plant Diseases and Proctection, Supplement*(21), 441-446.

Peco, B., De Pablos, I., Traba, J., & Levassor, C. (2005). The effect of grazing abandonment on species composition and functional traits: The case of dehesa grasslands. *Basic and Applied Ecology, 6*(2), 175-183.

doi:10.1016/j.baae.2005.01.002

Petropoulos, G. P., Kalaitzidis, C., & Prasad Vadrevu, K. (2012). Support vector machines and object-based classification for obtaining land-use/cover cartography from Hyperion hyperspectral imagery. *Computers and Geosciences, 41*, 99-107. doi:10.1016/j.cageo.2011.08.019

Petropoulos, G. P., Kontoes, C., & Keramitsoglou, I. (2011). Burnt area delineation from a uni-temporal perspective based on landsat TM imagery classification using Support Vector Machines. *International Journal of Applied Earth Observation and Geoinformation, 13*(1), 70-80. doi:10.1016/j.jag.2010.06.008

Poças, I., Cunha, M., & Pereira, L. S. (2012). Dynamics of mountain semi-natural grassland meadows inferred from SPOT-VEGETATION and field spectroradiometer data. *International Journal of Remote Sensing, 33*(14), 4334-4355. doi:10.1080/01431161.2011.645084

Potter, P., Ramankutty, N., Bennett, E. M., & Donner, S. D. (2010). Characterizing the spatial patterns of global fertilizer application and manure production. *Earth Interactions, 14*(2). doi:10.1175/2009EI288.1

Pu, R., Gong, P., Tian, Y., Miao, X., Carruthers, R. I., & Anderson, G. L. (2008). Using classification and NDVI differencing methods for monitoring sparse vegetation coverage: A case study of saltcedar in Nevada, USA. *International Journal of Remote Sensing, 29*(14), 3987-4011. doi:10.1080/01431160801908095

Ramoelo, A., Cho, M., Mathieu, R., & Skidmore, A. K. (2015). Potential of Sentinel-2 spectral configuration to assess rangeland quality. *Journal of Applied Remote Sensing, 9*(1). doi:10.1117/1.JRS.9.094096

Ramoelo, A., Skidmore, A. K., Cho, M. A., Schlerf, M., Mathieu, R., & Heitkönig, I. M. A. (2012). Regional estimation of savanna grass nitrogen using the red-edge band of the spaceborne rapideye sensor. *International Journal of Applied Earth Observation and Geoinformation, 19*(1), 151-162. doi:10.1016/j.jag.2012.05.009

Rango, A., Havstad, K., & Estell, R. (2011). The utilization of historical data and geospatial technology advances at the Jornada experimental range to support Western America ranching culture. *Remote Sensing, 3*(9), 2089-2109. doi:10.3390/rs3092089

Richter, R., & Schläpfer, D. (2004). Atmospheric and Topographic Correction for Satellite Imagery. ATCOR-2/3 User Guide, Version 8.3.1. Sep. 2014 https://www.rese-apps.com/software/download/index.html

Rihm, B., & Achermann, B. (2016). Critical Loads of Nitrogen and their Exceedances. Swiss contribution to the effects-oriented work under the Convention on Long-range Transboundary Air Pollution (UNECE). Federal Office for the Environment. Environmental studies. no. 1642: 78 p. Bern. May 26, 2017 https://www.bafu.admin.ch/bafu/en/home/topics/air/publications-studies/publications/Critical-Loads-of-Nitrogen-and-their-Exceedances.html

Rindfuss, R. R., Walsh, S. J., Turner Ii, B. L., Fox, J., & Mishra, V. (2004). Developing a science of land change: Challenges and methodological issues. *Proceedings of the National Academy of Sciences of the United States of America, 101*(39), 13976-13981.

Rinella, M. J., Vavra, M., Naylor, B. J., & Boyd, J. M. (2011). Estimating influence of stocking regimes on livestock grazing distributions. *Ecological Modelling, 222*(3), 619-625. doi:10.1016/j.ecolmodel.2010.10.004

Robinson, T. P., William Wint, G. R., Conchedda, G., Van Boeckel, T. P., Ercoli, V., Palamara, E., Cinardi, G., D'Aietti, L., Hay, S. I., & Gilbert, M. (2014). Mapping the global distribution of livestock. *PLoS ONE, 9*(5). doi:10.1371/journal.pone.0096084

Rose, R. A., Byler, D., Eastman, J. R., Fleishman, E., Geller, G., Goetz, S., Guild, L., Hamilton, H., Hansen, M., Headley, R., Hewson, J., Horning, N., Kaplin, B. A., Laporte, N., Leidner, A., Leimgruber, P., Morisette, J., Musinsky, J., Pintea, L., Prados, A., Radeloff, V. C., Rowen, M., Saatchi, S., Schill, S., Tabor, K., Turner, W., Vodacek, A., Vogelmann, J., Wegmann, M., Wilkie, D., & Wilson, C. (2015). Ten ways remote sensing can contribute to conservation. *Conservation Biology, 29*(2), 350-359. doi:10.1111/cobi.12397

Rounsevell, M. D. A., Arneth, A., Alexander, P., Brown, D. G., De Noblet-Ducoudré, N., Ellis, E., Finnigan, J., Galvin, K., Grigg, N., Harman, I., Lennox, J., Magliocca, N., Parker, D., O'Neill, B. C., Verburg, P. H., & Young, O. (2014). Towards decision-based global land use models for improved understanding of the Earth system. *Earth System Dynamics, 5*(1), 117-137. doi:10.5194/esd-5-117-2014

Roy, D. P., Wulder, M. A., Loveland, T. R., C.E, W., Allen, R. G., Anderson, M. C., Helder, D., Irons, J. R., Johnson, D. M., Kennedy, R., Scambos, T. A., Schaaf, C. B., Schott, J. R., Sheng, Y., Vermote, E. F., Belward, A. S., Bindschadler, R., Cohen, W. B., Gao, F., Hipple, J. D., Hostert, P., Huntington, J., Justice, C. O., Kilic, A., Kovalskyy, V., Lee, Z. P., Lymburner, L., Masek, J. G., McCorkel, J., Shuai, Y., Trezza, R., Vogelmann, J., Wynne, R. H., & Zhu, Z. (2014). Landsat-8: Science and product vision for terrestrial global change research. *Remote Sensing of Environment, 145*, 154-172. doi:10.1016/j.rse.2014.02.001

Rudel, T. K., Schneider, L., Uriarte, M., Turner Ii, B. L., DeFries, R., Lawrence, D., Geoghegan, J., Hecht, S., Ickowitz, A., Lambin, E. F., Birkenholtz, T., Baptista, S., & Grau, R. (2009). Agricultural intensification and changes in cultivated areas, 1970-2005. *Proceedings of the National Academy of Sciences of the United States of America, 106*(49), 20675-20680. doi:10.1073/pnas.0812540106

Running, S. W., Nemani, R. R., Heinsch, F. A., Zhao, M., Reeves, M., & Hashimoto, H. (2004). A continuous satellite-derived measure of global terrestrial primary production. *BioScience, 54*(6), 547-560. doi:10.1641/0006-3568(2004)054[0547:ACSMOG]2.0.CO;2

Running, S. W., & Zhao, M. (2000). Gross Primary Productivity 8-Day L4 Global 1Km (MOD17A2), v 5.0 and 5.5 NASA EOSDIS Land Processes DAAC, USGS Earth Resources Observation and Science (EROS) Center, Sioux Falls, South Dakota Jan. 16, 2017 https://lpdaac.usgs.gov

Sala, O. E., Stuart Chapin , F., III, Armesto, J. J., Berlow, E., Bloomfield, J., Dirzo, R., Huber-Sanwald, E., Huenneke, L. F., Jackson, R. B., Kinzig, A., Leemans, R., Lodge, D. M., Mooney, H. A., Oesterheld, M. n., Poff, N. L., Sykes, M. T., Walker, B. H., Walker, M., & Wall, D. H. (2000). Global Biodiversity Scenarios for the Year 2100. *Science, 287*(5459), 1770-1774. doi:10.1126/science.287.5459.1770

Sanderson, M. A., Feldmann, C., Schmidt, J., Herrmann, A., & Taube, F. (2010). Spatial distribution of livestock concentration areas and soil nutrients in pastures. *Journal of Soil and Water Conservation, 65*(3), 180-189. doi:10.2489/jswc.65.3.180

Schaepman, M. E., Jehle, M., Hueni, A., D'Odorico, P., Damm, A., Weyermann, J., Schneider, F. D., Laurent, V., Popp, C., Seidel, F. C., Lenhard, K., Gege, P., Küchler, C., Brazile, J., Kohler, P., De Vos, L., Meuleman, K., Meynart, R., Schläpfer, D., Kneubühler, M., & Itten, K. I. (2015). Advanced radiometry measurements and Earth science applications with the Airborne Prism Experiment (APEX). *Remote Sensing of Environment, 158*, 207-219. doi:10.1016/j.rse.2014.11.014

Schroeder, T. A., Cohen, W. B., Song, C., Canty, M. J., & Yang, Z. (2006). Radiometric correction of multi-temporal Landsat data for characterization of early successional forest patterns in western Oregon. *Remote Sensing of Environment, 103*(1), 16-26. doi:10.1016/j.rse.2006.03.008

Schulze, E. D., Ciais, P., Luyssaert, S., Schrumpf, M., Janssens, I. A., Thiruchittampalam, B., Theloke, J., Saurat, M., Bringezu, S., Lelieveld, J., Lohila, A., Rebmann, C., Jung, M., Bastviken, D., Abril, G., Grassi, G., Leip, A., Freibauer, A., Kutsch, W., Don, A., Nieschulze, J., BÖRner, A., Gash, J. H., & Dolman, A. J. (2010). The European carbon balance. Part 4: Integration of carbon and other trace-gas fluxes. *Global Change Biology, 16*(5), 1451-1469. doi:10.1111/j.1365-2486.2010.02215.x

Schüpbach, B., Zgraggen, K., & Szerencsits, E. (2008). Incentives for low-input land-use types and their influence on the attractiveness of landscapes. *Journal of Environmental Management, 89*(3), 222-233. doi:10.1016/j.jenvman.2007.01.060

Schuster, M. J., Smith, N. G., & Dukes, J. S. (2016). Responses of aboveground C and N pools to rainfall variability and nitrogen deposition are mediated by seasonal precipitation and plant community dynamics. *Biogeochemistry, 129*(3), 389-400. doi:10.1007/s10533-016-0240-6

Singh, A. (1989). Digital change detection techniques using remotely-sensed data. *International Journal of Remote Sensing, 10*(6), 989-1003. doi:10.1080/01431168908903939

Sinha, P., & Kumar, L. (2013). Independent two-step thresholding of binary images in inter-annual land cover change/no-change identification. *ISPRS Journal of Photogrammetry and Remote Sensing, 81*, 31-43. doi:10.1016/j.isprsjprs.2013.03.010

Siu-Ngan Lam, N., & Quattrochi, D. A. (1992). On the issues of scale, resolution, and fractal analysis in the mapping sciences. *Professional Geographer, 44*(1), 88-98. doi:10.1111/j.0033-0124.1992.00088.x

Skidmore, A. K., Bijker, W., Schmidt, K., & Kumar, L. (1997). Use of remote sensing and GIS for sustainable land management. *ITC Journal, 1997*(3-4), 302-315.

Smith, B., Wärlind, D., Arneth, A., Hickler, T., Leadley, P., Siltberg, J., & Zaehle, S. (2014). Implications of incorporating N cycling and N limitations on primary production in an individual-based dynamic vegetation model. *Biogeosciences, 11*(7), 2027-2054. doi:10.5194/bg-11-2027-2014

Smith, P. (2004). Carbon sequestration in croplands: the potential in Europe and

the global context. *European Journal of Agronomy, 20*(3), 229-236. doi:10.1016/j.eja.2003.08.002

Smith, P., Gregory, P. J., Van Vuuren, D., Obersteiner, M., Havlík, P., Rounsevell, M., Woods, J., Stehfest, E., & Bellarby, J. (2010). Competition for land. *Philosophical Transactions of the Royal Society B: Biological Sciences, 365*(1554), 2941-2957.

Socher, S. A., Prati, D., Boch, S., Müller, J., Baumbach, H., Gockel, S., Hemp, A., Schöning, I., Wells, K., Buscot, F., Kalko, E. K. V., Linsenmair, K. E., Schulze, E. D., Weisser, W. W., & Fischer, M. (2013). Interacting effects of fertilization, mowing and grazing on plant species diversity of 1500 grasslands in Germany differ between regions. *Basic and Applied Ecology, 14*(2), 126-136. doi:10.1016/j.baae.2012.12.003

Socher, S. A., Prati, D., Boch, S., Müller, J., Klaus, V. H., Hölzel, N., & Fischer, M. (2012). Direct and productivity-mediated indirect effects of fertilization, mowing and grazing on grassland species richness. *Journal of Ecology, 100*(6), 1391-1399. doi:10.1111/j.1365-2745.2012.02020.x

Song, C., Woodcock, C. E., Seto, K. C., Lenney, M. P., & Macomber, S. A. (2001). Classification and change detection using Landsat TM data: When and how to correct atmospheric effects? *Remote Sensing of Environment, 75*(2), 230-244. doi:10.1016/S0034-4257(00)00169-3

Spiess, E. (2011). Nitrogen, phosphorus and potassium balances and cycles of Swiss agriculture from 1975 to 2008. *Nutrient Cycling in Agroecosystems, 91*(3), 351-365. doi:10.1007/s10705-011-9466-9

Steffen, W., Richardson, K., Rockström, J., Cornell, S. E., Fetzer, I., Bennett, E. M., Biggs, R., Carpenter, S. R., de Vries, W., de Wit, C. A., Folke, C., Gerten, D., Heinke, J., Mace, G. M., Persson, L. M., Ramanathan, V., Reyers, B., & Sörlin, S. (2015). Planetary boundaries: Guiding human development on a changing planet. *Science, 347*(6223). doi:10.1126/science.1259855

Stevens, C. J., Lind, E. M., Hautier, Y., Harpole, W. S., Borer, E. T., Hobbie, S., Seabloom, E. W., Ladwig, L., Bakker, J. D., Chu, C., Collins, S., Davies, K. F., Firn, J., Hillebrand, H., La Pierre, K. J., MacDougall, A., Melbourne, B., McCulley, R. L., Morgan, J., Orrock, J. L., Prober, S. M., Risch, A. C., Schuetz, M., & Wragg, P. D. (2015). Anthropogenic nitrogen deposition predicts local grassland primary production worldwide. *Ecology, 96*(6), 1459-1465. doi:10.1890/14-1902.1.sm

Stoate, C., Boatman, N. D., Borralho, R. J., Carvalho, C. R., De Snoo, G. R., & Eden, P. (2001). Ecological impacts of arable intensification in Europe. *Journal of Environmental Management, 63*(4), 337-365. doi:10.1006/jema.2001.0473

Strijker, D. (2005). Marginal lands in Europe—causes of decline. *Basic and Applied Ecology, 6*(2), 99-106. doi:10.1016/j.baae.2005.01.001

Swain, D. L., Friend, M. A., Bishop-Hurley, G. J., Handcock, R. N., & Wark, T. (2011). Tracking livestock using global positioning systems are we still lost? *Animal Production Science, 51*(3), 167-175. doi:10.1071/AN10255

Swiss Constitution. (1999). Constitution fédérale de la Confédération suisse. Confédération suisse.

Swiss government. (1998). Ordonnance sur la terminologie agricole et la reconnaissance des formes d'exploitation (OTerm). Nov. 9, 2015 https://www.admin.ch/opc/fr/classified-

compilation/19983381/index.html
Swiss government. (2013). Ordonnance sur les paiements directs versés dans l'agriculture. Apr. 12, 2017 https://www.admin.ch/opc/fr/classified-compilation/20130216/index.html *RO 2013 4145*
Swisstopo. (2001). Digital Height Model, DHM25. Federal Office of Topography. . Jun. 3, 2015, http://www.swisstopo.admin.ch/internet/swisstopo/en/home/products/height/dhm25.html
Swisstopo. (2008). Swiss Map vector. Federal Office of Topography. Dec. 4, 2016 https://shop.swisstopo.admin.ch/en/products/maps/national/vector/smv25
Swisstopo. (2013). Swissimage. Dec. 6, 2016 https://shop.swisstopo.admin.ch/en/products/images/ortho_images/SWISSIMAGE
Swisstopo. (2014). Vector200. Federal Office of Topography Dec. 4, 2016 https://shop.swisstopo.admin.ch/en/products/landscape/vector200
Swisstopo. (2015). Digital Height Model, SwissALTI3D. Federal Office of Topography. . May 25, 2017 https://shop.swisstopo.admin.ch/de/products/height_models/alti3D
Temme, A. J. A. M., & Verburg, P. H. (2011). Mapping and modelling of changes in agricultural intensity in Europe. *Agriculture, Ecosystems and Environment, 140*(1-2), 46-56. doi:10.1016/j.agee.2010.11.010
Tilman, D., Fargione, J., Wolff, B., D'Antonio, C., Dobson, A., Howarth, R., Schindler, D., Schlesinger, W. H., Simberloff, D., & Swackhamer, D. (2001). Forecasting agriculturally driven global environmental change. *Science, 292*(5515), 281-284. doi:10.1126/science.1057544
Tscharntke, T., Klein, A. M., Kruess, A., Steffan-Dewenter, I., & Thies, C. (2005). Landscape perspectives on agricultural intensification and biodiversity - Ecosystem service management. *Ecology Letters, 8*(8), 857-874. doi:10.1111/j.1461-0248.2005.00782.x
Turner, B. L., & Doolittle, W. E. (1978). The concept and measure of agricultural intensity. *Professional Geographer, 30*(3), 297-301. doi:10.1111/j.0033-0124.1978.00297.x
Turner, B. L., & Robbins, P. (2008). Land-change science and political ecology: Similarities, differences, and implications for sustainability science. *Annual Review of Environment and Resources, 33*, 295-316. doi:10.1146/annurev.environ.33.022207.104943
Turner, D. P., Ritts, W. D., Cohen, W. B., Gower, S. T., Running, S. W., Zhao, M., Costa, M. H., Kirschbaum, A. A., Ham, J. M., Saleska, S. R., & Ahl, D. E. (2006). Evaluation of MODIS NPP and GPP products across multiple biomes. *Remote Sensing of Environment, 102*(3-4), 282-292. doi:10.1016/j.rse.2006.02.017
Turner, D. P., Ritts, W. D., Cohen, W. B., Gower, S. T., Zhao, M., Running, S. W., Wofsy, S. C., Urbanski, S., Dunn, A. L., & Munger, J. W. (2003). Scaling Gross Primary Production (GPP) over boreal and deciduous forest landscapes in support of MODIS GPP product validation. *Remote Sensing of Environment, 88*(3), 256-270. doi:10.1016/j.rse.2003.06.005
Turner, D. P., Ritts, W. D., Cohen, W. B., Maeirsperger, T. K., Gower, S. T., Kirschbaum, A. A., Running, S. W., Zhao, M., Wofsy, S. C., Dunn, A. L., Law,

B. E., Campbell, J. L., Oechel, W. C., Kwon, H. J., Meyers, T. P., Small, E. E., Kurc, S. A., & Gamon, J. A. (2005). Site-level evaluation of satellite-based global terrestrial gross primary production and net primary production monitoring. *Global Change Biology, 11*(4), 666-684. doi:10.1111/j.1365-2486.2005.00936.x

Turner II, B. L., Lambin, E. F., & Reenberg, A. (2007). The emergence of land change science for global environmental change and sustainability. *Proceedings of the National Academy of Sciences of the United States of America, 104*(52), 20666-20671. doi:10.1073/pnas.0704119104

Ustin, S. L., Gitelson, A. A., Jacquemoud, S., Schaepman, M., Asner, G. P., Gamon, J. A., & Zarco-Tejada, P. (2009). Retrieval of foliar information about plant pigment systems from high resolution spectroscopy. *Remote Sensing of Environment, 113*(SUPPL. 1), S67-S77. doi:10.1016/j.rse.2008.10.019

van Oudenhoven, A. P. E., Petz, K., Alkemade, R., Hein, L., & de Groot, R. S. (2012). Framework for systematic indicator selection to assess effects of land management on ecosystem services. *Ecological Indicators, 21*(0), 110-122. doi:10.1016/j.ecolind.2012.01.012

Van Wesemael, B., Paustian, K., Meersmans, J., Goidts, E., Barancikova, G., & Easter, M. (2010). Agricultural management explains historic changes in regional soil carbon stocks. *Proceedings of the National Academy of Sciences of the United States of America, 107*(33), 14926-14930. doi:10.1073/pnas.1002592107

Vankoughnett, M. R., & Henry, H. A. L. (2014). Soil freezing and N deposition: Transient vs multi-year effects on plant productivity and relative species abundance. *New Phytologist, 202*(4), 1277-1285. doi:10.1111/nph.12734

Vapnik, V. N. (1998). *The nature of statistical learning theory* (Second ed.). New York: Springer.

Verburg, P. H., Mertz, O., Erb, K. H., Haberl, H., & Wu, W. (2013). Land system change and food security: Towards multi-scale land system solutions. *Current Opinion in Environmental Sustainability, 5*(5), 494-502. doi:10.1016/j.cosust.2013.07.003

Verburg, P. H., van de Steeg, J., Veldkamp, A., & Willemen, L. (2009). From land cover change to land function dynamics: A major challenge to improve land characterization. *Journal of Environmental Management, 90*(3), 1327-1335. doi:10.1016/j.jenvman.2008.08.005

Verstraeten, W. W., Veroustraete, F., & Feyen, J. (2006). On temperature and water limitation of net ecosystem productivity: Implementation in the C-Fix model. *Ecological Modelling, 199*(1), 4-22. doi:10.1016/j.ecolmodel.2006.06.008

Vicente-Serrano, S. M., Pérez-Cabello, F., & Lasanta, T. (2008). Assessment of radiometric correction techniques in analyzing vegetation variability and change using time series of Landsat images. *Remote Sensing of Environment, 112*(10), 3916-3934. doi:10.1016/j.rse.2008.06.011

Volk, M., Obrist, D., Novak, K., Giger, R., Bassin, S., & Fuhrer, J. (2011). Subalpine grassland carbon dioxide fluxes indicate substantial carbon losses under increased nitrogen deposition, but not at elevated ozone concentration. *Global Change Biology, 17*(1), 366-376. doi:10.1111/j.1365-2486.2010.02228.x

Whitcraft, A. K., Becker-Reshef, I., Killough, B. D., & Justice, C. O. (2015). Meeting

earth observation requirements for global agricultural monitoring: An evaluation of the revisit capabilities of current and planned moderate resolution optical earth observing missions. *Remote Sensing, 7*(2), 1482-1503. doi:10.3390/rs70201482

Wulder, M. A., Hilker, T., White, J. C., Coops, N. C., Masek, J. G., Pflugmacher, D., & Crevier, Y. (2015). Virtual constellations for global terrestrial monitoring. *Remote Sensing of Environment, 170*, 62-76. doi:10.1016/j.rse.2015.09.001

Wulder, M. A., White, J. C., Goward, S. N., Masek, J. G., Irons, J. R., Herold, M., Cohen, W. B., Loveland, T. R., & Woodcock, C. E. (2008). Landsat continuity: Issues and opportunities for land cover monitoring. *Remote Sensing of Environment, 112*(3), 955-969. doi:10.1016/j.rse.2007.07.004

Wulder, M. A., White, J. C., Masek, J. G., Dwyer, J., & Roy, D. P. (2011). Continuity of Landsat observations: Short term considerations. *Remote Sensing of Environment, 115*(2), 747-751. doi:10.1016/j.rse.2010.11.002

Yang, Y., Donohue, R. J., McVicar, T. R., & Roderick, M. L. (2015). An analytical model for relating global terrestrial carbon assimilation with climate and surface conditions using a rate limitation framework. *Geophysical Research Letters, 42*(22), 9825-9835. doi:10.1002/2015GL066835

Zaehle, S., Bondeau, A., Carter, T. R., Cramer, W., Erhard, M., Prentice, I. C., Reginster, I., Rounsevell, M. D. A., Sitch, S., Smith, B., Smith, P. C., & Sykes, M. (2007). Projected changes in terrestrial carbon storage in Europe under climate and land-use change, 1990-2100. *Ecosystems, 10*(3), 380-401. doi:10.1007/s10021-007-9028-9

Zaehle, S., Friend, A. D., Friedlingstein, P., Dentener, F., Peylin, P., & Schulz, M. (2010). Carbon and nitrogen cycle dynamics in the O-CN land surface model: 2. Role of the nitrogen cycle in the historical terrestrial carbon balance. *Global Biogeochemical Cycles, 24*(1). doi:10.1029/2009GB003522,2010

Zaks, D. P. M., & Kucharik, C. J. (2011). Data and monitoring needs for a more ecological agriculture. *Environmental Research Letters, 6*(1). doi:10.1088/1748-9326/6/1/014017

Zhang, Y., Grant, R. F., Flanagan, L. B., Wang, S., & Verseghy, D. L. (2005). Modelling CO <inf>2</inf> and energy exchanges in a northern semiarid grassland using the carbon- and nitrogen-coupled Canadian Land Surface Scheme (C-CLASS). *Ecological Modelling, 181*(4), 591-614. doi:10.1016/j.ecolmodel.2004.07.007

Zhang, Y., Yu, G., Yang, J., Wimberly, M. C., Zhang, X., Tao, J., Jiang, Y., & Zhu, J. (2014). Climate-driven global changes in carbon use efficiency. *Global Ecology and Biogeography, 23*(2), 144-155. doi:10.1111/geb.12086

Zhao, M., Heinsch, F. A., Nemani, R. R., & Running, S. W. (2005). Improvements of the MODIS terrestrial gross and net primary production global data set. *Remote Sensing of Environment, 95*(2), 164-176. doi:10.1016/j.rse.2004.12.011

Zhao, M., Running, S. W., & Nemani, R. R. (2006). Sensitivity of Moderate Resolution Imaging Spectroradiometer (MODIS) terrestrial primary production to the accuracy of meteorological reanalyses. *Journal of Geophysical Research: Biogeosciences, 111*(1). doi:10.1029/2004JG000004

# Curriculum vitae

**MARTA GOMEZ GIMENEZ**
**11/07/1986**
**Spanish**

## Education

2013-2017 Ph.D (Dr. sc. nat) in Earth Observation, Department of Geography, Remote Sensing Laboratories, University of Zurich (CH).

2011 Master's degree in Geographic Information Technologies (60 ECTS), Department of Geography, University of Alcala (ESP).

Thesis: *Use of satellite images to Emergency and Security management.* Supervised by Dr. María Julia Yagüe Ballester and Dr. Isabel Montoya Montes.

2010 Bachelor's degree in Environmental Sciences (345 ECTS), Biology and Geology Department, University Rey Juan Carlos (ESP).

Thesis: *Use of multispectral images to study a glacier.* Supervised by Dr. Iván López Ruiz-Labranderas and Dr. Francisco Carreño Conde.

2004 Baccalaureate in Natural and Health Sciences. SEK Ciudalcampo International School, (ESP).

2002 Secondary education. SEK Ciudalcampo International School, (ESP).

## Teaching experience, Department of Geography, University of Zurich

2016 Principles of Remote Sensing "Labs" (GEO 233.2: Fall semester).
2016 Specialization in Remote Sensing: Research colloquium (GEO 441.1: Spring semester).
2015 Fernerkundung und Geographische Informationswissenschaft I (GEO 113: Fall semester).
2015 Small group teaching (GEO 299: Fall semester).
2015 Small group teaching (GEO 299: Spring semester).
2014 Small group teaching (GEO 299: Fall semester).
2014 Fernerkundung und Geographische Informationswissenschaft II, (GEO 123: Spring semester).

## Previous professional experience in Earth Observation

2011-2012 Remote sensing and GIS analyst, Remote Sensing Applications and Services division, Payload Data Processing and Application Business Unit, GMV, Spain.

**Graduate school courses and training (selected)**

- Ph.D. Seminars I—II.
- Principles and theory in Geography.
- Retreat seminar I—II.
- Spectroscopy of the Earth System.
- Voice training and presentation skills.
- Scientific writing.
- Resource stressed-focused oriented.
- ESA 5th Advanced training course in land remote sensing.
- Project management.
- Time and self-management.
- Introductory R for spatial analysis and visualization.
- R4all. A recipe for success with R.
- Introduction to Python applied to cartography, GIS, and remote sensing.

**Peer-review publications**

**Gómez Giménez, M.,** de Jong, R., Keller, A., Rihm B., and Schaepman, M.E. Nitrogen deposition mostly predicts gross primary production response in Swiss croplands, grasslands, and natural vegetation mosaic. Submitted to *Agriculture and Forest Meteorology.*

**Gómez Giménez, M.,** de Jong, R., Della Peruta, R., Keller, A., and Schaepman, M.E. (2017). Determination of grassland use intensity based on multi-temporal remote sensing data and ecological indicators. *Remote Sensing of Environment, 198*, 126-139.

**Gómez Giménez, M.** Della Peruta, R., de Jong, R, Keller, A., and Schaepman, M.E. (2016). Spatial Differentiation of Arable Land and Permanent Grassland to Improve a Land Management Model for Nutrient Balancing. *IEEE Journal of Selected Topics in Applied Earth Observations and Remote Sensing, 9*, 5655-5665.

**Conference contributions**

**Gómez Giménez, M.** Della Peruta, R., de Jong, R., Keller, A., and Schaepman, M.E., Arable land and grassland differentiation to improve a Land Management Model *American Geophysical Union (AGU) Fall Meeting*, 14-18th December, 2015, San Francisco (USA).

Keller, A., Della Peruta, R., Mann, S., Zimmermann, A., Schulin, R., **Gómez Giménez, M.,** de Jong, R., and Schaepman, M.E. (2015). A regional monitoring tool for agricultural land management and to assess the impact on soil functions (iMSoil): part 1 *III Conference of NRP68: Soil as a Resource*. 12-13th November, 2015, Montreaux (CH).

**Gómez Giménez, M.,** Della Peruta, R., Keller, A., Schaepman, M.E., and de Jong, R. Land cover differentiation to improve a Land Management Model using remote sensing sources. *International Symposium: Recent Advances in Quantitative Remote Sensing*, 22-26th September, 2014, Valencia (ESP) & *12th Swiss Geoscience Meeting*, 21-22nd, November, 2014, Fribourg (CH).

Keller, A., Della Peruta, R., Mann, S., Schulin, R., **Gómez Giménez, M.,** de Jong, R., and Schaepman, M.E., A regional soil monitoring tool to assess the impact of agricultural land management to soil functions (iMSoil) *NRP68 Conference,* 20-21st November, 2014, Fribourg, (CH).

## Acknowledgements

First of all, I am sincerely grateful for the opportunity that I have been given to pursue a Ph.D. at the Remote Sensing Laboratories, University of Zurich, and at the Swiss centre of excellence for agricultural research, Agroscope. During these years, I have had the privilege of working at two different facilities. This has provided me with a large number of new and challenging situations that have taught me precious lessons. I am taking away very valuable experiences that have broadened my way of thinking. I am absolutely sure that these memorable four years will accompany me in the future. Now, I would like to express my gratitude to all the people who have made this journey interesting, enjoyable and unforgettable.

I would like to thank my supervisors Dr. Rogier de Jong, Dr. Armin Keller, Prof. Dr. Michael E. Schaepman, and my Ph.D. committee member, PD. Dr. Guido Wiesenberg, for their time and feedback, which have helped me improve my work. I am particularly thankful to Dr. Raniero Della Peruta for his valuable contributions to this Ph.D. Thanks for a whole year going back and forth to the field with me, your proactive attitude towards my Ph.D., very interesting discussions about a wide range of topics, and contributing to having a good work environment. It was easy to work with you. I would also like to highlight the role of Prof. Dr. Michael E. Schaepman in this Ph.D. I honestly believe that I could not have started, carried out, and finished this Ph.D. on time without your support. Every discussion, conversation, and chat meant a step forward in any matter of concern. It has been a great pleasure to come to Zurich to not only to work with you but also to learn from you.

There are many people at LIDARLab, MMRS, NABO, SARLab, and SpectroLab, who have made my working life more enjoyable. Most especially, my gratitude goes to my office mates: Carla Guillén Escribà, Daniel Kükenbrink, Fabian D. Schneider, and Jonas Böhler for so many hilarious moments, trips, and table football breaks. Moreover, I wish to acknowledge the contributions of Daniel, Fabian, and Jonas in translating the summary of this thesis into German and in teaching me Swiss words. I also extend this special thanks to my colleagues from Agroscope: Julia Franzen, Leta Klauser, Lucie Greiner, and Michael Müller. I feel

grateful for the time we have spent together playing table tennis and sharing many enjoyable conversations. In addition, I would like to acknowledge the contributions of Rita Ott and Sandra Altorfer in making my life easier over the last four years. You both are amazing!

Not a single performance could be successfully played without crucial work behind the scenes. Therefore, I express my profound gratitude to my close relatives, friends, and teachers who have left their mark on me, inspired me, and pushed me forward. Among them, I would like to highlight my personal "crew": Encarnación, Francisco, and Javier —things are just easy when you break your leg and the next day someone decides to take a holiday and travel 1,700 km to take care of you— Arturo, who has shared these four years and more with me in Madrid, Cannes, Zurich, and Darmstadt. I am certain that having met you is one of the greatest things that will ever happen in my life. Thanks to my old and new friends who have paid me visits and given me so many happy moments, including scuba diving and skiing trips, Friday's beers and *aperitivos* on Sundays! Eva, thanks for still being there.

Finally, I would like to dedicate this work to my *titita*, Milagros Gascón Vélez, who believed in me so strongly. I think of you every day.

ISBN Nr. 978-3-906894-04-1